UDK 66:54(05) CODEN HMIDA 8 ISSN 0367–598X

4

Hemijska industrija

Vol. 79

Časopis Saveza hemijskih inženjera Srbije

Chemical Industry

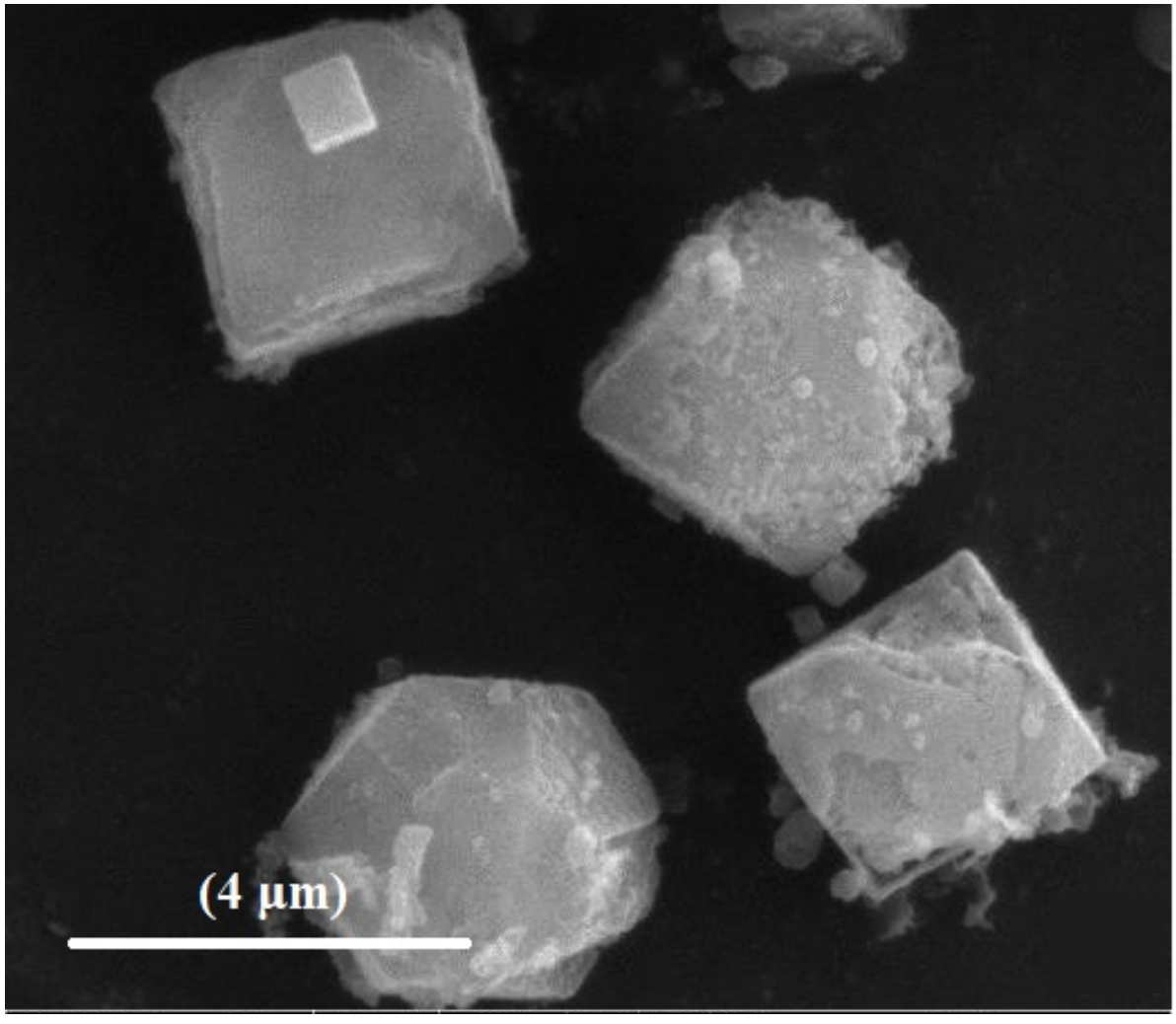

BEOGRAD, OKTOBAR-DECEMBAR 2025. HMIDA 8, 79(4) 191-252 (2025)

Aktivnosti Saveza hemijskih inženjera Srbije pomažu:

**MINISTARSTVO NAUKE,
TEHNOLOŠKOG RAZVOJA
I INOVACIJA
REPUBLIKE SRBIJE**

Tehnološko-metalurški fakultet
Univerziteta u Beogradu

Prirodno-matematički fakultet
Univerziteta u Novom Sadu

Institut za tehnologiju nuklearnih i
drugih mineralnih sirovina, Beograd

Tehnološki fakultet
Univerziteta u Novom Sadu

Institut za hemiju, tehnologiju i metalurgiju
Univerziteta u Beogradu

Fakultet tehničkih nauka
Univerziteta u Novom Sadu

Tehnološki fakultet
Univerziteta u Nišu, Leskovac

Fakultet tehničkih nauka
Univerziteta u Prištini
Kosovska Mitrovica

Institut IMS, Beograd

DCP HEMIGAL
Leskovac

Barič

Elixir Prahovo

SHI Beograd Srbija

Chemical Industry
Химическая промышленность

Hemijska industrija

Časopis Saveza hemijskih inženjera Srbije
Journal of the Association of Chemical Engineers of Serbia
Журнал Союза химических инженеров Сербии

VOL. 79 **Beograd, oktobar – decembar 2025.** **Broj 4**

Izdavač
Savez hemijskih inženjera Srbije
Beograd, Kneza Miloša 9/I

Glavni urednik
Bojana Obradović

Zamenica glavnog i odgovornog urednika
Emila Živković

Pomoćnik glavnog i odgovornog urednika
Ivana Drvenica

Urednici
Jelena Bajat, Dejan Bezbradica, Ivana Banković-Ilić, Dušan Mijin, Marija Nikolić, Snežana Stanković, Đorđe Veljović, Tatjana Volkov-Husović

Članovi uredništva
Nikolaj Ostrovski, Milorad Cakić, Željko Čupić, Miodrag Lazić, Slobodan Petrović, Milovan Purenović, Aleksandar Spasić, Dragoslav Stoiljković, Radmila Šećerov-Sokolović, Slobodan Šerbanović, Nikola Nikačević, Svetomir Milojević

Članovi uredništva iz inostranstva
Dragomir Bukur (SAD), Jiri Hanika (Češka Republika), Valerij Meshalkin (Rusija), Ljubiša Radović (SAD), Constantinos Vayenas (Grčka)

Likovno-grafičko rešenje naslovne strane
Milan Jovanović

Redakcija
11000 Beograd, Kneza Miloša 9/I
Tel/fax: 011/3240-018
E-pošta: shi@ache.org.rs
www.ache.org.rs

Izlazi kvartalno, rukopisi se ne vraćaju

Za izdavača: Ivana T. Drvenica

Sekretar redakcije: Slavica Desnica

Izdavanje časopisa pomaže
Republika Srbija, Ministarstvo nauke, tehnološkog razvoja i inovacija

Uplata pretplate i oglasnog prostora vrši se na tekući račun Saveza hemijskih inženjera Srbije, Beograd, broj 205-2172-71, Komercijalna banka a.d., Beograd

Menadžer časopisa i kompjuterska priprema
Aleksandar Dekanski

Štampa
Razvojno-istraživački centar grafičkog inženjerstva, Tehnološko-metalurški fakultet, Univerzitet u Beogradu, Karnegijeva 4, 11000 Beograd

Indeksiranje

Radovi koji se publikuju u časopisu *Hemijska Industrija* ideksiraju se preko *Clarivate* servisa *Science Citation Index - Expanded™* i *Journal Citation Reports™ (JCR)*, kao i *Scopus* servisa *CiteScore™*

SADRŽAJ/CONTENTS

E-waste recycling: an overview of hydrometallurgical processes used for metal recovery*

Nallely G. Picazo-Rodríguez[1], Gabriela Baltierra-Costeira[1], Ma de Jesús Soria-Aguilar[2], Zeferino Gamiño Arroyo[3], Norman Toro[4], Manuel Saldana[4,5], Jesús R. de la Garza de Luna[1] and Francisco Raúl Carrillo-Pedroza[2]

[1]*Instituto Tecnológico Superior de Monclova, Tecnológico Nacional de México, Monclova, México*
[2]*Facultad de Metalurgia, Universidad Autónoma de Coahuila, Monclova, México*
[3]*Departamento de Ingeniería Química, División de Ciencias Naturales y Exactas, Universidad de Guanajuato, Guanajuato, México*
[4]*Faculty of Engineering and Architecture, Universidad Arturo Prat, Iquique, Chile*
[5]*Departamento de Ingeniería Química y Procesos de Minerales, Universidad de Antofagasta, Antofagasta, Chile*

Abstract

Exponential population growth resulted in exponential demands for metals, especially for production of electronic devices, which are mainly sent to landfills at the end of their functional life. This practice poses a significant environmental hazard due to the presence of metals within these discarded materials, termed electronic waste or e-waste, which necessitate appropriate management strategies to avert adverse effects on both the ecosystem and human health. E-waste contains valuable metals often in concentrations rendering their recovery economically viable. Furthermore, the escalating demand for metals, driven by technological progress, has made the recycling of e-waste a crucial element of sustainable resource management. This work provides an overview of hydrometallurgical processing techniques for the recovery of valuable metals from the waste from electrical and electronic equipment, where hydrometallurgy plays a determinant role in the recovery of valuable metals such as copper, gold, and silver. These methodologies employ aqueous chemistry to facilitate the metal extraction, presenting a cost-effective and environmentally sustainable alternative when compared to production of metals by conventional mining practices. However, the economic viability of these alternative processes may fluctuate based on the specific type and concentration of metals present within the waste.

Keywords: hydrometallurgy; e-waste management; valuable metals; extraction; environmental sustainability.

Available on-line at the Journal web address: http://www.ache.org.rs/HI/

REVIEW PAPER

UDC: 669.054.8:628.5

Hem. Ind. **79(4)** 191-207 (2025)

1. INTRODUCTION

Waste from electrical and electronic equipment (WEEE), arising from both private homes and professional uses, may contain heavy metals such as Be, Cr, Cd, Ar, Se, Sb, Hg, Pb, as well as Au, Ag and Cu [1,2]. Improvements in the processing power of computers have shortened their average life. Every year, the amount of WEEE increases three times faster than that of the other forms of municipal waste [3].

As reported in literature [4], the copper content in electronic waste (e-waste) can be around 20 % while in primary metallic resources it ranges from 0.5 to 1 %. It should be thus profitable to develop feasible and environmentally friendly

Corresponding authors:
N. G. Picazo-Rodríguez, Instituto Tecnológico Superior de Monclova, Tecnológico Nacional de México, Monclova, México;
E-mail: nallely.pr@monclova.tecnm.mx; https://orcid.org/0000-0002-5780-2747
G. Baltierra-Costeira, Instituto Tecnológico Superior de Monclova, Tecnológico Nacional de México, Monclova, México;
E-mail: gabriela.bc@monclova.tecnm.mx; https://orcid.org/0000-0001-6269-1183
F. R. Carrillo-Pedroza, Facultad de Metalurgia, Universidad Autónoma de Coahuila, Monclova, México; https://orcid.org/0000-0002-0413-0676
E-mail: raul.carrillo@uadec.edu.mx
Co-authors: M. de J. Soria-Aguilar https://orcid.org/0000-0003-3910-7772, Z. Gamiño Arroyo https://orcid.org/0000-0002-6228-8586, N. Toro https://orcid.org/0000-0001-6269-1183, M. Saldana https://orcid.org/0000-0001-9265-1529, J. R. de la Garza de Luna https://orcid.org/0000-0002-6522-9514

Paper received: 18 November 2024; Paper accepted: 28 November 2025; Paper published: 16 December 2025.
https://doi.org/10.2298/HEMIND241118015D

*This manuscript is an expanded and peer-reviewed version of the preprint previously published as: Picazo-Rodríguez NG; Baltierra-Costeira G; Soria-Aguilar MJ, Gamiño-Arroyo Z, Toro, N, de la Garza de Luna JR, Carrillo-Pedroza FR, E-waste Recycling: An Overview of Hydrometallurgical Processes Used to Metals Recovery. *Preprints* 2023, 2023110933. https://doi.org/10.20944/preprints202311.0933.v1

methods to recover copper from such waste. Treatment of e-waste has consequently gained relevance in recent years, especially in developed countries. In addition, these wastes will become an important source of metals, especially when the primary sources are running out [5].

E-waste has increased significantly in all regions of the world because the use of electronic devices and equipment occurs massively in different sectors of human life (industrial, services, economic) [6]. According to literature [7], consumption of electrical and electronic devices is strongly linked to the development and economy of countries and in 2019 53.6 Mt of e-waste was generated globally (7.3 kg *per* capita) and it is expected that by 2030 74.7 Mt of this waste will be produced, almost double what was generated in 2019. It was also stated that computers, TV devices, and mobile phones constitute most of the e-waste and that in some advanced countries this waste makes up more than 80 % of municipal waste [8].

Nowadays, industrial waste is generally incinerated, which is detrimental to the environment due to the large number of metals it contains [9]. As reported in literature [5] incineration and thermal treatment of e-waste have raised concerns because of emissions of organic pollutants, which are toxic and can cause serious problems. However, recovery of metals from these wastes could be more economical than extraction them from their primary sources [10].

For example, as reported by Cui and Zhang [4], printed circuit boards (PCB) are the components of electronic scrap that contain the highest number of valuable metals in significant concentrations such as ~3300 ppm Ag, 80 ppm Au and 26.8 % Cu. Au and Ag are contained in native or alloy forms, mainly coated on the pins and holes of electronic components and the board, or within microprocessors [11]. Hsu *et al.* [12], mention in their research that PCBs represent 3 % of the total mass of e-waste worldwide appearing in the form of a copper-coated fiberglass and resin laminate.

To achieve optimal extraction of gold and silver, it is necessary to eliminate the common metals mentioned above and thus avoid the extra consumption of reagents that would be required by their presence. For example, the extraction of copper from computer PCBs has been investigated using inorganic acid leaching. These reagents dissolve other metallic elements such as iron, nickel, lead, and zinc, thereby removing a substantial portion of the base-metal matrix. As a result, the relative concentrations of gold and silver in the remaining solid residue increase, rising from 131.29 to 345.9 g t^{-1} for Au and from 310 to 864.8 g t^{-1} for Ag, respectively [13].

The technologies for metal recovery from electronic waste encompass pre-treatment operations (classification, dismantling, shredding, and physical separation), as well as hydrometallurgical routes based on acid or alkaline-oxidant and complexing systems, whose efficiency and selectivity have been extensively documented [14-22]. Emerging processes such as electrochemically assisted leaching, ionic-liquid extraction, and kinetic modelling for multicomponent systems have further optimized the dissolution and recovery of critical metals under controlled conditions [23-26]. In parallel, advances in catalytic pyrolysis, carbothermic treatments, and selective smelting contribute to the valorization of refractory metallic fractions [18,19,27,28]. Biohydrometallurgy, driven by microorganisms and microbial consortia capable of oxidizing or reducing metallic phases, has gained recognition as a sustainable alternative for complex WEEE matrices [29,30], while integrated physicochemical-biotechnological approaches increasingly support circular recovery schemes with reduced environmental impact. This paper presents a review of the main hydrometallurgical processes used in the recovery of metals from WEEE.

2. HYDROMETALLURGICAL PROCESSES: EXTRACTION AND RECOVERY FROM E-WASTE

Hydrometallurgical processes involve chemical reactions carried out in aqueous or organic solutions. The main steps are leaching, concentration/purification of metals and recovery, offering advantages such as the ability to control the level of impurities, low investment cost, lower environmental impact, and high metal recovery potentials [9,31].

If the hydrometallurgical route is to be followed for copper recovery sulfuric acid is used for leaching [32] as it provides copper extraction in high quantities, in addition to other heavy metals [33]. Park *et al.* [34], determined that the efficiency of the sulfuric acid leaching process increased with increasing agitation speed, temperature, oxygen flow and initial Cu^{2+} content so that the following conditions were proposed as optimal: sulfuric acid concentration (1 mol dm^{-3}), temperature (90 °C), stirring speed (600 rpm), pulp density (1 %), initial copper concentration (10 g dm^{-3}) and oxygen flow rate (1 dm^3 min^{-1}). Dávila-Pulido *et al.* [35] carried out copper leaching in a 2 mol L^{-1} H_2SO_4-H_2O_2 0.2 mol L^{-1} system, which allowed complete dissolution of copper present in the electronic waste samples. The same leaching system was recirculated in another study for up to 5 cycles, resulting in reduction of acid consumption by 60 % [36]. Other acid

leaching media include ferric chloride with hydrochloric acid system, which was used to extract copper and antimony from PCBs followed by recovery them by electrodeposition, managing to obtain 96 % copper and 81 % antimony [37].

A study of the effectiveness of a new leaching system consisting of ionic hydrogen sulphate liquids to dissolve copper from PCBs showed that copper could be leached in large quantities, but with the presence of an oxidant such as H_2O_2 [38,39]. In other works where ionic liquids of hydrogen sulphate and hydrogen peroxide were used, it was found that the particle size had a great influence on the process [40].

Other researchers, such as Kavousi *et al.* [41], employed hydrogen peroxide in an HBF_4 leaching medium to simultaneously dissolve copper and the Sn-Pb solder phases, achieving a copper extraction efficiency of 99.99%. In another approach, hydrogen peroxide was combined with an environmentally benign lixiviant, sodium citrate, while ammonium phosphate was incorporated as a chemical inhibitor to suppress the co-dissolution of base metals, resulting in copper concentrations exceeding 30 g L^{-1} [42].

Other methods have been also used to leach copper such as application of electrogenerated chlorine in hydrochloric acid solution [43]. In specifically, in one experimental series generation of chlorine was carried out simultaneously with copper leaching, while in another two reactors were used, one for chlorine generation and the other for copper leaching. Better results were obtained in the latter case, achieving a recovery of copper of 71 % together with 98 % zinc, 96 % tin and 96 % lead using a 2 mol L^{-1} HCl solution at a current density of 714 A m^{-2}, 323 K and 400 rpm for 240 min.

After copper leaching from e-waste, the residue is further leached to recover the precious metals [1]. The most used chemical reagents during this leaching process are cyanide, halides, thiourea, thiosulfate, ethylenediaminetetraacetic acid (EDTA), oxalates, aqua regia, sodium hypochlorite, nitric acid, ferric chloride, and organic solvents [9].

According to Akcil *et al.* [5], cyanide leaching has been a successful technology worldwide for the recovery of precious metals (especially Au and Ag) from ores/concentrates/waste materials, because it is an effective, economical, and easy to implement leaching agent. However, its use requires treatment of the effluents generated during the recovery process. In response to the toxic nature and handling problems of cyanide, several non-cyanide leaching processes have been developed using non-toxic leaching agents such as thiourea, thiosulfate, aqua regia and iodine. Consequently, various recycling technologies have been established utilizing both cyanide or non-cyanide leaching methods to recover precious and valuable metals.

An example of a process for recovering precious metals from e-waste through the hydrometallurgical route was implemented by Mudila *et al.* [44] processed waste printed circuit boards from mobile phones by mechanically grinding and delaminating them to obtain powdered and liberated metallic fractions. The resulting material was then subjected to a two-stage leaching process: an initial nitric acid leaching step (3 M HNO_3, 30 °C) to dissolve base metals such as copper, followed by a second leach using a 3 M H_2SO_4 and 3 M NaBr system at 70 °C to solubilize the gold present in the residue. Recovery of gold from e-waste containing high copper content was carried out by applying chemical pretreatment first with inorganic acids (HCl, HNO_3 and H_2SO_4), organic substances (EDTA and citrate) and oxidants (air, ozone and hydrogen peroxide) resulting in more than 90 % of copper extracted when using peroxide and HCl or citrate [45]. In the second step, thiourea was used resulting in more than 90 % of the gold recovering after 1 h [45]. Table 1 shows a review of leaching processes of e-waste with the use of cyanide as well as other leaching agents considered as "green".

Table 1 shows hydrometallurgical processes carried out under alkaline and acid conditions. In the former case, leaching media such as cyanide, glycine, sodium, and ammonium thiosulfate are used. Glycine has been successfully employed for copper extraction under alkaline conditions; however, efficient leaching requires proper sample preparation. Since copper and other metals may remain trapped within solder joints and composite layers, Huan et al. [46] recommend a preliminary pretreatment step to expose the metallic fractions typically involving mechanical liberation and, when necessary, selective dissolution of solder using nitric acid prior to conducting glycine-based leaching [46]. On the other hand, in alkaline conditions glycinate ion ($H_2NCH_2COO^-$) is found in solutions, which can form complexes with cuprous (Cu^+) and cupric (Cu^{2+}) ions when in the presence of an oxidant such as ambient O_2 at room temperature. However, base metals such as Ni, Al, Sn, Zn, and Co are extracted simultaneously with their extraction favoured under alkaline conditions. In the case of gold and silver, their extraction does not exceed 2 %, as it requires a catalyst such as cyanide, which could be mixed with glycine in minimum permissible proportions for recovery. This step should occur recovering copper and other base metals since these metals interact with cyanide.

On the other hand, acid leaching in the presence of an oxidant such as H_2O_2 has been used for leaching copper, gold, and silver. Petter *et al.* [47] determined that nitric acid can dissolve up to 100 % of silver contained in PCB residues, while using aqua regia 882 g t^{-1} of gold and 417.9 kg t^{-1} of copper were achieved. However, in the case of silver, low recovery was obtained since it tends to form insoluble AgCl. Even though acid solutions offer good results in the extraction of metals such as copper, gold and silver, these leaching agents have some disadvantages such as high cost and high toxicity to the environment and health.

Table 1. Electronic waste leaching processes using cyanide and alternative leaching methods for PCBs treatment

Leaching medium	Preparation of sample	Conditions of leaching	Metal recovery (%)	Ref.
Glycine	Pulverized feed	0.5 M glycine pH 10, *t* = 72 h, particle size= <2 mm	• Au = 2 • Ag = 2; Pb = 16 • Cu = 96.5; Al = 12.6 • Ni = 9.3; Zn = 92.5 • Co = 3.1	[46]
Sodium ammonium thiosulfate	Particle size less than 1 mm obtained in a blade mill	8 M HNO_3, 0.1 M $Na_2S_2O_3$ and 0.1 M $(NH_4)_2S_2O_3$, pH 9.5 to 11 solid/liquid ratio = 1:20	• HNO_3- Ag = 100 • $Na_2S_2O_3$ and $(NH_4)_2S_2O_3$- Au = 15	[47]
Sodium ammonium thiosulfate and cyanide based pickling solution	Intact PCBs were used	0.12 M $Na_2S_2O_3$, 0.12 M $(NH_4)_2S_2O_3$ *t* = 4 and 24 h, *T* = 30 °C, pH 10	• Cyanide base pickling solution - Au = 88 • $(NH_4)_2S_2O_3$- Au = 75	[48]
Sodium thiosulfate	Crushed and toasted material at 800 °C	4 M HNO_3, 0.7 M $Na_2S_2O_3$ pH 10.5, shake for 6 h, *T* = 25 °C	• Au = 81 • Ag = 88 • Cu = 32	[49]
Thiosemicarbazide	Intact PCBs were used	2 M NaOH, 0.5 M CH_5N_3S, pH 11.5, *T* = 55 °C, stirring rate 1000 rpm, *t* = 220 min	• Au = 95.8 • Ag = 60 • Cu = 77.7	[50]
Sodium thiosulfate	Intact PCBs were used	2 M NaOH, 0.5 M $Na_2S_2O_3$, pH 12, *T* = 50 °C, stirring rate 900 rpm, *t* = 180 min	• Cu = 99.82	[51]
Sulfuric acid and hydrogen peroxide	PCBs milled	2 M H_2SO_4, 0.2 M H_2O_2, *t* = 150 min, stirring rate 200 rpm, *T* = 25 °C	• Cu = 100	[35]
Cyanide solution for characterization and sodium ammonium thiosulfate	Intact PCBs were used	0.1 M $(NH_4)_2S_2O_3$, 0.2 M NH_4OH, 0.1 M H_2O_2	• Commercial cyanide: 86.23 g ton^{-1} Au • $(NH_4)_2S_2O_3$: Au = 11 %	[52]
Thiourea	PCBs <106 mm	0.1 M H_2SO_4 , 0.25 M CH_4N_2S	• Au = 17.3; Ag = 49.5	[53]
Thiourea	SH SIZE	24 g L^{-1} CH_4N_2S, 0.6 % Fe^{3+} *T* = ambient, *t* = 2 h	• Au = 90 • Ag = 50	[54]
Iodine-iodide	PCBs incinerated at 800 °C	Iodine-iodid mass ratio = 1:6, stirring speed 500 rpm, *T* = 40 °C, *t* = 24 h	• Au = 99 • Ag = 1 • Pd = 1	[55]
Iodine-iodide	Particle size less than 0.75 mm	8 mmol L^{-1} I_2, 70 mmol L^{-1} KI 30 mmol L^{-1} H_2O_2	• Au = 31.5	[56]

Batnasan *et al.* [55], used 1 mol L^{-1} thiourea and 0.25 mol L^{-1} H_2SO_4 at an acidic pH, achieving 17.3 % and 49.5 % Au and Ag dissolution, respectively. These authors found that a high redox potential and acidity of the solution increase leaching of Au and Pd, while decrease Ag leaching. Jing *et al.* [54], determined that a gold and silver leaching process by thiourea can be optimized by decreasing the particle size, due to the increased specific surface area. Extraction of 90 % gold and 50 % silver from PCB samples was achieved using the following conditions: 24 g L^{-1} solution of thiourea and Fe^{3+} at room temperature and 100 mesh particle size. Still, the authors mention that the thiourea process is expensive compared to conventional processes such as cyanidation. On the other hand, the iodine-iodide system at acidic pH has been used for the recovery of precious metals; it is worth mentioning that this system is selective towards gold [55].

In one study, the use of sodium and ammonium thiosulfate did not result in positive results reaching a maximum gold extraction of 15 %, and it was concluded that more than one leaching agent is needed to extract all the metals from PCBs [47]. Still, in another treatment process of intact PCBs also by using sodium and ammonium thiosulfate 70 and 75 % of gold was extracted, respectively, which was attributed to the size of the PCB samples since, according to this research, the use of intact PCB samples inhibits dissolution of base metals, whose release is favoured by grinding and once in solution they compete for the leaching reagent with gold [48].

On the other hand, Gámez *et al.* [52], found that dissolving copper with nitric acid before carrying out leaching with thiosulfate improved the recovery of gold and silver, reaching extraction efficiencies of 81 and 88 % respectively. The addition of H_2O_2 to the thiosulfate system a slight increase in the extraction of gold and silver. When base metals are completely separated, gold recovery is greatly improved, which can be also achieved by cyanide. According to Birich *et al.* [56], thiosulfate and thiourea are less sensitive to metallic impurities than other leaching agents; however, when these impurities are removed from PCBs, gold recovery improves. Based on the above, it could be concluded that while leaching PCB samples at acidic pH yields good results, it also presents the drawback of high reagent costs and toxicity. Conversely, glycine is an alternative that offers advantages such as low cost and environmental friendliness Additionally, it can be used in two stages: first, to eliminate base metals and second, to add a small amount of cyanide as a catalyst to extract metals such as gold and silver.

Recovery of metals from the solutions generated from leaching processes can be carried out by different methods, such as solvent extraction, ion exchange, adsorption, precipitation and cementation. Choice of the method depends on properties of the e-waste and the solution originating from leaching [4,18]. Examples of some metal recovery processes from e-waste leach solutions are shown in Table 2.

Table 2. Alternative metal recovery processes from e-waste leach solutions

Treated sample	Recovery method	Conditions	Recovery, %	Ref.
Thiosulfate leach solution	Solvent extraction (SX) and electrowinning (EW)	LIX984 N with kerosene for copper	SX - Cu=92 EW - Cu=99 EW - Au=87	[57]
3 M nitric acid solution used for Cu and 3 mol L^{-1} H_2SO_4 and Sodium Bromide solution used for Au.	Solvent extraction	ACORGA M5640 dissolved in kerosene and Tertiary amide extractant 0.1 mol L^{-1} dissolved in toluene.	Cu = 99 Au = 99.9	[58]
Solution containing Cu^{2+}, Zn^{2+}, Ni^{2+}, Pb^{2+} and Al^{3+} ions	Multi-element ion exchange	Three resins were used: Amberlite IRA 743, Lewatit TP 208 and Lewatit TP 260 at a dose of 90-100 g L^{-1}	Cu = 90	[59]
Mixture of chlorate and chitosan in HCl	Adsorption	Chitosan granules cross-linked with glutaraldehyde (GCC) were used as adsorbent at a dose of 1 g L^{-1}.	Au = 100	[60]
Leaching solution with hydrophilic quaternary salts from a CPU	Precipitation	Tetrabutylammonium based salts were added	Au = 91.4	[61]
16 % HCl leach solution	Cementation	Iron powder of commercial grade was used for precipitating Cu, at a stoichiometric ratio of 1:1	Cu = 85	[62]

Murali *et al.* [57] used the extractant LIX984 N with kerosene and found that pH and temperature are two parameters that significantly influence solvent extraction of copper. An increase in pH can enhance formation of complexes with the extractant, so that carrying out the process at pH below 2 was recommend, to avoid the risk of coprecipitation of other metals. Regarding the temperature, room temperature was recommended, since a decrease in copper extraction from 94 to 87 % was noted as temperature was increased from 30 to 45 °C. Similarly, extraction of copper and gold with the ACORGA M560 reagent in kerosene was found to be the best at pH in the range 1 to 2.5 [58], and by using the extractant in a ratio of 1:1, pH 2 and 4 mol L^{-1} H_2SO_4 as the extraction agent, 99.9 % of copper was recovered. As for gold, the use of a secondary amide enabled 99 % recovery.

Nekouei *et al.* [59], proposed sorption as another option for the recovery of metal ions from leaching solutions, being efficient and easy to operate. In this process a porous resin is commonly used as an ion exchanger. Cementation was proposed as an efficient method for copper recovery, reaching 90 % cemented with iron, while also recovering Al (5.8 %), Co (0.8 %) and Ni (1.5 %) [62]. Then, other authors have proposed a precipitation method as an effective and economical option for the recovery of metals, providing separation by stages [62].

According to Hsu *et al.* [12], successive electrowinning of multiple metals, particularly with Cu and Ni, and Cu and Au, in sulfuric acid and aqua regia baths, presents a promising option for combining individual electrowinning steps; this process takes advantage of the differences in electrode potentials of different metals.

The mentioned recovery techniques are effective; however, each has its advantages and limitations. In the case of the solvent extraction technique, a disadvantage is the need for the use of a wide variety of additives, while in

cementation these are the high consumption of reagents and occurrence of coprecipitation of base metals. During the ionic exchange the need for regeneration of the adsorbents presents a drawback while although electrowinning provides metals of high purity, but at high energy consumption.

3. PATENTS AND INDUSTRIAL PROCESSES

Urban mining has recently gained significant relevance because it offers commercial, economic, social, and environmental opportunities. For this reason, many developed countries already have e-waste management technologies, know-how and systems in place [63]. Nevertheless, some developed countries export this waste to developing countries [64]. Arya and Kumar [63] highlight that India still lacks adequate waste management services, consisting mainly of collection, which hampers the implementation of industrial processes for waste treatment as accurate estimation of electronic waste generation is essential. In contrast, they note that the electronic waste management model in China is regarded as one of the preferred methodologies, involving collection, recycling, and value recovery [63].

As mentioned above, millions of tons of e-waste are generated annually, making recycling crucial for environmental protection. Current industrial processes for treating these materials include dismantling and granulation to particles in the range 0.17 mm to 5 cm, used for plastics and non-ferrous materials recovery. Additionally, industrial scale circuit board recycling machines utilize drum-type screwdrivers to separate metals such as copper from other components [65]. Table 3 presents focused on e-waste recycling.

Table 3. Examples of recovery of metals and other valuable materials from electronic waste

Overview	Items recovered	Types of e-waste	Recovery method	Ref.
It investigates the potentials and barriers for tantalum recovery from WEEE, highlighting the low current recycling rate of less than 1 % for tantalum. The study reveals challenges in accurately separating tantalum from PCBs, leading to the loss of other valuable metals like silver.	Tantalum, particularly from tantalum capacitors. Other significant materials that can be recovered include silver, manganese, silicon, aluminium, copper, iron, and nickel, with silver being noted for its surprisingly high content. The recovery processes for tantalum and silver are highlighted as essential due to their market value and scarcity.	Mobile phones, smartphones, tablets, notebooks, desktop personal computers (PCs), hard disk drives (HDDs), flat screen monitors, and servers, devices selected based on their expected high tantalum capacitor content and significant share of new electric and electronic products put on the market (POM).	Identification, liberation, separation, and concentration of tantalum capacitors from printed circuit boards. Manual removal of visually identifiable components is the primary method. Mechanical processing techniques include crushing and sieving. Acid leaching is also employed to separate tantalum from other materials.	[66]
It discusses the development of an eco-friendly and cost-effective process for recovering precious metals from electronic board waste, particularly focusing on a non-profit organization in Quebec, Canada.	The primary items recovered from electronic boards include precious metals such as gold, silver and palladium.	It discusses various types of e-waste, particularly focusing on electronic boards from telecommunications devices, computers, mobile phones, and smartphones.	The recovery methods for precious metals from electronic boards include bio metallurgy, pyrometallurgy, and hydrometallurgy, each with distinct advantages and limitations.	[67]
It focuses on the environmental and technological assessment of e-waste recycling, specifically targeting the extraction and concentration of metallic CU from PCBs. Results indicate that concentrated products contain approximately 78 % Cu.	Copper, which constitutes approximately 10 to 20 % of the PCB mass. Other metals that can be recovered include iron, zinc, nickel, silver, gold, and manganese, as indicated in the analysis of the concentrated class.	PCBs can contain approximately 28 metals, including copper, gold, and palladium, along with 23 polymers and ceramic materials. Other components in e-waste may include toxic elements such as lead, cadmium, mercury, arsenic, and chromium.	Dismantling, comminating, particle size classification, magnetic separation, and electrostatic separation. Initially, the pre-treatment aims to release metals, primarily copper, which is crucial for subsequent metallurgical processes.	[68]
It discusses the recovery of rare-earth elements from phosphor powder in spent fluorescent lamps as a critical step towards a bio-based economy. It emphasizes the importance of urban mining and bio-based technologies in achieving sustainable development goals.	Rare-earth elements such as europium, yttrium, and terbium from phosphor powder in spent fluorescent lamps. Other metals that can be recovered from E-waste include copper, nickel, iron, aluminium, and zinc, which also have known economic value.	E-waste encompasses a variety of discarded electrical and electronic devices, including but not limited to fluorescent lamps, high-intensity discharge lamps, and LED lamps. The composition of E-waste typically includes materials such as glass, metals, plastics, and toxic compounds.	Biohydrometallurgical processes (bioleaching and biosorption). Bioleaching utilizes microorganisms to secrete acids that enhance metal solubilization, while biosorption employs biosorbents to selectively remove metals through various mechanisms.	[69]

Overview	Items recovered	Types of e-waste	Recovery method	Ref.
It presents a systematic selective disassembly approach for WEEE, focusing on maximizing disassembly profit while adhering to environmental regulations. A case study on Changhong liquid crystal display televisions demonstrates the effectiveness of the approach.	Components such as metal fixing plates, metal washers, top metal supports, toughened glass seats, steel plates, rubber gaskets, control buttons, power switches, loudspeakers, control receiver boards, power supply boards, main boards, metal boards, surface frames, LCD screens, and cover plates.	E-waste can be categorized into five end-of-life types: reuse; repair; remanufacture; recycling; and disposal.	The recovery method discussed in the research paper focuses on a systematic selective disassembly approach for WEEE, particularly targeting components with recycling potential.	[70]
It examines the impact of eco-design measures on the recycling of plastics from WEEE in the EU. It identifies that while some measures, like improved disassembly, are beneficial, others, such as polymer marking, are underutilized and ineffective.	The contexts do not provide specific information regarding the items or types of metals recovered from e-waste recycling.	Encompasses a variety of discarded electrical and electronic devices, including but not limited to computers, televisions, mobile phones, and household appliances such as vacuum cleaners and coffee machines.	Manual dismantling and automated separation techniques. Froth flotation is a complex separation process that utilizes the hydrophobic properties of polymers. Electrical conductivity properties are leveraged to separate clean and dry plastics. The sink-float method is commonly used for sorting polymers due to its low cost.	[71]
It focuses on substance flow analysis (SFA) to quantify and characterize the flows of precious metals (silver, gold, palladium) during the preprocessing of WEEE. It highlights that despite high recovery rates for mass-relevant elements, only a quarter of gold and palladium is recoverable post-processing.	Precious metals such as silver, gold, and palladium. The recovery rates for these precious metals are notably low, with only 11.5 % of silver, 25.6 % of gold, and 25.6% of palladium reaching output fractions from which they may potentially be recovered. In addition to precious metals, mass-relevant materials such as copper and iron are also recovered, with recovery rates of 60 % for copper and 95.6 % for iron.	WEEE, which can be categorized into several groups. Common categories include IT and telecommunications equipment, consumer electronics, and large household appliances. Specific examples of electronic waste are mobile phones, computers, televisions, and kitchen appliances.	The recovery method for precious metals from WEEE involves a preprocessing phase that concentrates valuable materials into specific output streams. State-of-the-art metallurgical processes are employed to recover precious metals during the copper recovery process, which is designed to also capture these metals.	[72]
It discusses the significant growth of the electrical and electronic equipment (EEE) market in the Gulf Cooperation Council (GCC) region, driven by the oil and gas sector, leading to increased electronic waste (e-waste) due to shorter product lifespans. It proposes industrial remanufacturing as a viable strategy for e-waste management.	The focus is primarily on the recovery of reusable components from end-of-life electronic devices, rather than metals.	E-waste primarily includes discarded industrial EEE that has reached its end-of-life stage, such as computers, printers, televisions, and mobile phones, or industrial equipment like programmable logic controllers (PLCs), drives, and controllers also contribute to e-waste generation.	The recovery methods for end-of-life electronic products include five primary strategies: repair, refurbishment, remanufacturing, cannibalization and recycling.	[73]
It addresses the economic impact of recycling car electronics, particularly in light of increasing waste from end-of-life vehicles (ELVs) due to new European environmenttal policies. The findings confirm profitability across all analysed scenarios, emphasizing the importance of effective waste management in the automotive sector.	It discusses the recovery of metals from electronic components in ELVs, particularly focusing on gold recovery, which plays a decisive role in the economic impact of car electronics recycling processes. Its indicates that the metals extracted during the recycling process are assumed to be 95 % pure.	E-waste includes various types of WEEE of vehicle industry, with waste printed circuit boards (WPCBs) being a significant component.	Hydrometallurgy. This method involves extracting desired metals from metal-rich leached liquor through various techniques such as electrorefining, precipitation, cementation, absorption, ion exchange, or solvent extraction. The focus is primarily on recovering valuable metals like gold and silver.	[74]

Overview	Items recovered	Types of e-waste	Recovery method	Ref.
It reviews and summarizes advanced technologies for the recycling of waste electrical and electronic components (WECs), highlighting the need for a comprehensive approach to address the economic and environmental challenges associated with WEC recycling. It discusses various physical recovery methods, leaching systems, and their advantages and disadvantages, emphasizing the importance of efficiency and environmental safety.	Copper was recovered with rates of 98.21 and 99.16 %, with a purity of 92.75 % from various waste materials. Gold recovery rates were reported, although they were still quite low. Silver was recovered with a rate of 93 % from leach liquor using cementation with copper and zinc. A selective recovery of 99.94 % of silver was achieved using KCl from nitric acid leaching solution.	E-waste primarily includes WPCB and waste electronic components (WECs). E-waste encompasses various devices such as computers, mobile phones, digital cameras, and other electronic equipment that have reached the end of their life cycle. Specific components within e-waste include central processing units (CPUs), random access memory (RAM), tantalum capacitors (TCs), and aluminium electrolytic capacitors (AECs).	Disassembly, physical separation, and various metallurgical processes. Disassembly is the initial step, followed by classification of components for reuse or recycling. Physical methods such as crushing, sieving, and magnetic separation are employed to separate metals from non-metals. Pyrometallurgical processes, including smelting and refining, are widely used for metal recovery, while hydrometallurgical methods involve chemical leaching and bioleaching for selective recovery of metals from leachates.	[75]

Recycling e-waste is a critical environmental and economic challenge due to the rapid growth of discarded electronic devices. The papers provided in Table 3 explore various aspects of e-waste recycling, including methodologies, environmental impacts, and the role of remanufacturing in promoting a circular economy.

Recycling processes often include novel mechanical and physical processing, pyrometallurgical and hydrometallurgical methods, and biohydrometallurgical innovations. E-waste recycling often begins with mechanical processes such as dismantling, grinding, and separation based on different density and magnetic properties, processes that are crucial for preparing materials for further metallurgical recovery and enhancing the efficiency of subsequent extraction methods [68]. Then, pyrometallurgical or hydrometallurgical methods may be used offering advantages and weaknesses as discussed in the previous section [75]. And finally, emerging biohydrometallurgical techniques utilize activity of microorganisms to recover metals, presenting a more sustainable alternative to traditional methods [69]. These processes are gaining attention for their potential to reduce environmental impacts and improve resource recovery from complex e-waste streams.

In the estimation of environmental and economic impacts, life cycle analysis (LCA) is used to evaluate the environmental performance of e-waste recycling processes, highlighting the significant impacts of crushing and screening activities. LCA helps identifying opportunities for reducing carbon emissions and improving sustainability of recycling operations [64]. Efficient recycling can reduce the need for virgin material extraction, contributing to economic sustainability and resource conservation [75].

Remanufacturing extends the life of electronic products by restoring them to a near-original state, which reduces waste and conserves resources. Additionally, as a cost-effective strategy it supports the circular economy by promoting the reuse of materials and minimizing the environmental impact of new production [73]. Recycling of e-waste is a multifaceted challenge that requires a combination of mechanical, chemical, and biological processes to maximize the resource recovery and minimize environmental impacts. Advancements in biohydrometallurgical methods and integration of remanufacturing into the circular economy offer promising pathways for sustainable e-waste management.

On the other hand, extraction of metals from electronic waste can be dangerous [76] and industrial operations require the use of personal protective equipment as well as dust collector systems to minimize the presence of dust in air, since e-waste recycling may expose workers to toxic metals. In a study carried out by Gravel *et al.* [77], six electronic and commercial recycling facilities were investigated in which metal exposure was measured, and the presence of metals such as lead, beryllium, mercury, arsenic, barium, cadmium and chromium was found in the blood of the workers, as well as in the dust present in the air. It is worth mentioning that in this place the dust control was inadequate and personal protective equipment was not used.

Many business models for treating e-waste involve industries operating as isolated systems disconnected from other production chains. Marconi *et al.* [78] argue that this isolation leads to the loss of consistent residual economic value and they propose implementing an industrial symbiosis system as a solution. Zeng *et al.* [79] describes an eco-industrial park as the practical application of supply chain management at the industrial park level. Park *et al.* [80] reviewed the first phase of South Korea's National Ecological Program, which aimed to develop an industrial park, with achieving

industrial symbiosis. The main focus was to bring together interested parties from companies, governments and research centres to facilitate industrial symbiosis projects. These efforts yielded significant environmental benefits, including reduction in greenhouse gases that achieved 51 % of the program's target.

Recycling industries are looking for alternatives to reduce the environmental impact and establish a successful business model, including several companies dedicated to the field of e-waste recovery by different methods. Today the academic and industrial sectors have combined theoretical and practical knowledge to provide practical solutions for society, resulting in scientific publications and registered patents, allowing in the long-term circular waste management [81]. Table 4 shows some of the recent patents that have been implemented in e-waste treatments.

Table 4. Recent patents related e-waste recycling

Patent number	Patent title	Invention	State	Country	Date	Ref.
MX 391678 B	Gold and copper recovery method from PCBs with an ionic solution	Ionic solution with low environmental and energy impact, made with leaching organic salts	Granted	Mexico	April 2022	[82]
MX/a/2018/006178	Process for the recovery of non-ferrous metals obtained from electronic scrap through physical-mechanical refining	Mechanical physical refining of a production line using mechanical and wind equipment	Applied	Mexico	Novembe r 2019	[83]
CN113732005A	Cleaning treatment method to efficiently recycle useful substances in electronic waste	Cleaning treatment to efficiently recycle useful substances, does not generate secondary pollution	Granted	China	December 2021	[84]
CN106520152A	Recovery processing of electronic waste by pyrolysis	Metal recovery system and an organic matter reaction system, by high efficiency pyrolysis method and notable energy savings	Granted	China	March 2017	[85]
US202217583385A	Simplified method of recovering gold from e-waste	2-step method, the first one uses a combination of acid weak with oxidant and the second solvents, water and wetting agent/surfactant	Granted	USA	July 2022	[86]
CN110639438A	Preparation for hollow polyaniline microspheres, method for recovering precious metals in electronic waste and method of recycling the recovery product	polyaniline hollow microspheres can efficiently recover materials	Granted	Canada	January 2022	[87]
US11608544B2	Recovery process from electronic waste	Use of biohydrometallurgical techniques; microorganisms	Granted	USA	March 2023	[88]
US11608544B2	Recovery process from e- waste	Use of biohydrometallurgical techniques; microorganisms	Granted	USA	March 2023	[89]
WO2023087114A1	A process to recover a metallic fraction of electronic waste and produce value-added products	Al, Zn, Ni, Cu, Au, Ag, Pt and Pd recovery, pyrolysis oil and added value to produce a conditioned material	Granted	Canada	May-23	[90]
CN110983031A	Comprehensive method of separation and recovery of electronic waste	Two leaching are carried out and subsequent solid- liquid separation and a second leaching, screening, screening, recovery of noble and basic metals	Granted	China	April 2020	[91]

In the invention of Alarcón *et al.* [82] an ionic solution is described comprising inorganic salts to recover gold and copper from e-waste PCBs with low environmental and energy impact. This method produces an Au/Cu precipitate obtained and offers an innovative alternative to traditional recovery processes, generating fewer toxic residues.

Berrueta *et al.* [83], focused on obtaining non-ferrous metals from electronic scrap by a four-stage physical-mechanical refining process. They formed a production line which uses different mechanical and wind equipment and includes: (1) reduction, pre-cleaning and cleaning of light contaminants, (2) elimination of heavier materials such as ferrous and other contaminants, (3) drying and a size homogenization, and (4) final cleaning and classification.

A clean treatment method is patented [84] aiming to efficiently recycle beneficial substances in WEEE, with saving resources at the same time without generating secondary pollution. A completely new treatment technology and a completely new processing device are described, which can almost completely recycle all useful substances in e-waste

except filters, without producing secondary pollution. It not only solves the environmental pollution caused by traditional e-waste processing technology but also recycles various resources into electrons as much as possible.

Minjie *et al.* [85] developed a pyrolysis-based system for treating WEEE, which includes material treatment, metal recovery, and organic matter reactions. The process uses grinding and classifying equipment, acid leaching and electrolytic tanks, and an electronic waste pyrolysis reactor, with heating and separation systems. This integrated approach aims to recover metals, process non-metallic components, and maximize resource utilization from e-waste. This integrated approach aims to recover metals, process non-metallic parts, and maximize resource utilization from e-waste.

The invention of Lynn *et al.* [86] describes a two-step method for recovering gold from e-waste. In the first step a solution containing a weak acid in combination with an oxidant is used followed by the second step in which the delaminated gold from chip debris is isolated and purified by using solvents, water, and a wetting agent/surfactant shown to be effective without the need for leaching or the use of harsh or expensive chemicals.

Bin *et al.* [87] developed a method for preparing hollow polyaniline microspheres for efficient recovery of precious metals from e-waste without additional energy use. The polyaniline/precious metal nanocomposites obtained during the recovery process can be used as new electroactive materials to prepare electronic devices, promoting sustainable recycling.

Reece *et al.* [88] introduced bio-metallurgical techniques for recovering precious metals from WEEE. The process begins with removing at least a portion of non-target materials from e-waste or grinding it to the desired particle size. The pre-processed e-waste is then treated with a leach solution to dissolve at least a portion of the target metal. Next, microorganisms are added to adsorb the dissolved metal ions, resulting in metal-laden microorganisms. These microorganisms are subsequently separated from the solution, and the target metal(s) are recovered from the microorganisms.

Marlin *et al.* [89] developed a method for obtaining metals from group 8 to 14, raw copper, from WEEE. The process involves melting a mixed feed comprising WEEE in a smelting reactor to form separate metallic and slag phases. In the next step, the slag is removed, and the remaining first metallic phase is refined with an oxygen-containing gas, producing a second copper-enriched slag phase. This slag can be separated and the refining step repeated, if needed. The first refined metal phase is collected from the smelter reactor, and additional e-waste can be added to the copper-enriched slag to continue the recovery process.

The invention Mohamed *et al.* [90] includes recovering organic and metallic fractions of e-waste by conditioning the e-waste followed by pyrolysis resulting in gaseous and solid phases, wherein the latter comprises an organic and a metal fraction. The recovery further includes separating the metal fraction to recover at least one of the metals Al, Zn, Ni, Cu, Au, Ag, Pt and Pd. In the described process at least 95 wt.% of the e-waste can be recovered in the form of recovered metals, pyrolysis oil and value-added products.

Finally, the invention of Xiaohui *et al.* [91] provides an integrated method for separating and recovering materials from WEEE. The process involves mixing e-waste particles with acid liquor, low-temperature roasting, and performing sequential leaching and solid-liquid separations to obtain different components. If e-waste contains noble metals, HCl/Cl is used for the first leaching process. Depending on the presence of precious metals, specific leaching agents are used to recover noble and base metals. The remaining residues are screened to separate glass fibres and polymer roasting products. Thus, by this method precious metals, base metals, glass fibres, and polymer roasting products are separated, achieving comprehensive separation and recovery of e-waste.

4. FUTURE OF E-WASTE RECYCLING

The future of e-waste recycling is principally determined by technological advances, policy frameworks, and sustainable practices aimed at mitigating environmental impacts and maximizing resource recovery. With e-waste continuing to grow, fed by the demand for rapid technological change and consumerism, creative solutions are being developed worldwide to face the challenges that arise with e-waste management. These solutions encompass a variety of strategies, from improving recycling technologies to implementing comprehensive policy measures.

From the technological point of view, the future of e-waste management will likely focus on modular and upgradeable electronic devices, since they generate less waste, have a prolonged product life and are easier to repair and recycle [92]. Other recycling technologies, involving hydrometallurgical and biometallurgical processes, are also under

scrutiny for applications in the recovery of valuable materials from e-waste. All these techniques are forecasted to be greener, more economically feasible, and to include several recycling technologies that ensure better performances [93,94]. In addition, AI and internet of things (IoT) technologies create new promising opportunities not only for automation in e-waste sorting and categorization but also for optimization of recycling processes and tracking/monitoring of e-waste flows along the value chain [92].

The implementation of extended producer responsibility (EPR) frameworks will be a fundamental aspect of future e-waste management from a regulatory and policy perspective. This includes designing devices for easy disassembly and recycling and creating efficient collection networks [92]. Then again, formal e-waste recycling, in line with circular economic principles, reduces much of the generated waste to a minimum while recovering resources maximally. Meanwhile, LCA tools increasingly have been applied for carrying out environmental performance evaluation of various approaches for dealing with e-waste management. This will result in significantly more environmentally friendly practices than those used today [95]. Public education and awareness play a crucial role in fostering sustainability. By increasing education on responsible consumption and proper recycling practices, a culture of sustainability can be cultivated. This involves promoting the longer use of devices and encouraging recycling [88]. In developing countries, integrating informal recycling sectors into structured management programs can improve the efficiency of e-waste recycling and reduce the environmental and health risks associated with informal practices [96].

The global electronics recycling market is expected to increase noticeably, reaching $65.8 billion by the year 2026. This, in turn, creates different opportunities for entrepreneurship and economic development regarding e-waste recycling industry [96]. However, despite all the advantages, WEEE management in developing countries seriously suffers because of poor infrastructure, lack of appropriate collection systems, and low level of awareness of the public. Solving these problems is very significant for effective recycling of WEEE [97]. Hydrometallurgical processes are an excellent option for recovering metals from e-waste, offering advantages such as higher selectivity and lower energy consumption compared to pyrometallurgical methods. However, they can also generate significant environmental impacts, mainly due to the production of liquid effluents containing dissolved metals, toxic compounds, and acidic residues. To prevent, reduce, or eliminate these impacts, specific measures should be implemented, including the use of less toxic leaching agents, the recirculation of solutions within closed-loop systems, the application of advanced wastewater treatment technologies, and the integration of tools like life cycle assessment and real-time monitoring. These strategies would help optimize the process and promote a safer and more sustainable approach to hydrometallurgy.

While the prospect for e-waste recycling is highly promising, several challenges continue to persist. Specifically, informal recycling activities, especially in developing countries, pose serious environmental and health hazards due to improper handling and disposal. Apart from this, the problem of e-waste materials' complexity and the demands on advanced recycling technologies have not yet been overcome. However, this can be elaborated by an integrated approach: one holistic method which embeds technological innovations, policy measures, and sustainable practices in the development of a more sustainable future for e-waste management.

CONCLUSIONS

From a circular economy and environmental sustainability perspective, the identification of alternative applications for waste materials has become a critical driver influencing social, economic, and ecological systems. The rapid growth of the global population and technological advancement have led to an exponential increase in the use of electronic devices, consequently generating large volumes of e-waste. This waste stream contains both hazardous substances and valuable metals such as copper, gold, and silver, whose recovery is essential for resource conservation and pollution prevention.

Various technologies have been developed to recover metals from e-waste, including pyrometallurgical, hydro-metallurgical, and bio-hydrometallurgical processes. Pyrometallurgical methods are effective in recovering metals rapidly and at high throughput but are energy-intensive and generate toxic emissions. Hydrometallurgical processes offer greater selectivity, operate at lower temperatures, and are more suitable for decentralized applications; however, they often involve corrosive leaching agents and produce liquid effluents that require advanced treatment. Bio-hydrometallurgical methods represent an environmentally friendly alternative using microbial activity to solubilize

metals, yet they are limited by slower reaction kinetics and challenges in industrial scalability. Therefore, the selection of a recovery route must balance technical, environmental, and economic criteria.

In this work, an overview of leaching agents used in hydrometallurgical processes was presented, emphasizing the need to optimize these systems through the development of eco-friendly reagents and scalable designs. Future e-waste recycling strategies will depend on technological innovation, robust regulatory frameworks, and the integration of sustainable practices. Advances in artificial intelligence (AI) and the internet of things (IoT) hold promise for improving traceability and automation in e-waste processing. Likewise, policy mechanisms such as extended producer responsibility (EPR), supported by public awareness campaigns, will play a vital role in formalizing the recycling sector. Although the global market for e-waste recovery is projected to expand, significant barriers remain, particularly in developing regions where infrastructure is limited and informal practices persist. An integrated approach that combines technological, environmental, and policy-based solutions will be essential to advancing the efficiency and sustainability of e-waste recycling systems.

*Declaration of interest statement***:** The authors declare they have no conflict of interest.

Acknowledgements: The authors appreciate the support provided by the UAdeC and the Tec NM. Manuel Saldana acknowledges the infrastructure and support from Doctorado en Ingeniería de Procesos de Minerales at the Universidad de Antofagasta.

REFERENCES

[1] Pinna EG, Sebastián Drajlin D, Toro N, Rodriguez MH. Kinetic modeling of the leaching of $LiCoO_2$ with phosphoric acid. *J Mater Res Technol.* 2020; 9(6): 14017-14028. https://doi.org/10.1016/J.JMRT.2020.09.109

[2] Toro Villarroel NR, Torres Albornoz DA. *La fuerza del litio*. Santiago de Chile: Memoria Creativa; 2023. https://doi.org/10.61303/978-956-416-471-7

[3] Chen J-J, Gamiño Arroyo Z, Recovery of copper from printed circuit and electronic waste. *Jóvenes Cienc.* 2017; 3(2); 2412-2416. https://www.jovenesenlaciencia.ugto.mx/index.php/jovenesenlaciencia/article/view/1997

[4] Cui J, Zhang L, Metallurgical recovery of metals from electronic waste. *J Hazard Mater.* 2008; 158(2-3): 228-256. https://doi.org/10.1016/j.jhazmat.2008.02.001

[5] Akcil A, Erust C, Sekhar C, Ozgun M, Sahin M, Tuncuk A, Precious metal recovery from waste printed circuit boards using cyanide and non-cyanide lixiviants. *Waste Manag.* 2015; 45: 258-271. https://doi.org/10.1016/j.wasman.2015.01.017

[6] Araiza JA, Escobar K, Nájara JA, Diagnóstico de generación y manejo de los residuos eléctricos y electrónicos en instituciones educativas: un caso de estudio. *Ing Rev Acad Fac Ing UADY.* 2016; 20: 115-126. https://www.revista.ingenieria.uady.mx/ojs/index.php/ingenieria/article/view/34 (in Spanish)

[7] Forti V, Balde CP, Kuehr R, Bel G, The global E-waste monitor 2020: Quantities, flows and the circular economy potential. Bonn, Geneva and Rotterdam: United Nations University/United Nations Institute for Training and Research, International Telecommunication Union, and International Solid Waste Association. https://ewastemonitor.info/wp-content/uploads/2020/11/GEM_2020_def_july1_low.pdf Accessed October 23, 2024.

[8] Dehchenari M, Hosseinpoor S, Aali R, Salighehdar N, Mehdipour M, Simple method for extracting gold from electrical and electronic wastes using hydrometallurgical process. *Environ Health Eng Manag J.* 2017; 4(1): 55-58. http://dx.doi.org/10.15171/EHEM.2017.08

[9] Krishnan S, Syahidah N, Kamyab H, Mat S, Fadhil M, Abd Z, Chaiprapat S, Kenzo I, Ichikawa Y, Nasrullah M, Chelliapan S, Othman N, Current technologies for recovery of metals from industrial wastes: An overview. *Environ Technol Innov.* 2021; 22: 101525. https://doi.org/10.1016/j.eti.2021.101525

[10] Yao Z, Xu Z, Shuai Q, Chen X, Jiang Z, Peng X, Li H, Solidification of municipal solid waste incineration fly ash through co-mechanical treatment with circulation fluidized bed combustion fly ash. *Materials*. 2020; 13(1): 141. https://doi.org/10.3390/ma13010141

[11] Li H, Oraby E, Eksteen J, Cyanide consumption minimisation and concomitant toxic effluent minimisation during precious metals extraction from waste printed circuit boards. *Waste Manag.* 2021; 125: 87-97. https://doi.org/10.1016/j.wasman.2021.02.033

[12] Hsu E, Barmak K, West A, Hyung A, Park A, Advancements in the Treatment and Processing of Electronic Waste with Sustainability: A Review of Metal Extraction and Recovery Technologies. *Green Chem.* 2019; 21: 919-936. https://doi.org/10.1039/C8GC03688H

[13] Pinillo GA. Lixiviación de cobre contenido en tarjetas de computador PCB para la extracción de metales preciosos. *Rev Ing Investig Desarr.* 2018; 18(2): 15-21. https://doi.org/10.19053/1900771X.v18.n2.2018.11873 (in Spanish)

[14] Barragan J, Alemán J, Peregrina A, Amaya M, Rivero E, Larios E. Leaching of Metals from e Waste: From Its Thermodynamic Analysis and Design to Its Implementation and Optimization. *ACS.* 2021; 6(18): 12063-12071. https://doi.org/10.1021/acsomega.1c00724

[15] Chatterjee S. Sustainable Electronic Waste Management and Recycling Process. *Am J Environ Eng.* 2012; 2(1): 23-33. http://dx.doi.org/10.5923/j.ajee.20120201.05

[16] Lee H, Molstad E, Brajendra M, Recovery of Gold and Silver from Secondary Sources of Electronic Waste Processing by Thiourea Leaching. *J Miner Metals Mater Soc.* 2018; 70: 1616-1621. https://doi.org/10.1007/s11837-018-2965-2

[17] Tuncuk A, Akcil A, Yazici E, Deveci H, Aqueous metal recovery techniques from e-scrap: Hydrometallurgy in recycling. *Miner Eng.* 2012; 25(1): 28-37. https://doi.org/10.1016/j.mineng.2011.09.019

[18] Ashiq A, Kulkarni J, Vithanage M, *Hydrometallurgical recovery of metals from e-waste* in: Vara M, Vithanage M, eds. *Electronic Waste Management and Treatment Technology*, Elsevier Inc.; 2019: 225-246. https://doi.org/10.1016/B978-0-12-816190-6.00010-8

[19] Leiva-Guajardo SI, Toro N, Fuentealba E, Morel MJ, Soliz A, Portillo C, Galleguillos Madrid, FM, Contribution of Copper Slag to Water Treatment and Hydrogen Production by Photocatalytic Mechanisms in Aqueous Solutions: A Mini Review. *Materials* (Basel) 2024; 17(22): 5434. https://doi.org/10.3390/MA17225434

[20] Tamayo-Soriano DA, Soria-Aguilar M de J, Picazo-Rodríguez NG, Almaguer-Guzman I, Chaidez-Felix J, Carrillo-Pedroza FR, Acid Leaching of La and Ce from Ferrocarbonatite-Related REE Ores. *Minerals* 2024; 14(5): 504. https://doi.org/10.3390/MIN14050504

[21] Najera Ibarra JM, Soria-Aguilar M de J, Martínez-Luevanos A, Picazo-Rodriguez NG, Martínez-Luévanos A, Carrillo-Pedroza FR, Figueroa-López U, Valenzuela García JL, Zinc Extraction from Primary Lead Smelting Slags by Oxidant Alkaline Leaching. *Processes* 2024; 12(7): 1409. https://doi.org/10.3390/PR12071409

[22] González-Ibarra AA, Nava-Alonso F, Dávila-Pulido GI, Carrillo-Pedroza FR, Rodríguez-Flores AM, Dissolution behavior of elemental tellurium and tellurium dioxide in alkaline cyanide solutions. *Hydrometallurgy* 2021; 203: 105702. https://doi.org/10.1016/J.HYDROMET.2021.105702

[23] Garza-Román MR, Carrillo-Pedroza FR, Picazo-Rodríguez NG, Soria-Aguilar M de J, Almaguer-Guzmán I, Chaidez-Félix J. Effects of pretreatment and leaching medium on the extraction efficiency of Au and Ag from a chalcopyrite leaching by-product. DYNA 2021; 88(218): 119-26. https://doi.org/10.15446/dyna.v88n218.90284

[24] Ramos-Cano J, González-Zamarripa G, Carrillo-Pedroza FR, Soria-Aguilar MDJ, Hurtado-Macías A, Cano-Vielma A, Kinetics and statistical analysis of nickel leaching from spent catalyst in nitric acid solution. *Int J Miner Process.* 2016; 148: 41-47. https://doi.org/10.1016/J.MINPRO.2016.01.006

[25] Soria-Aguilar MDJ, Davila-Pulido GI, Carrillo-Pedroza FR, Gonzalez-Ibarra AA, Picazo-Rodriguez N, de Jesus Lopez-Saucedo F, Ramos-Cano J, Oxidative Leaching of Zinc and Alkalis from Iron Blast Furnace Sludge. *Metals.* 2019; 9(9): 1015. https://doi.org/10.3390/MET9091015

[26] Cháidez J, Parga J, Valenzuela J, Carrillo R, Almaguer I, Leaching Chalcopyrite Concentrate with Oxygen and Sulfuric Acid Using a Low-Pressure Reactor. *Metals.* 2019; 9(2): 189. https://doi.org/10.3390/MET9020189

[27] Hossain R, Sahajwalla V, Current recycling innovations to utilize e-waste in sustainable green metalmanufacturing. *Phil Trans R Soc A.* 2024; 382: 20230239. https://doi.org/10.1098/rsta.2023.0239

[28] Gulliani S, Volpe M, Messineo A, Volpe R. Recovery of metals and valuable chemicals from waste electric and electronic materials: a critical review of existing technologies. *RSC Sustainability 2023*; 1: 1085-1108. https://doi.org/10.1039/d3su00034f

[29] Magoda K, Mekuto, L. Biohydrometallurgical Recovery of Metals from Waste Electronic Equipment: Current Status and Proposed Process. *Recycling.* 2022; 7: 67. https://doi.org/10.3390/recycling7050067

[30] Nagarajan N, Panchatcharam P, A Comprehensive Review on Sustainable Metal Recovery from E-Waste Based on Physiochemical and Biotechnological Methods. *Eng Sci.* 2023; 22(844): 844. https://dx.doi.org/10.30919/es8d844

[31] Mura M, Castillo I, Torres D, Galleguillos Madrid FM, Gálvez E, Gallegos S, Castillo J, Varas M, Jamett, I, Toro N, Global Overview of the Lithium Market and Opportunities for Chile. *Resources.* 2025; 14(2): 33. https://doi.org/10.3390/RESOURCES14020033

[32] Rocchetti L, Vegliò F, Kopacek B, Beolchini F, Environmental impact assessment of hydrometallurgical processes for metal recovery from WEEE residues using a portable prototype plant. *Environ Sci Technol.* 2013; 47(3): 1581-1588. https://doi.org/10.1021/es302192t

[33] Hossain MS, Ahmad Yahaya AN, Suhaila Yacob L, Zulkhairi Abdul Rahim M, Mohamad Yusof NN, Bachmann RT, Selective recovery of Copper from waste mobile phone printed circuit boards using Sulphuric acid leaching. *Mater Today Proc.* 2018; 5(10): 21698-21702. https://doi.org/10.1016/j.matpr.2018.07.021

[34] Park Y, Eom Y, Yoo K, Jha MK, Leaching of copper from waste-printed circuit boards (Pcbs) in sulfate medium using cupric ion and oxygen. *Metals (Basel).* 2021; 11(9): 1369. https://doi.org/10.3390/met11091369

[35] Dávila-Pulido GI, Salinas-Rodríguez A, Carrillo-Pedroza FR, González-Ibarra AA, Méndez-Nonell J, Garza-García M, Leaching kinetics of electronic waste for the recovery of copper: Rate-controlling step and rate process in a multisize particle system. *Int J Chem Kinet.* 2021; 53(3): 379-389. https://doi.org/10.1002/kin.21450

[36] Rajahalme J, Perämäki S, Budhathoki R, Väisänen A, Effective Recovery Process of Copper from Waste Printed Circuit Boards Utilizing Recycling of Leachate. *JOM.* 2021; 73: 980-987. https://doi.org/10.1007/s11837-020-04510-z

[37] Barragan JA, Ponce De León C, Alemán Castro JR, Peregrina-Lucano A, Gómez-Zamudio F, Larios-Durán ER, Copper and Antimony Recovery from Electronic Waste by Hydrometallurgical and Electrochemical Techniques. *ACS Omega.* 2020; 5(21): 12355-12363. https://doi.org/10.1021/acsomega.0c01100

[38] Wstawski S, Emmons-Burzyńska M, Rzelewska-Piekut M, Skrzypczak A, Regel-Rosocka M, Studies on copper(II) leaching from e-waste with hydrogen sulfate ionic liquids: Effect of hydrogen peroxide. *Hydrometallurgy.* 2021; 205: 105730. https://doi.org/10.1016/j.hydromet.2021.105730

[39] Huang J, Chen M, Chen H, Chen S, Sun Q, Leaching behavior of copper from waste printed circuit boards with Brønsted acidic ionic liquid. *Waste Manag.* 2014; 34(2): 483-488. https://doi.org/10.1016/j.wasman.2013.10.027

[40] Zhang D-J, Dong L, Li Y-T, Wu Y, Ma Y-X, Yang B, Copper leaching from waste printed circuit boards using typical acidic ionic liquids recovery of e-wastes' surplus value. *Waste Manag.* 2018; 78: 191-197. https://doi.org/10.1016/j.wasman.2018.05.036

[41] Kavousi M, Sattari A, Alamdari EK, Firozi S, Selective separation of copper over solder alloy from waste printed circuit boards leach solution. *Waste Manag.* 2017; 60: 636-642. https://doi.org/10.1016/j.wasman.2016.07.042

[42] Segura-Bailón B, Lapidus GT, Selective recovery of copper contained in waste PCBs from cellphones with impurity inhibition in the citrate-phosphate system. *Hydrometallurgy.* 2021; 203: 105699. https://doi.org/10.1016/j.hydromet.2021.105699

[43] Kim EY, Kim MS, Lee JC, Jeong J, Pandey BD, Leaching kinetics of copper from waste printed circuit boards by electro-generated chlorine in HCl solution. *Hydrometallurgy.* 2011; 107(3-4): 124-132. https://doi.org/10.1016/j.hydromet.2011.02.009

[44] Mudila R, Singh KK, Morrison C, Love J, Recycling copper and gold from e-waste by a two-stage leaching and solvent extraction process. *Sep Purif Technol.* 2021; 263: 118400. https://doi.org/10.1016/j.seppur.2021.118400

[45] Torres R, Lapidus G, Copper leaching from electronic waste for the improvement of gold recycling. *Waste Manag.* 2016; 57: 131-139. https://doi.org/10.1016/j.wasman.2016.03.010

[46] Huan L, Oraby E, Eksteen J, Extraction of copper and the co-leaching behaviour of other metals from waste printed circuit boards using alkaline glycine solutions. *Resour Conserv Recycl.* 2020; 154: 104624. https://doi.org/10.1016/j.resconrec.2019.104624

[47] Petter P, Veit H, Bernardes A, Evaluation of gold and silver leaching from printed circuit board of cellphones. *Waste Manag.* 2014; 34(2): 475-482. https://doi.org/10.1016/j.wasman.2013.10.032

[48] Kasper A, Veit H, Gold recovery from printed circuit boards of mobile phones scraps using a leaching solution alternative to cyanide. *Braz J Chem Eng.* 2018; 35(3): 931-942. https://doi.org/10.1590/0104-6632.20180353s20170291

[49] Gámez S, Garcés K, De la Torre E, Guevara A, Precious metals recovery from waste printed circuit boards using thiosulfate leaching and ion exchange resin. *Hydrometallurgy* 2019; 186: 1-11. https://doi.org/10.1016/j.hydromet.2019.03.004

[50] Cerecedo-Sáenz E, Cárdenas-Reyes EA, Rojas-Calva AH, Reyes-Valderrama MI, Rodríguez-Lugo V, Toro N, Gálvez E, Acevedo-Sandoval OA, Hernández-Ávila J, Salinas-Rodríguez E, Use of the O_2-Thiosemicarbazide System, for the Leaching of: Gold and Copper from WEEE & Silver Contained in Mining Wastes. *Materials* 2021; 14(23): 7329. https://doi.org/10.3390/MA14237329

[51] Salinas-Rodríguez E, Hernández-ávila J, Cerecedo-Sáenz E, Arenas-Flores A, Veloz-Rodríguez MA, Toro N, del P. Gutiérrez-Amador M, Acevedo-Sandoval OA, Leaching of Copper Contained in Waste Printed Circuit Boards, Using the Thiosulfate-Oxygen System: A Kinetic Approach. *Materials* 2022; 15(7): 2354. https://doi.org/10.3390/MA15072354

[52] Halmenshlager P, Veit H, Bernardes A, Leaching of gold and silver from printed circuit board of mobile phones. *Rev Esc Minas.* 2015; 68(1): 61-68. https://doi.org/10.1590/0370-44672015680152

[53] Batnasan A, Haga K, Shibayama A, Recovery of Precious and Base Metals from Waste Printed Circuit Boards Using a Sequential Leaching Procedure. *JOM.* 2018; 70: 124-128. https://doi.org/10.1007/s11837-017-2694-y

[54] Jing L, Xiu X, Wen, L, Thiourea leaching gold and silver from the printed circuit boards of waste mobile phones. *Waste Manag.* 2012; 32(6): 1209-1212. https://doi.org/10.1016/j.wasman.2012.01.026

[55] Batnasan A, Haga K, Shibayama A, *Recovery of Valuable Metals from Waste Printed Circuit Boards by Using Iodine-Iodide Leaching and Precipitation i*n: Kim H, Wesstrom B, Alam S, Ouchi T, Azimi G, Neelameggham NR, Wang S, GuanedsX. *Rare Metal Technology 2018. TMS 2018. The Minerals, Metals & Materials Series.* Springer, Cham. 2018; 131-142. https://doi.org/10.1007/978-3-319-72350-1_12

[56] Birich A, Gao Z, Vrucak D, Friedrich B, Sensitivity of Gold Lixiviants for Metal Impurities in Leaching of RAM Printed Circuit Boards. *Metals (Basel)*. 2023; 13(5): 969. https://doi.org/10.3390/met13050969

[57] Murali A, Zhang Z, Shine A, Free M, Sarswat P, E-wastes derived sustainable Cu recovery using solvent extraction and electrowinning followed by thiosulfate-based gold and silver extraction. *J Hazard Mater Adv.* 2022; 8: 100196. https://doi.org/10.1016/j.hazadv.2022.100196

[58] Rao M, Singh K, Morrison C, Love J, Recycling copper and gold from e-waste by a two-stage leaching and solvent extraction process. *Sep Purif Technol.* 2021; 263: 118400. https://doi.org/10.1016/j.seppur.2021.118400

[59] Nekouei R, Pahlevani F, Assefi M, Maroufi S, Sahajwalla V. Selective isolation of heavy metals from spent electronic waste solution by macroporous ion-exchange resins. *J Hazard Mater.* 2019; 371: 389-396. https://doi.org/10.1016/j.jhazmat.2019.03.013

[60] Bui T, Jeon S, Lee Y, Facile recovery of gold from e-waste by integrating chlorate leaching and selective adsorption using chitosan-based bioadsorbent. *J Environ Chem Eng.* 2021; 9(1): 104661. https://doi.org/10.1016/j.jece.2020.104661

[61] Nogueira A, Carreira A, Vargas S, Passos H, Schaffer N, Simple gold recovery from e-waste leachate by selective precipitation using a quaternary ammonium salt. *Sep Purif Technol.* 2023; 316: 123797. https://doi.org/10.1016/j.seppur.2023.123797

[62] Mahapatra RP, Srikant SS, Rao RB, Recovery of basic valuable metals and alloys from E-waste using microwave heating followed by leaching and cementation process. *Sādhanā.* 2019; 44: 209. https://doi.org/10.1007/s12046-019-1193-y
[63] Arya S, Kumar S, E-waste in India at a glance: Current trends, regulations, challenges and management strategies. *J Clean Prod.* 2020; 271(): 122707. https://doi.org/10.1016/j.jclepro.2020.122707
[64] Ramesh M, Paramasivan M, Akshay P, Jarin T, A review on electric and electronic waste material management in 21st century. *Mater Today Proc.* 2023. https://doi.org/10.1016/j.matpr.2023.01.057
[65] Islam A, Ahmed T, Rabiul M, Rahman A, Sultana M, Abd A, Uddin M, Hwa S, Hasan M, Advances in sustainable approaches to recover metals from e-waste-A review. *J Clean Prod.* 2019; 244: 118815. https://doi.org/10.1016/j.jclepro.2019.118815
[66] Ueberschaar M, Dariusch Jalalpoor D, Korf N, Rotter VS, Potentials and Barriers for Tantalum Recovery from Waste Electric and Electronic Equipment. *J Ind Ecol.* 2017; 21(3): 700-714. https://doi.org/10.1111/JIEC.12577
[67] Blais C, Le Dinh AQ, Loranger É, Abdul-Nour G, Precious Metals Recovery Process from Electronic Boards: Case Study of a Non-Profit Organization (QC, Canada). *Sustainability.* 2024; 16(6): 2509. https://doi.org/10.3390/SU16062509
[68] Dias J, Pereira Silva AG, França de Holanda JN, Martins Delatorre F, Oliveira da Conceição A, Mendonça de Miranda G, Futuro A, Cardinal Pinho S. Environmental and Technological Assessment of Operations for Extraction and Concentration of Metals in Electronic Waste. *Sustainability.* 2023; 15(17): 13175. https://doi.org/10.3390/SU151713175
[69] Giese EC, E-waste mining and the transition toward a bio-based economy: The case of lamp phosphor powder. *MRS Energy Sustain.* 2022; 9(2): 494-500. https://doi.org/10.1557/s43581-022-00026-y
[70] Jin G, Li W, Wang S, Gao S. A systematic selective disassembly approach for Waste Electrical and Electronic Equipment with case study on liquid crystal display televisions. *Proc Inst Mech Eng B.* 2017; 231(13): 2261-2278. https://doi.org/10.1177/0954405415575476
[71] Fenwick C, Mayers K, Lee J, Murphy R, Recycling plastics from e-waste: Implications for effective eco-design. *J Ind Ecol.* 2023; 27(5): 1370-1388. https://doi.org/10.1111/JIEC.13409
[72] Chancerel P, Meskers CEM, Hagelüken C, Rotter VS, Assessment of Precious Metal Flows During Preprocessing of Waste Electrical and Electronic Equipment. *J Ind Ecol.* 2009; 13(5): 791-810. https://doi.org/10.1111/J.1530-9290.2009.00171.X
[73] Alkouh A, Keddar KA, Alatefi S, Remanufacturing of Industrial Electronics: A Case Study from the GCC Region. *Electronics.* 2023; 12(9): 1960. https://doi.org/10.3390/ELECTRONICS12091960
[74] Cozza G, D'Adamo I, Rosa P, Circular manufacturing ecosystems: Automotive printed circuit boards recycling as an enabler of the economic development. *Prod. Manuf. Res.* 2023; 11(1): 2182837. https://doi.org/10.1080/21693277.2023.2182837
[75] Wu C, Awasthi AK, Qin W, Liu W, Yang C, Recycling value materials from waste PCBs focus on electronic components: Technologies, obstruction and prospects. *J Environ Chem Eng.* 2022; 10(5): 108516. https://doi.org/10.1016/j.jece.2022.108516
[76] Brindhadevi K, Barceló D, Lan C, Rene E, E-waste management, treatment options and the impact of heavy metal extraction from e-waste on human health: Scenario in Vietnam and other countries. *Environ Res.* 2023; 217: 114926. https://doi.org/10.1016/j.envres.2022.114926
[77] Gravel S, Roberge B, Calosso M, Gagné S, Lavoie J, Labrèche F, Occupational health and safety, metal exposures and multi-exposures health risk in Canadian electronic waste recycling facilities. *Waste Manag.* 2023; 165: 140-149. https://doi.org/10.1016/j.wasman.2023.04.026
[78] Marconi M, Gregori F, Germani M, Papetti A, Favi C, An approach to favor industrial symbiosis: The case of waste electrical and electronic equipment. *Procedia Manuf.* 2018; 21: 502-509. https://doi.org/10.1016/j.promfg.2018.02.150
[79] Zeng H, Chen X, Xiao X, Zhou Z, Institutional pressures, sustainable supply chain management, and circular economy capability: Empirical evidence from Chinese eco-industrial park firms. *J Clean Prod.* 2017; 155: 54-65. https://doi.org/10.1016/j.jclepro.2016.10.093
[80] Park JM, Park JY, Park HS, A review of the National Eco-Industrial Park Development Program in Korea: Progress and achievements in the first phase, 2005-2010. *J Clean Prod.* 2016; 114: 33-44. https://doi.org/10.1016/j.jclepro.2015.08.115
[81] Ye Q, Umer Q, Zhou R, Asmi A, Asmi F, How publications and patents are contributing to the development of municipal solid waste management: Viewing the UN Sustainable Development Goals as ground zero. *J Environ Manag.* 2023; 325: 116496. https://doi.org/10.1016/j.jenvman.2022.116496
[82] Alarcón A. Method for recovering gold and silver from printed circuit boards using an ionic solution. MX 391678 B, 2022. https://patents.google.com/patent/MX391678B/en
[83] Berrueta F. Non-ferrous metals obtained from electronic scrap through physical-mechanical refining. MX/a/2018/006178, 2019. https://patents.google.com/patent/MX2018006178A/en
[84] Zhang Y. Cleaning treatment method to efficiently recycle useful substances of electronic garbage. CN113732005A, 2021. https://patents.google.com/patent/CN113732005A/en
[85] Minjie S. System and method for electronic waste pyrolysis recovery processing. CN106520152A, 2017. https://patents.google.com/patent/CN106520152A/en
[86] Lynn W. Simplified method of gold recovery from electronic waste. US20220235433A1, 2022. https://patents.google.com/patent/US20220235433A1/en
[87] Bin Z. Preparation for hollow polyaniline microspheres, method for recovering precious metals in electronic waste and method of recycling the recovery product. CN110639438A, 2022. https://patents.google.com/patent/CN110639438A/en

[88] Reece W. Process for recovering metal from electronic waste. US11608544B2, 2023. https://patents.google.com/patent/US11608544B2/en

[89] Marlin F. Method for the recovery of metals from electronic waste. CA3189365A1, 2022. https://patents.google.com/patent/CA3189365A1/en

[90] Mohamed K. A process to recover a metallic fraction of electronic waste and produce value-added products. WO2023087114A1, 2023. https://patents.google.com/patent/WO2023087114A1/en

[91] Xiaohui L. Comprehensive method of separation and recovery of electronic waste. CN110983031A, 2020. https://patents.google.com/patent/CN110983031A/en

[92] Kumar Sahoo P, Environmental Aspects of E-waste Management. In *Futuristic Trends in Chemical Material Sciences & Nano Technology*. 2024; 3: 306-318. https://doi.org/10.58532/V3BDCS1CH21

[93] Mishra K, Siwal SS, Thakur VK, E-waste recycling and utilization: A review of current technologies and future perspectives. *Curr. Opin. Green Sustain Chem.* 2024; 47: 100900. https://doi.org/10.1016/J.COGSC.2024.100900

[94] Alam T, Golmohammadzadeh R, Faraji F, Shahabuddin M. E-Waste Recycling Technologies: An Overview, Challenges and Future Perspectives. In: *Paradigm Shift in E-waste Management*, Editor1 A.; Editor2 B., Eds.; CRC Press: Boca Raton, FL, USA; 2022: 143-176. https://doi.org/10.1201/9781003095972-10

[95] He Y, Kiehbadroudinezhad M, Hosseinzadeh-Bandbafha H, Kumar Gupta V, Peng W, Lam SS, Tabatabaei M, Aghbashlo M, Driving sustainable circular economy in electronics: A comprehensive review on environmental life cycle assessment of e-waste recycling. *Environ Pollut.* 2024; 342: 123081. https://doi.org/10.1016/J.ENVPOL.2023.123081

[96] Seif R, Salem FZ, Allam NK. E-waste recycled materials as efficient catalysts for renewable energy technologies and better environmental sustainability. *Environ Dev Sustain.* 2023; 26: 5473-5508. https://doi.org/10.1007/S10668-023-02925-7

[97] Senthilnathan J, Philip L. Persistent Toxic Substances Released from Uncontrolled E-waste Recycling and Action for the Future. In: Jawaid, M, Khan, A, eds. *Conversion of Electronic Waste in to Sustainable Products. Sustainable Materials and Technology.* Singapore: Springer; 2023: 103-126. https://doi.org/10.1007/978-981-19-6541-8_4

Reciklaža elektronskog otpada: pregled hidrometalurških procesa koji se koriste za ekstrakciju metala

Nallely G. Picazo-Rodríguez[1], Gabriela Baltierra-Costeira[1], Ma de Jesús Soria-Aguilar[2], Zeferino Gamiño Arroyo[3], Norman Toro[4], Manuel Saldana[4,5], Jesús R. de la Garza de Luna[1] and Francisco Raúl Carrillo-Pedroza[2]

[1] Instituto Tecnológico Superior de Monclova, Tecnológico Nacional de México, Monclova, México
[2]Facultad de Metalurgia, Universidad Autónoma de Coahuila, Monclova, México
[3]Departamento de Ingeniería Química, División de Ciencias Naturales y Exactas, Universidad de Guanajuato, Guanajuato, México
[4]Faculty of Engineering and Architecture, Universidad Arturo Prat, Iquique, Chile
[5]Departamento de Ingeniería Química y Procesos de Minerales, Universidad de Antofagasta, Antofagasta, Chile

(Pregledni rad)

Izvod

Eksponencijalni rast stanovništva doveo je do eksponencijalne potražnje za metalima, posebno za proizvodnju elektronskih uređaja, koji se na kraju svog funkcionalnog veka najčešće odlažu na deponije. Ova praksa predstavlja značajnu opasnost po životnu sredinu zbog prisustva metala u ovim odbačenim materijalima, nazvanim elektronski otpad ili e-otpad. To zahteva odgovarajuće strategije upravljanja e-otpadom, kako bi se sprečili negativni efekti na ekosistem i na ljudsko zdravlje. E-otpad sadrži vredne metale, često u koncentracijama koje čine njihovu reciklažu ekonomski isplativom. Štaviše, rastuća potražnja za metalima, vođena tehnološkim napretkom, učinila je reciklažu e-otpada ključnim elementom održivog upravljanja resursima. Ovaj rad pruža pregled hidrometalurških tehnika obrade za reciklažu vrednih metala iz otpada od električne i elektronske opreme, pre svega metala kao što su bakar, zlato i srebro. Ove metodologije koriste vodene rastvore kako bi olakšala ekstrakcija metala, predstavljajući isplativu i ekološki održivu alternativu proizvodnji metala konvencionalnim rudarenjem. Međutim, ekonomska isplativost ovih alternativnih procesa može varirati zavisno od vrste i koncentracije metala prisutnih u otpadu.

Ključne reči: hidrometalurgija; upravljanje elektronskim otpadom; vredni metali; ekstrakcija; ekološka održivost

3D biomaterials produced by near-field electrospinning and melt electrowriting

Ilda Kola[1], Jnanada Shrikant Joshi[2], Nonsikelelo Sheron Mpofu[2,3] and Andrea Ehrmann[2]

[1]Department of Textile and Fashion, Polytechnic University of Tirana, Tirana, Albania
[2]Faculty of Engineering Sciences and Mathematics, Bielefeld University of Applied Sciences and Arts, Bielefeld, Germany
[3]School of Engineering, Moi University, Eldoret, Kenya

Abstract

Near-field electrospinning and melt electrowriting are attractive techniques that can be used to produce polymeric nano- or microfibres and build three-dimensional (3D) shapes that can be used in biotechnology and biomedicine. Preferred patterns can be designed due to the possibility to define nozzle and collector movements. Opposite to conventional electrospinning, near-field electrospinning enables formation of very fine fibres assembled in structures with much larger pore sizes, tailored according to the requirements of cells, which makes such scaffolds highly interesting for cell culture, tissue engineering applications and similar biomedical and biotechnological applications. In addition, this technique is relatively simple, reproducible and inexpensive. Melt electrowriting can be used to draw microfibres from a solution or a melt through an electrostatic field allowing precise deposition with high accuracy, leading to highly porous scaffolds that facilitate homogeneous cell distribution. This review provides an overview of new theoretical and experimental findings related to near-field electrospinning and melt electrowriting for applications in biotechnology and biomedicine, such as printing scaffolds for tissue engineering and cell culture, producing wound dressings, and others. Near-field electrospinning and melt electrowriting processes are briefly explained, and the most relevant polymers for biomedical applications are presented. Finally, recent challenges and suggestions for future research directions are given.

Keywords: 3D porous scaffolds; biomedicine; nanofibers; three-dimensional shapes.

Available on-line at the Journal web address: http://www.ache.org.rs/HI/

MINI-REVIEW PAPER

UDC: 544.275.7: 678.076

Hem. Ind. **79(4)** 209-217 (2025)

1. INTRODUCTION

Fibrous scaffolds have been used in biotechnology and biomedicine for decades [1-3]. Electrospinning is usually applied to produce polymeric nanofibers for biotechnological and other applications [4-8]. This electrostatically driven process enables spinning of polymers, polymer blends, and polymers with embedded nanoparticles to create nanofiber mats with arbitrarily oriented fibres [9]. Oriented nanofiber bundles are advantageous for many applications [10,11] and can be produced by several techniques, such as a fast-rotating collector electrospinning, spinning on the gaps between grounded electrodes, structuring the electric field by dielectric or conductive materials, magnetic field-assisted electrospinning, centrifugal electrospinning, or post-processing to draw the fibres [9,12-15]. However, certain randomness is always present due to the bending instability of the jet travelling to the collector, resulting from the repulsive forces between surface charges that are necessary for jet stretching and correspondingly small fibre diameters [9].

Near-field electrospinning differs regarding the distance between the needle, through which the polymer solution is inserted into the strong electric field, and the collector is much smaller than in common electrospinning, typically below 10 mm [16-18]. At this distance, the jet is still stable, so that highly aligned and complex patterns can be written by producing nano- or microfibres [9].

As an alternative, melt electrowriting has emerged, which combines additive manufacturing with electrohydrodynamical stabilization of the molten jet, resulting in a possible printing resolution around 1 µm [19].

Corresponding author: Andrea Ehrmann, Faculty of Engineering Sciences and Mathematics, Bielefeld University of Applied Sciences and Arts, 33619 Bielefeld, Germany; E-mail: andrea.ehrmann@hsbi.de, https://orcid.org/0000-0001-6063-5989
Co-authors: I. Kola https://orcid.org/0009-0007-6967-4475, J. S. Joshi https://orcid.org/0000-0001-6063-5989,
N. S. Mpofu https://orcid.org/0000-0001-8419-3388

Paper received: 11 January 2025; Paper accepted: 11 September 2025; Paper published: 29 September 2025.
https://doi.org/10.2298/HEMIND250111013K

The possibility to create highly aligned fibres by near-field electrospinning (NFES) and melt electrowriting (MEW) makes these techniques promising for tissue engineering and other biomedical and biotechnological applications. In the next sections, both processes as well as the most common biomedical polymers are briefly described, followed by the most recent applications reviewed in detail, and an outlook on overcoming recent challenges in utilization of these technologies.

2. NEAR-FIELD ELECTROSPINNING

Near-field electrospinning is a technique quite similar to the more common far-field electrospinning, where usually a syringe containing a polymer solution is placed opposite to a collector, with a strong electric field applied in-between (Fig. 1a). This leads to the formation of a so-called Taylor cone at the end of the needle from which a jet is initiated that is only stable for a short distance, before it becomes instable and shows a whipping action, which leads to stretching and thinning of the polymeric jet before it reaches the substrate [20]. In a homogeneous electric field, the resulting nanofibers are thus more or less arbitrarily positioned on the substrate. In NFES the nozzle-to-collector distance and voltage are strongly reduced (Fig. 1b), resulting in much better-controlled patterning (Fig. 1d) than in the common far-field electrospinning process (Fig. 1c) [20]. The nanofiber thickness depends not only on the polymers used, but also on the voltage and other spinning parameters, where low voltages of a few hundred Volts result in fine fibres of a few tens of nanometres in diameter [20,21]. It should be mentioned that even the length of the needle can modify the NFES results, which is rarely mentioned in the literature [22,23].

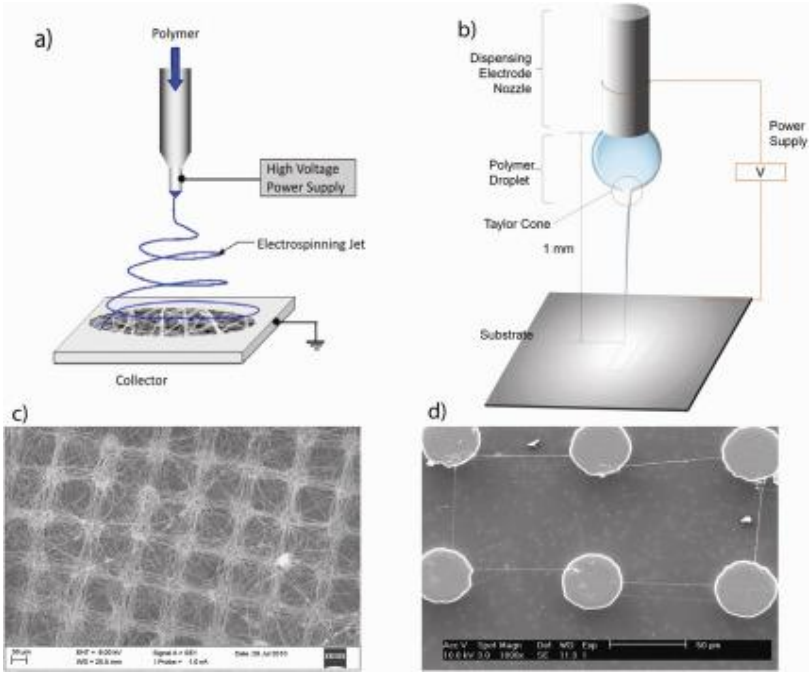

Figure 1. Far-field electrospinning (FFES) (a, c) compared with low-voltage near-field electrospinning (NFES; b, d). The fibres are chaotically deposited on carbon 3D posts in FFES (c), whereas NFES allows more controlled patterning (d). From [20], originally published under a CC BY-NC-ND 4.0 license

3. MELT ELECTROWRITING

Melt electrowriting can be regarded as a hybrid technology, combining extrusion 3D printing with electrospinning. Figure 2a shows the principle of this technique, while Figure 2b depicts an exemplary scaffold printed from poly(caprolactone) (PCL) using melt electrowriting [24]. In addition to common planar substrates, MEW is also often performed on cylindrical rotating substrates to prepare tubular scaffolds [25]. Interestingly, MEW printers have recently been made available at low costs by an open-source device called MEWron, thus making MEW possible for many research groups to obtain microfibres with a diameter range of around 1.5 to 100 µm, depending on the material and device

configuration [24,26]. Important parameters, influencing the printing results and fibre diameters, are voltage and pressure, collector speed, nozzle diameter and the temperature of the molten polymer, besides the environmental parameters temperature and relative humidity which have also significant impacts [27,28]. In addition, the substrate should be conductive to support well-aligned fibre placement [29].

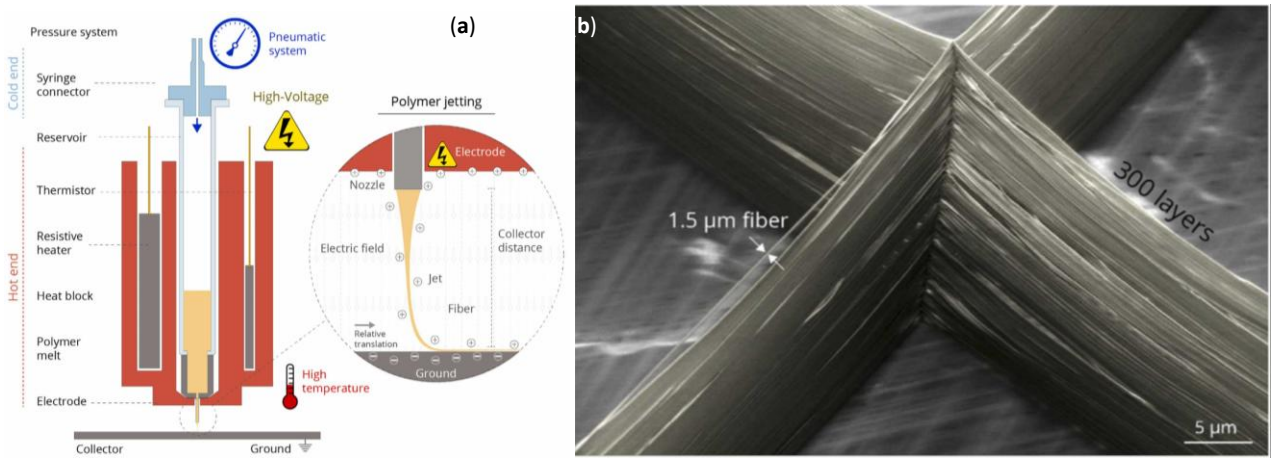

Fig. 2. Melt electrowriting (MEW): (a) Schematic including the main components and working mechanism of MEW; (b) poly(caprolactone) square scaffold with 500 µm interspace, 1.5 µm fibres and 300 layers. From [24], originally published under a CC-BY 4.0 license

4. BIOMATERIALS USED FOR NEAR-FIELD ELECTROSPINNING AND MELT ELECTROWRITING

Several polymers have been successfully used in near-field electrospinning and melt electrowriting.

Poly(caprolactone) (PCL) is often used in NEFS, but also biopolymers like alginate, chitosan, collagen, gelatine as well as poly(g-benzyl-l-glutamate) (PBLG), poly(L-lactic acid) (PLLA), polydioxanone (PDO), polymethyl methacrylate (PMMA), poly(ethylene oxide) (PEO), poly(2-ethyl-2-oxazoline) (PEtOx), poly(2-ethyl-2-oxazine) (PEtOzi), and various other polymers, copolymers and polymer blends [30].

PCL is also most often used in MEW due to its biocompatibility, good thermal stability and printability, either solely or blended with other polymers [31,32]. In addition, different other polyesters can be used, such as poly(hydroxymethyl-glycolide-*co*-*ε*-caprolactone) (pHMGCL) or thermoplastic elastomers (TPEs) as well as water-soluble polymers like poly(2-ethyl-2-oxazoline) (PEtOx), hydrogels like poly(2-ethyl-2-oxazine) (PEtOzi) or non-biodegradable polymers like polypropylene (PP) [31]. Mixing these polymers with different fillers, such as hydroxyapatite (HA), bioactive glass, metal or metal-oxide nanoparticles, reduced graphene oxide (rGO) etc. can be used to improve cell adhesion and proliferation, mechanical or electrical properties, reduce degradation or modify hydrophobicity of the material [32].

As this wide range of potential materials, combined with the high degree of freedom offered by the selected structures, which are built from nano- and microfibres with a wide range of diameters, shows, near-field electrospinning and melt electrowriting enable a wide variety of applications in biomedicine, biotechnology, and similar fields [33]. A selection of the most recent interesting applications is given in the next sections.

5. BIOMEDICAL APPLICATIONS OF NEAR-FIELD ELECTROSPINNING

Several studies of near-field electrospinning to prepare scaffolds for tissue engineering can be found in literature. Poly(vinyl alcohol) (PVA) blended with chitosan was used in NFES, with a distance of 3 mm between the needle and the collector under a voltage of 2 kV [34]. It was shown that higher collector speeds were advantageous for well-defined fibre placement and thus suggested to use this strategy for obtaining tissue engineering scaffolds.

PDO was used for preparation of near-field electrospun small-diameter vascular graft scaffolds with micron-sized polymer fibres [35]. These tubular scaffolds had similar mechanical properties as native vessels and expanding pores, to support transmural endothelialization. Comparing NFES with far-field electrospinning to prepare PDO scaffolds, the same research group showed a higher neutrophil innate immune response of DNA extrusion to form neutrophil

extracellular traps due to the possibility to tailor the pore sizes and mechanical properties [36]. Other researchers prepared PDO near-field electrospun bioresorbable vascular grafts whose fibrous architecture aimed to mimic the arterial extracellular matrix with the native vessel properties regarding tensile strength, suture retention, and burst pressure, which was best achieved by fibre alignment angles of 15°/75° [37].

Using partly branched PCL microfibres prepared by NFES on a valley-shaped collector, Qavi and Tan tried to mimic the arteriole-capillary-venule structure by spinning stem-branch-stem fibrous structures [38]. Concentrating on relatively thin fibres only, Davis *et al.* [40] used NFES of gelatine to prepare fibres with a diameter of 2.3 µm [39], which is similar to gelatine fibres prepared with far-field electrospinning.

Besides tissue engineering, other biomedical and biotechnological applications of NFES can be found in the literature. NFES was applied to prepare medical wound dressings based on PCL blended with collagen type I in different ratios and added erythromycin, used to prevent wound infections due to Gram-positive and Gram-negative bacteria [41]. Good mechanical properties, thermal stability, antibacterial, slow-release and moisturizing functions of this wound dressing were reported.

PCL was functionalized with collagen and the natural drug usnic acid [42]. The authors found that the electrospun fibre structures were hydrophilic due to the addition of collagen and inhibited the growth of Gram-positive and Gram-negative bacteria due to the usnic acid, as shown in Figure 3. In addition, crosslinking the collagen with genipin resulted in improved mechanical properties, thermal stability and drug release performance.

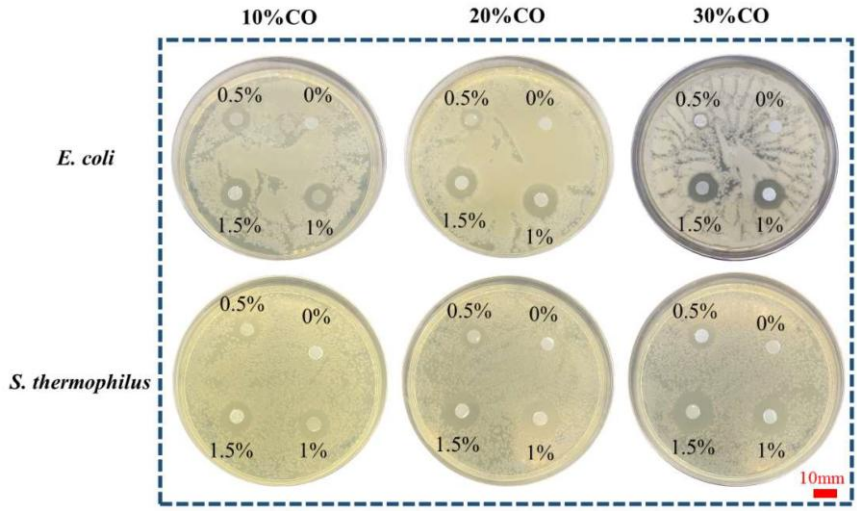

Fig. 3. Effect of composite fibres with different contents of collagen (CO) and usnic acid (the number in the culture dish is the acid content) on antibacterial properties against E. coli and S. thermophilus. From [42], originally published under a CC-BY 4.0 license.

6. BIOMEDICAL APPLICATIONS OF MELT ELECTROWRITING

Similar to the aforementioned MEWron device, a custom-made MEW device was used to prepare PCL box-structure and triangular scaffolds by applying a temperature of 73 °C, a pressure of 1.2 bar in the syringe and an acceleration voltage of 6 kV, while the nozzle-collector distance was 4 mm, and the collector was rotated at the rate of 400 mm min^{-1} [43]. By varying the scaffold design, the authors could tailor the scaffolds especially for osteoblasts or for keratinocytes and connective tissue, so that a bilayer scaffold combining the optimum designs could be produced by connecting these surface layers by a casted PCL film. A custom-made MEW device was also used by Eichholz and Hoey, who showed significant differences in the morphology, spreading and cytoskeletal tension of human skeletal stem cells depending on the architecture of 10 µm PCL fibres [44].

Tubular melt-electrowritten PCL scaffolds were used to investigate the influence of these scaffolds, applied blank or seeded with ovine bone marrow mesenchymal stem cells, on ovine tibial segmental defects in merino-cross sheep [45]. The authors reported a positive impact of seeded scaffolds, while also mentioning the problems of up-scaling from *in vitro* and small animal models to *in vivo* application on surgically relevant scales. By filling PCL melt electrowritten scaffolds with

nano-HA, Chen *et al.* [46,47] reported improved bone marrow mesenchymal stem cell proliferation as well as high structural regularity and fibre conformity combined with good mechanical stability.

Gwiazda *et al.* [48] investigated the influence of fibre orientation on cell alignment. Comparing different PCL matrices with three different patterns assembled of 20 µm fibres, human mesenchymal stem cells seeded on these scaffolds were found to align spontaneously along these patterns. Large cellularized bone-ligament-bone constructs with complex geometries were thus proposed for increased mechanical resilience and elasticity. In another study, MEW was combined with fused deposition modelling (FDM) 3D printing to prepare PCL scaffolds with aligned and orthogonal fibres, partly coated with collagen [49]. Human adipose-derived stem cells (hADSCs) were found to proliferate on the obtained scaffolds (Fig. 4), while the aspect ratio of cells on the aligned fibres was significantly higher than that on orthogonal fibres. Besides, osteogenic and tenogenic differentiation of hADSCs was found depending on HA addition in different regions.

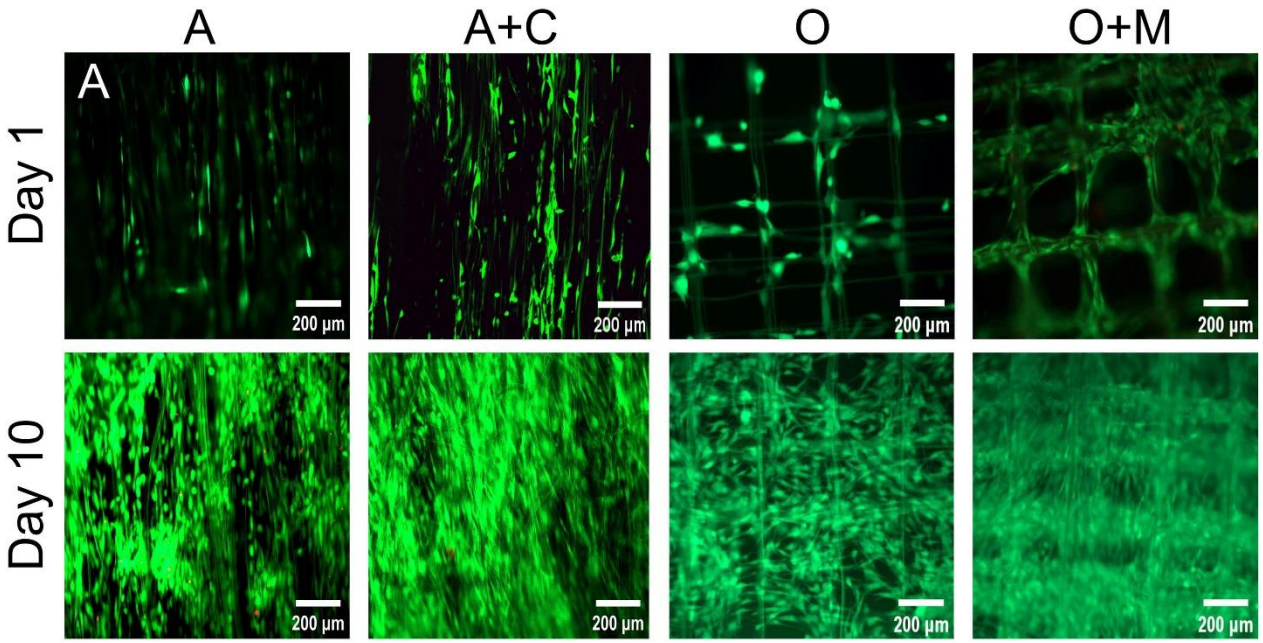

Fig. 4. Live/dead staining of human adipose-derived stem cells on aligned (A), collagen-coated aligned (A+C), orthogonal (O), and mineral-coated orthogonal (O+M) PCL scaffolds, taken on day 1 and day 10. From [49], originally published under a CC-BY-NC 3.0 license

While PCL is most often used for melt electrowriting, some authors also applied other materials. PLLA electrowritten scaffolds with 40 µm fibre diameter and 200 µm pore size were successfully tested *in vitro* for bone tissue engineering [50]. Combining PCL with PLA led to slightly increased viability of L929 mouse murine fibroblast and human umbilical vein endothelial cells compared to pure PCL and PLA scaffolds [51].

Finally, it should be mentioned that the relatively low voltages used in MEW allow even for printing of polymer-DNA composites [52] or of cell-laden polymers, which is sometimes described as electrohydrodynamic bioprinting. This technique was for example reported for printing of alginate-based bioinks with C2C12 cells [53] or human chondrocytes [54].

7. CONCLUSION AND OUTLOOK

Near-field electrospinning and melt electrowriting are recently developed techniques to prepare nano- and microfibres and place them at well-defined positions. The possibility to tailor pore sizes and geometries, independent of fibre diameters, is supportive for cell culture and tissue engineering applications.

Nevertheless, there are still challenges to overcome. On the one hand, while several polymers have already been investigated for NFES or MEW, nowadays especially MEW is mostly performed with PCL or PCL blends, suggesting that more research is needed on the use of other polymers. Additionally, the large number of custom-made setups for NFES and MEW reduces the reproducibility of studies [36]. The situation is even more complicated by sometimes missing information such as the needle length in NFES or environmental parameters. Also, the fibre throughput in these

techniques is still slower than in common far-field electrospinning and several attempts have been made to speed up the fibre production. Finally, freely available programs to translate CAD data of diverse shapes into instructions for NFES or MEW devices are still missing [55].

We hope that this review can help gaining more interest in developing these techniques further.

REFERENCES

[1] Smith LA, Ma PX. Nano-fibrous scaffolds for tissue engineering. *Colloids Surf B.* 2004; 3: 125-131. https://doi.org/10.1016/j.colsurfb.2003.12.004

[2] Jun ID, Han HS, Edwards JR, Jeon HJ. Electrospun fibrous scaffolds for Tissue engineering: viewpoints on architecture and fabrication. *Int J Mol Sci*. 2018; 19: 745. https://doi.org/10.3390/ijms19030745

[3] Rahman M, Dip TM, Nur MG, Padhye R, Houshyar S. Fabrication of Silk Fibroin-Derived Fibrous Scaffold for Biomedical Frontiers. *Macromol Mater Eng.* 2024; 309: 2300422. https://doi.org/10.1002/mame.202300422

[4] Ji DX, Lin YG, Guo XY, Ramasubramanian B, Wang RW, Radacsi N, Jose R, Qin XH, Ramakrishna S. Electrospinning of nanofibres. *Nat Rev Methods Primers.* 2024; 4: 1. https://doi.org/10.1038/s43586-023-00278-z

[5] Maran BAV, Jeyachandran S, Kimura M. A review on the electrospinning of polymer nanofibers and Its Biomedical Applications. *J Comp Sci.* 2024; 8: 32. https://doi.org/10.3390/jcs8010032

[6] Wang CL, Su YJ, Xie JW. Advances in Electrospun Nanofibers: Versatile materials and diverse biomedical applications. *Acc Mater Res.* 2024; 5: 987-999. https://doi.org/10.1021/accountsmr.4c00145

[7] Teyeb C, Grothe T, Dotter M, Kola I, Ehrmann A. Homogeneity of physical properties of electrospun gelatin nanofiber mats. *Sust Green Mater.* 2024; 1-14, https://doi.org/10.1080/29965292.2024.2404716

[8] Morina E, Dotter M, Döpke C, Kola I, Spahiu T, Ehrmann A. Homogeneity of Needleless Electrospun Nanofiber Mats. *Nanomaterials.* 2023; 13: 2507. https://doi.org/10.3390/nano13182507

[9] Robinson AJ, Pérez-Nava A, Ali SC, González-Campos JB, Holloway JL. Comparative analysis of fiber alignment methods in electrospinning. *Matter.* 2021; 4: 821-844. https://doi.org/10.1016/j.matt.2020.12.022

[10] Blachowicz T, Malczyk M, Kola I, Ehrmann A. Textiles for Very Cold Environments. *Processes.* 2024; 12: 927. https://doi.org/10.3390/pr12050927

[11] Blachowicz T, Mpofu NS, Ehrmann A. Measuring Physical and Chemical Properties of Single Nanofibers for Energy Applications—Possibilities and Limits. *Nanoenergy Adv.* 2024; 4: 300-317. https://doi.org/10.3390/nanoenergyadv4040018

[12] Blachowicz T, Ehrmann A. Methods and Engineering of Electrospinning. In: Das R, ed. *Electrospun Nanofibrous Technology for Clean Water Production. Nanostructure Science and Technology*. Springer, Singapore; 2023:7-35. https://doi.org/10.1007/978-981-99-5483-4_2

[13] Hellert C, Storck JL, Grothe T, Kaltschmidt B, Hütten A, Ehrmann A. Positioning and Aligning Electrospun PAN Fibers by Conductive and Dielectric Substrate Patterns. *Macromol Symp.* 2021; 395: 2000213. https://doi.org/10.1002/masy.202000213

[14] Storck JL, Grothe T, Mamun A, Sabantina A, Klöcker M, Blachowicz T, Ehrmann A. Orientation of Electrospun Magnetic Nanofibers Near Conductive Areas. *Materials.* 2020; 13: 47. https://doi.org/10.3390/ma13010047

[15] Storck JL, Brockhagen B, Grothe T, Sabantina L, Kaltschmidt B, Tuvshinbayar K, Braun L, Tanzli E, Hütten A, Ehrmann A. Stabilization and Carbonization of PAN Nanofiber Mats Electrospun on Metal Substrates. *C* 2021; 7: 12. https://doi.org/10.3390/c7010012

[16] Kameoka J, Orth R, Yang Y, Czaplewski D, Mathers R, Coates GW, Craighead H. A scanning tip electrospinning source for deposition of oriented nanofibres. *Nanotechnology.* 2003; 14: 1124. https://doi.org/10.1088/0957-4484/14/10/310

[17] Sun D, Chang C, Li S, Lin L. Near-field electrospinning. *Nano Lett.* 2006; 6: 839-842. https://doi.org/10.1021/nl0602701

[18] Mpofu NS, Blachowicz T, Ehrmann A, Ehrmann G. Wearable Electrospun Nanofibrous Sensors for Health Monitoring. *Micro.* 2024; 4: 798-822. https://doi.org/10.3390/micro4040049

[19] Mieszczanek P, Robinson TM, Dalton PD, Hutmacher DW. Convergence of machine vision and melt electrowriting. *Adv Mater.* 2021; 33: 2100519. https://doi.org/10.1002/adma.202100519

[20] Bisht G, Nesterenko S, Kulinsky L, Madou M. A computer-controlled near-field electrospinning setup and its graphic user interface for precision patterning of functional nanofibers on 2D and 3D substrates. *SLAS Technology.* 2012; 17: 302-308. https://doi.org/10.1177/2211068212446372

[21] Khodabandeh AR, Yousefi AA, Vasheghani-Farahani E. The effect of process variables on near-field electrospinning of polycaprolactone studied by response surface methodology. *Iran Polym J.* 2024; 33: 1569-1581. https://doi.org/10.1007/s13726-024-01339-0

[22] Yang Y, Jia Z, Liu J, Li Q, Hou L, Wang L, Guan Z. Effect of electric field distribution uniformity on electrospinning. *J Appl Phys.* 2008; 103: 104307. https://doi.org/10.1063/1.2924439

[23] Hekmati A, Rashidi A, Ghazisaeidi R, Drean JY. Effect of needle length, electrospinning distance, and solution concentration on morphological properties of polyamide-6 electrospun nanowebs. *Text Res J.* 2013; 83: 1452-1466. https://doi.org/10.1177/0040517512471746

[24] Reizabal A, Kangur T, Saiz PG, Menke S, Moser C, Brugger J, Menke S, Moser C, Brugger J, Dalton PD, Luposchainsky S. MEWron: An open-source melt electrowriting platform. *Addit Manuf.* 2023; 71: 103604. https://doi.org/10.1016/j.addma.2023.103604

[25] Peng ZL, Wang MJ, Lv H, Zhang JY, Li YN, Wu JY, Zhang SL, Wang F, Zhang GM, Zhu XY, Xu L, Lan HB. Electric field-driven microscale 3D printing of flexible thin-walled tubular mesh structures of molten polymers. *Mater Des.* 2023; 225: 111433. https://doi.org/10.1016/j.matdes.2022.111433

[26] Reizabal A, Devlin BL, Paxton NC, Saiz PG, Liashenko I, Luposchainsky S, Woodruff MA, Lanceros-Mendez S, Dalton PD. Melt electrowriting of nylon-12 microfibers with an open-source 3D printer. *Macromol Rapid Comm.* 2023; 44: 2300424. https://doi.org/10.1002/marc.202300424

[27] Vazquez-Armendariz J, Tejeda-Alejandre R, Bahhur A, Rodriguez CA, Dean D. Meltelectrowriting of polycaprolactone thin membranes with high porosity. *Proc CIRP.* 2022; 110: 282-286. https://doi.org/10.1016/j.procir.2022.06.051

[28] O'Neill KL, Dalton PD. A decade of melt electrowriting. *Small Methods.* 2023; 7: 2201589. https://doi.org/10.1002/smtd.202201589

[29] Ding HZ, Cao K, Zhang FC, Boettcher W, Chang RC. A fundamental study of charge effects on melt electrowritten polymer fibers. *Mater Des.* 2019; 178: 107857. https://doi.org/10.1016/j.matdes.2019.107857

[30] King III WE, Bowlin GL. Near-field electrospinning and melt electrowriting of biomedical polymers – progress and limitations. *Polymers.* 2021; 13: 1097. https://doi.org/10.3390/polym13071097

[31] Kade JC, Dalton PD. Polymers for melt electrowriting. *Adv Healthcare Mater.* 2020; 10: 2001232. https://doi.org/10.1002/adhm.202001232

[32] Saiz PG, Reizabal A, Vilas-Vilela JL, Dalton PD, Lanceros-Mendez S. Materials and strategies to enhance melt electrowriting potential. *Adv Mater.* 2024; 36: 2312084. https://doi.org/10.1002/adma.202312084

[33] Loewner S, Heene S, Baroth T, Heymann H, Cholewa F, Blume H, Blume C. Recent advances in melt electro writing for tissue engineering for 3D printing of microporous scaffolds for tissue engineering. *Front Bioeng Biotechnol.* 2022; 10: 896719. https://doi.org/10.3389/fbioe.2022.896719

[34] Yan FF, Chen HP, Zheng LL, Chen WH, Liu YY, Hu QX. The controllable PVA-Chitosan fiber prepared by the near-field electro spinning for tissue engineering. *Adv J Food Sci Technol.* 2013; 5: 1073-1078. https://maxwellsci.com/print/ajfst/v5-1073-1078.pdf

[35] King III WE, Bowlin GL. Near-field electrospinning of polydioxanone small diameter vascular graft scaffolds. *J Mech Behav Biomed Mater.* 2022; 130: 105207. https://doi.org/10.1016/j.jmbbm.2022.105207

[36] King III WE, Bowlin GL. Mechanical characterization and neutrophil NETs response of a novel hybrid geometry polydioxanone near-field electrospun scaffold. *Biomed Mater.* 2021; 16: 065002. https://doi.org/10.1088/1748-605X/ac1e43

[37] Snyder AE, Sandridge JK, Nordmoe AE, Main EN, Bowlin GL. Fabrication and mechanical characterization of near field electrospun bioresorbable vascular grafts with fibrous architecture mimicking the arterial extracellular matrix. *J Bioact Compat Pol.* 2024; 39: 455-466. https://doi.org/10.1177/08839115241262038

[38] Qavi I, Tan GZ. Near-field electrospinning polycaprolactone microfibers to mimic arteriole-capillary–venule structure. *Progr Biomater.* 2021; 10: 223-233. https://doi.org/10.1007/s40204-021-00165-4

[39] Davis ZG, Hussain AF, Fisher MB. Processing variables of direct-write, near-field electrospinning impact size and morphology of gelatin fibers. *Biomed Mater.* 2021; 16: 045017. https://doi.org/10.1088/1748-605X/abf88b

[40] Wehlage D, Blattner H, Sabantina L, Böttjer R, Grothe T, Rattenholl A, Gudermann F, Lütkemeyer D, Ehrmann A. Sterilization of PAN/gelatine nanofibrous mats for cell growth. *Tekstilec.* 2019; 62: 78-88. https://doi.org/10.14502/Tekstilec2019.62.78-88

[41] Li DF, Lin DS, Li Y, Xu SK; Cao QY, Zhou WY. Preparation and characterization of novel multifunctional wound dressing by near-field direct-writing electrospinning and its appliation. *Polymers.* 2024; 16: 1573. https://doi.org/10.3390/polym16111573

[42] Mai ZR, Liu QL, Bian YS, Wang P, Fu XW, Lin DS, Kong NZ, Huang YQ, Zeng ZJ, Li DF, Zheng WX, Xia YJ, Zhou WY. PCL/collagen/UA composite biomedical dressing with ordered microfiberous structure fabricated by a 3D near-field electrospinning process. *Polymers.* 2022; 15: 223. https://doi.org/10.3390/polym15010223

[43] Fuchs A, Youssef A, Seher A, Hartmann S, Brands RC, Müller-Richter UDA, Kübler AC, Linz C. A new multilayered membrane for tissue engineering of oral hard- and soft tissue by means of melt electrospinning writing and film casting – An in vitro study. *J Craniomaxillofac Surg.* 2019; 47: 695-703. https://doi.org/10.1016/j.jcms.2019.01.043

[44] Eichholz KF, Hoey DA. Mediating human stem cell behaviour via defined fibrous architectures by melt electrospinning writing. *Acta Biomater.* 2018; 75: 140-151. https://doi.org/10.1016/j.actbio.2018.05.048

[45] Black C, Kanczler JM, de Andrés MC, White LJ, Savi FM, Bas O, Saifzadeh S, Henkel J, Zannettino A, Gronthos S, Woodruff MA, Hutmacher D W, Oreffo ROC. Characterisation and evaluation of the regenerative capacity of Stro-4+ enriched bone marrow mesenchymal stromal cells using bovine extracellular matrix hydrogel and a novel biocompatible melt electro-written medical-grade polycaprolactone scaffold. *Biomaterials.* 2020; 247: 119998. https://doi.org/10.1016/j.biomaterials.2020.119998

[46] Chen Z J, Liu YB, Huang J, Wang H, Hao M, Hu XD, Qian XM, Fan JT, Yang HJ, Yang B. Enhanced in vitro biocompatible polycaprolactone/nano-hydroxyapatite scaffolds with near-field direct-writing melt electrospinning technology. *J Funct Biomater.* 2022; 13: 161. https://doi.org/10.3390/jfb13040161

[47] Chen ZJ, Liu YB, Huang J, Hao M, Hu, XD, Qian XM, Fan JT, Yang HJ, Yang B. Influences of process parameters of near-field direct-writing melt electrospinning on performances of polycaprolactone/nano-hydroxyapatite scaffolds. *Polymers.* 2022; 14: 3404. https://doi.org/10.3390/polym14163404

[48] Gwiazda M, Kumar S, Swieszkowski W, Ivanovski S, Vaquett C. The effect of melt electrospun writing fiber orientation onto cellular organization and mechanical properties for application in Anterior Cruciate Ligament tissue engineering. *J Mech Behav Biomed Mater.* 2020; 104: 103631. https://doi.org/10.1016/j.jmbbm.2020.103631

[49] Ma SS, Zheng SY, Li D, Hu WH, Wang LM. Melt Electrowriting Combined with Fused Deposition Modeling Printing for the Fabrication of Three-Dimensional Biomimetic Scaffolds for Osteotendinous Junction Regeneration. *Int J Nanomed.* 2024; 19: 3275-3293. https://doi.org/10.2147/IJN.S449952

[50] Meng J, Boschetto F, Yagi S, Marin E, Adachi T, Chen XF, Pezzotti G, Sakurai S, Yamane H, Xu HZ. Design and manufacturing of 3D high-precision micro-fibrous poly (l-lactic acid) scaffold using melt electrowriting technique for bone tissue engineering. *Mater Des.* 2021; 210: 110063. https://doi.org/10.1016/j.matdes.2021.110063

[51] Shahverdi M, Seifi S, Akbari A, Mohammadi K, Shamloo A, Movahhedy MR. Melt electrowriting of PLA, PCL, and composite PLA/PCL scaffolds for tissue engineering application. *Sci Rep*. 2022; 12: 19935. https://doi.org/10.1038/s41598-022-24275-6

[52] Soukarie D, Nocete L, Bittner AM, Santiago I. DNA data storage in electrospun and melt-electrowritten composite nucleic acid-polymer fibers. *Mater Bio Today.* 2024; 24: 100900. https://doi.org/10.1016/j.mtbio.2023.100900

[53] Qiu ZN, Wang YT, Kasimu A, Li DC, He JK. Functionalized alginate-based bioinks for microscale electrohydrodynamic bioprinting of living tissue constructs with improved cellular spreading and alignment. *Bio-Des Manufact.* 2023; 6: 136-149. https://doi.org/10.1007/s42242-022-00225-z

[54] Ross MT, Kilian D, Lode A, Ren JY, Allenby MC, Gelinsky M, Woodruff MA. Using melt-electrowritten microfibres for tailoring scaffold mechanics of 3D bioprinted chondrocyte-laden constructs. *Bioprinting.* 2021; 23: e00158. https://doi.org/10.1016/j.bprint.2021.e00158

[55] Paxton NC, Lanaro M, Bo A, Crooks N, Ross MT, Green N, Tetsworth K, Allenby MC, Gu YT, Wong CS, Powell SK, Woodruff MA. Design tools for patient specific and highly controlled melt electrowritten scaffolds. *J Mech Behav Biomed Mater.* 2020; 105: 103695. https://doi.org/10.1016/j.jmbbm.2020.103695

3D biomaterijali proizvedeni elektropredenjem u bliskom polju i elektropisanjem rastopljenim materijalom

Ilda Kola[1], Jnanada Shrikant Joshi[2], Nonsikelelo Sheron Mpofu[2,3] i Andrea Ehrmann[2]

[1]Department of Textile and Fashion, Polytechnic University of Tirana, Tirana, Albania
[2]Faculty of Engineering Sciences and Mathematics, Bielefeld University of Applied Sciences and Arts, Bielefeld, Germany
[3]School of Engineering, Moi University, Eldoret, Kenya

(Mini pregledni rad)

Izvod

Elektropredenje u bliskom polju (engl. near-field electrospinning) i elektropisanje rastopljenim materijalom (engl. melt electrowriting) predstavljaju atraktivne tehnike koje se mogu koristiti za proizvodnju polimernih nano- ili mikrovlakana i izradu trodimenzionalnih (3D) struktura koje nalaze primenu u biotehnologiji i biomedicini. Poželjne strukture se mogu projektovati zahvaljujući mogućnosti definisanja kretanja dizne i kolektora. Za razliku od konvencionalnog elektropredenja, elektropredenje u bliskom polju omogućava formiranje veoma finih vlakana koja se organizuju u strukture sa znatno većim porama, prilagođene zahtevima ćelija, što ove nosače čini izuzetno zanimljivim za kulture ćelija, inženjerstvo tkiva i slične biomedicinske i biotehnološke primene. Pored toga, ova tehnika je relativno jednostavna, ponovljiva i jeftina. Elektropisanje rastopljenim materijalom može se koristiti za izvlačenje mikrovlakana iz rastvora ili topljenog polimera kroz elektrostatičko polje, omogućavajući precizno nanošenje sa visokom tačnošću, što dovodi do veoma poroznih nosača koji olakšavaju ravnomernu raspodelu ćelija. Ovaj pregledni rad pruža uvid u nova teorijska i eksperimentalna saznanja vezana za elektropredenje u bliskom polju i elektropisanje rastopljenim materijalom, sa primenama u biotehnologiji i biomedicini, kao što su štampanje nosača za inženjerstvo tkiva i kulture ćelija, izrada obloga za rane i druge primene. Procesi su ukratko objašnjeni, a zatim su predstavljeni i najrelevantniji polimeri za biomedicinske primene. Na kraju, izloženi su aktuelni izazovi i predlozi za buduće pravce istraživanja.

Ključne reči: 3D porozni nosaci, nanovlakna, biomedicina

Phase transformations kinetics in barium titanate synthesis by mechanochemical processing

Nataša G. Đorđević[1], Srđan D. Matijašević[1], Nenad M. Vušović[2], Slavica R. Mihajlović[1] and Milica M. Vlahović[3]

[1]*Institute for Technology of Nuclear and Other Mineral Raw Materials, Belgrade, Serbia*
[2]*University of Belgrade, Technical Faculty in Bor, Bor, Serbia*
[3]*University of Belgrade, Institute of Chemistry, Technology and Metallurgy-National Institute of the Republic of Serbia, Belgrade, Serbia*

Abstract

This article presents the research results on a dry mechanochemical synthesis of barium titanate at a low temperature in which the reaction model and kinetics were determined during the activation of a powder mixture of titanium dioxide and barium oxide. The solid-state reaction achieved high degree of conversion (0.99). Successive analyses were conducted throughout the reaction, revealing the presence of both the starting powders and newly formed intermediate compounds. Phase transformations were monitored via X-ray diffraction, allowing the dynamics of the synthesis to be characterized. It was established that, for the given system, 440 min of mechanical activation in a high-energy vibration mill was required to complete the neutralization reaction and produce barium titanate. The reaction mixture composition was tracked by sampling at five intervals, confirming the presence of intermediate compounds and mapping the reaction pathway from the initial barium and titanium oxides to the final $BaTiO_3$ product.

Keywords: Solid-state reaction; BaO; TiO_2; reaction mechanism; kinetics; mechanochemical synthesis.

Available on-line at the Journal web address: http://www.ache.org.rs/HI/

ORIGINAL SCIENTIFIC PAPER

UDC: 544.275.7: 678.076

Hem. Ind. **79(4)** 219-231 (2025)

1. INTRODUCTION

Barium titanate is a material that has long been of great interest due to its properties. It is a very stable (mechanically and chemically) material with ferroelectric properties that is easy to prepare. It has found application in capacitors, superconductors, piezoelectric devices and PTC thermistors thanks to its high dielectric constant and low loss characteristics [1].

However, dielectric properties of barium titanate nanoparticles are greatly influenced by the applied synthesis method. There are several methods for the synthesis of barium titanate: hydrothermal, microwave-assisted hydrothermal, electrochemical, polymer precursor (Pechini) and the dry process synthesis, *i.e.* mechanochemical synthesis [2]. The aim of the latter studies was not to improve the dielectric properties of barium titanate, but to examine the possibility of obtaining it by a dry mechanochemical process and to monitor the kinetics of this process, which is continued in the present work.

Solid-state reactions have long captured the interest of researchers, particularly when these processes offer advantages such as simpler synthesis methods and reduced energy consumption compared to equivalent liquid-phase reactions. In recent years, mechanochemical synthesis has gained prominence in the production of various compounds. Understanding the specific parameters characteristic of solid-state matter is crucial for this type of research [3]. In addition to their advantages, solid-state reactions also have disadvantages that can make them challenging for certain applications [4] such as the often requirement for high temperatures (above 700 °C), presenting an additional economic

Corresponding author: Nataša G. Đorđević, Institute for Technology of Nuclear and Other Mineral Raw Materials, Franchet d'Esperey Blvd 86, Belgrade, Serbia; E-mail: djordjevic@itnms.ac.rs, https://orcid.org/0000-0002-2353-6751
Co-authors: S. D. Matijašević https://orcid.org/0000-0002-2353-6751, N. M. Vušović https://orcid.org/0000-0001-5246-4243, S. R. Mihajlović https://orcid.org/0000-0003-0904-3878, M. M. Vlahović https://orcid.org/0000-0002-7893-9101

Paper received: 22 October 2024; Paper accepted: 15 September 2025; Paper published: 25 September 2025.
https://doi.org/10.2298/HEMIND241022014D

investment in the desired process. Also, due to the necessary diffusion of reactants in the solid phase, the process rate is lower than in liquid-phase reactions. Due to the nature of the process, it is difficult to control the morphology of the product and formation of new, secondary phases due to incomplete reactions and diffusion limited processes. Another problem is the presence of mechanically hard, strongly bonded agglomerates at high processing temperatures, which are difficult to disintegrate. In contrast to solid-state reactions, in reactions that take place in sol-gel systems, better control of the final product in terms of homogeneity, stoichiometry and purity is possible.

Unlike liquid-phase reactions, where particles exhibit greater mobility due to the presence of ions in a fluid medium, solid-state reactions require direct contact between the initial components, which have not decomposed into ions. Not all reactions that occur in the liquid phase can be replicated in the solid phase. For such reactions to be feasible, they must be thermodynamically favourable, meaning that the activation energy necessary to initiate the chemical reaction must be adequately supplied. The energy input to the system has to meet or exceed the activation energy required for the reaction to proceed in the solid state [5-8].

When the starting components are ground in their solid state, bringing the particles into contact without dissociation and a chemical reaction occurring with sufficient energy input, the process is referred to as mechanochemical synthesis, which typically occurs in a reactor. These reactions differ from classic acid-base neutralization reactions. However, if the product of a mechanochemical reaction is salt formed from a base and an acid, with the initial components being a base anhydride and an acid anhydride, the reaction can still be categorized as a neutralization reaction. This reaction occurs due to the collision of mechanically activated particles, coupled with the sufficient energy input that leads to dissociation. The system becomes excited, the crystal lattice is disrupted, and new bonds are formed between particles. The presence of broken bonds and excited electrons, which act as carriers for the formation of new bonds, drives the reaction forward. In this context, only the Lewis definitions of acid-base reactions apply [9,10]. Bases serve as electron donors, while acids are electron acceptors under the newly established conditions of the mechanochemical neutralization reaction. The most significant factor influencing such complex reactions is the input of mechanical energy, which determines the reaction time necessary to achieve a complete reaction in the solid phase [11]. When titanium dioxide and barium oxide are the initial components in such a system, it is possible to synthesize barium titanate as the final product [12-17].

A mechanochemical process for obtaining barium bismuth titanate was described, whereby the synthesis was carried out in a planetary ball mill in air atmosphere followed by a comprehensive analysis of the resulting product [12]. Also, mechanochemical activation of a stoichiometric powder mixture $2Bi_2O_3{\cdot}3TiO_2$ was performed to obtain $Bi_4Ti_3O_{12}$ [13]. X-ray powder diffraction was used to monitor the intermediate as well as the final product, and the results were used to establish the kinetics of the process. In another study mechanochemical activation of a $2Bi_2O_3{\cdot}3TiO_2$ mixture was performed in a planetary ball mill and the crystallite size, amount of the amorphous phase and the transformed fraction were monitored using the X-ray diffraction analysis method. The authors established that there was deformation of the crystal lattice and destruction of the structure of the starting material [14]. Also, after a certain amount of grinding time, a very disordered, amorphous/nanocrystalline structure was obtained. There are some other papers describing synthesis of $BaTIO_3$ by solid-state synthesis methods with lower energy of activation of the initial samples; those methods produced poorly uniform $BaTiO_3$ at higher temperatures, with intermediate phases such as Ba_2TiO_4 or $BaTi_2O_5$ [18-20].However, in one study it was indicated that $BaTiO_3$ can be obtained at lower temperatures in contrast to results previously reported in the literature [21].

To comprehend this synthesis process fully, it is essential to identify intermediate compounds and monitor both the reaction mechanism and kinetics [22-28]. The aim of this research was to derive the reaction mechanism and investigate the kinetics of barium titanate synthesis via mechanochemical activation in a vibrating mill with rings.

2. EXPERIMENTAL

Mechanochemical neutralization reactions involving barium oxide (BaO) and titanium dioxide (TiO_2) were conducted using a high-energy vibration mill with torsion springs and annular working elements, manufactured by KHD Humboldt Wedag A.G., Germany (model MH954/3). The mill comprises a base and a horizontally positioned shutter. The working vessel is a cylindrical container made of stainless steel, with a depth of 40 mm and an internal diameter of 170 mm. The

working elements consist of two freely moving concentric rings, also made of stainless steel, with a total weight of 3 kg. The grinding process lasted for 440 min, with a motor power of 0.8 kW, the energy input to the system equivalent to a grinding disc speed of 800 rpm.

Atomic absorption spectrophotometry (AAS) was selected as a precise and reliable method for monitoring the reaction kinetics, and based on literature data and blank tests, 10 % acetic acid was chosen as the most suitable solvent. Chemical analysis was carried out using a Perkin Elmer Analyst 703 (USA) atomic absorption spectrophotometer. The concentrations of unreacted Ba^{2+} (λ = 553.6 nm) and Ti^{4+} (λ = 364.3 nm) ions were determined in the reaction mixture at specific time intervals, after dissolving the samples in this solvent. In this solution, only the oxide of the corresponding metal dissolves, forming acetate, while titanium dioxide and possibly synthesized titanate remain undissolved as a product of the reaction. The measurement uncertainty was 0.49 %. Practically, kinetic diagrams of the mechanochemical neutralization reactions were determined as follows: during the experiment, samples of the system in the amount of 0.1 g (analytical balance AE 165 MX 104 (Mettler, Switzerland) were taken at certain time intervals. The samples were dissolved in 250 ml of 10 % acetic acid solution. After filtering the suspension in the clear solution, the content of the appropriate alkaline metal (Ba^{2+}) and titanium was determined by using an AAS. Based on the obtained results, the degree of synthesis of the appropriate sample was calculated. From a set of calculations for the time series of mechanochemical synthesis, a kinetic diagram for the corresponding mechanochemical reactions was constructed.

The identification of crystalline phases formed during the solid-state reaction was carried out using X-ray powder diffraction (XRD). The samples were recorded and analysed using an automated diffractometer PW-1710 (Philips, Netherlands) equipped with a copper tube, operating at 40 kV and 35 mA. The device features a graphite monochromator and a proportional counter filled with xenon gas. The scanning angle (2θ) ranged from 4 to 65° with step of 0.02° and holding time 0.5 s. Phase identification was achieved by comparing the results with standard patterns from the JCPDS database. The XRD analysis enabled the determination of the types and quantities of crystalline phases present. Detection limit was below 2 % [29].

For these experiments, barium oxide (BaO *p.a.*, Fluka, Switzerland) was used as the basic reactant, and titanium dioxide (TiO_2 *p.a.*, Merck, Germany) as the acidic reactant. No specific preconditions regarding the crystal structure or particle size distribution of the starting components were imposed. The used mechanochemical reactor was designed for an optimal batch size of 50 to 150 g. In this study, 0.5 mol (76.7 g) of BaO and 0.5 mol (39.9 g) of TiO_2, giving a total of 116.6 g as calculated from the stoichiometric Equation (1), were used, which is within the optimal range.

$$BaO_{(s)} + TiO_{2(s)} = BaTiO_{3(s)}(BaO{\cdot}TiO_2) \quad (1)$$

To identify the crystal structure of BaO, a qualitative XRD analysis was performed, as shown in Table 1 (*d*-interplanar spacing, 2θ - diffraction angle) and Figure 1.

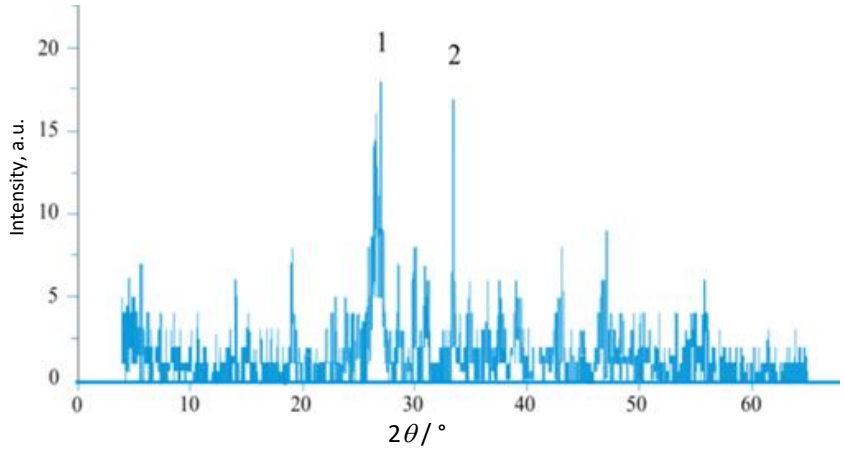

Figure 1. XRD analysis of BaO, (JCPDS-No. 22-1056)

Table 1. XRD peaks of BaO

Peak (from Fig. 1)	*d* / nm	2θ / °
1	0.32895	27.085
2	0.26771	33.445

Analysing the X-ray diffraction (XRD) pattern in Figure 1 confirmed the presence of a significant amount of amorphous material. The diffraction peaks (d-values 3.2895 and 2.6771) indicate that the analysed sample corresponds to (poorly crystallized) barium oxide (BaO), (JCPDS-No. 22-1056). The XRD pattern of the starting titanium dioxide and its characteristic diffraction peaks are provided in Table 2 and Figure 2.

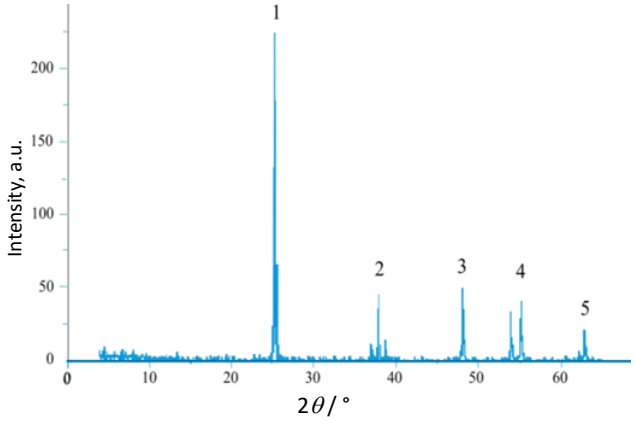

Figure 2. XRD analysis of TiO_2, (JCPDS card No. 21-1272)

Table 2. XRD peaks of TiO_2

Peak (from Fig. 2)	*d* / nm	2θ / °
1	0.35133	25.330
2	0.23778	37.805
3	0.18926	48.035
4	0.16667	55.055
5	0.14806	62.700

Throughout 440 min required for the complete synthesis of barium titanate via the mechanochemical process, samples were taken five times (at 30, 110, 200, 290, and 440 min) and each was analysed using XRD. The atomic absorption spectrophotometric (AAS) method was employed to analyse the chemical composition of the system corresponding to the activation time.

Based on the chemical analysis results, the degree of synthesis *S* [30], was calculated using Equation (2):

$$S = \left(1 - \frac{0.25\left(m - bm_{Ti}\right)}{m_0 a}\right) 100 \quad (2)$$

where m_{Ti} / g L^{-1} is the mass concentration of titanium in the solution, m / g L^{-1} is the concentration of barium in solution, m_0 / g L^{-1} is the mass concentration of the initial sample, a denotes the mass fraction of barium in the initial sample with the value of 0.5885, b represents the equivalence factor for barium's participation in the assumed intermediate compound of stoichiometric composition $BaTiO_3$, with b = 2.8604 for the tested reaction system (BaO + TiO_2). The fundamental chemical-thermodynamic data, along with the corresponding equilibrium constant for the neutralization reaction between BaO and TiO_2, are as follows [31]: ΔH_r = -161.5 kJ mol^{-1}, ΔS^o_r = -12.69 J mol^{-1}, ΔG^o_r = -157.8 kJ mol^{-1}, $K_r = 1.31 \times 10^{28}$.

All data refer to a temperature of 20 °C: $\Delta H°_r$ (change in the enthalpy of the reaction), $\Delta S°_r$ (change in the entropy of the reaction), $\Delta G°_r$ (change in the Gibbs free energy of the reaction), and K_r (equilibrium constant of the reaction). All experiments were performed in triplicate.

3. RESULTS AND DISCUSSION

In our research, we also used X-ray structural analysis to monitor the results of activation and final synthesis as a function of activation time. To monitor dynamics of the formation of a new phase (*i.e.* the reaction product), samples of the reaction mixture were taken at specific time intervals (30 to 440 min) throughout the experiments, followed by qualitative XRD analyses. This approach allowed for the identification and monitoring of both the initial components and the products of the mechanochemical neutralization reactions. The XRD analysis of the sample after 30 min of mechanochemical activation was shown in a previous study [32]. The results demonstrated that high-energy milling

induced significant changes in the crystal structure of the starting components, with trace amounts of barium titanate being detected.

The next sample was taken from the reaction system after 110 min of mechanochemical treatment. The XRD analysis of this sample is presented in Table 3 and Figure 3.

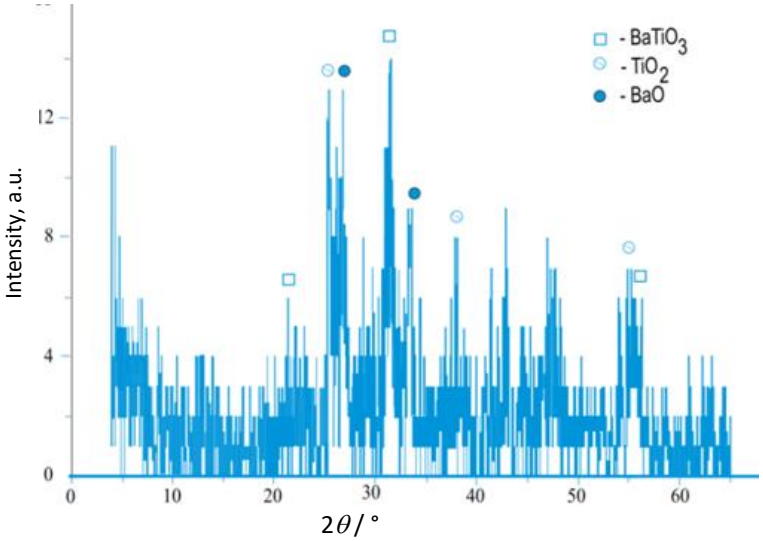

Figure 3. XRD analysis of the reaction system ($BaO+TiO_2$) after 110 min of the mechanochemical treatment

Table 3. XRD peaks of the reaction system ($BaO+TiO_2$) after 110 min of the treatment (8 peaks registered)

Peak (from Fig. 3)	Assigned phase	*d* / nm	2θ / °
1-□	$BaTiO_3$	0.39852	22.29
2-○	TiO_2	0.35093	25.36
3-●	BaO	0.33142	26.88
4-□	$BaTiO_3$	0.28480	31.38
5-●	BaO	0.26873	33.31
6-□	$BaTiO_3$	0.23432	38.38
7-□	$BaTiO_3$	0.16541	55.51
8-○	TiO_2	0.16060	57.32

XRD peaks of the investigated system after 200 min of mechanochemical treatment are given in Table 4. As illustrated in Figure 4, the crystalline structure of the reaction system continues to degrade, bringing the entire reaction mixture to an almost entirely amorphous state.

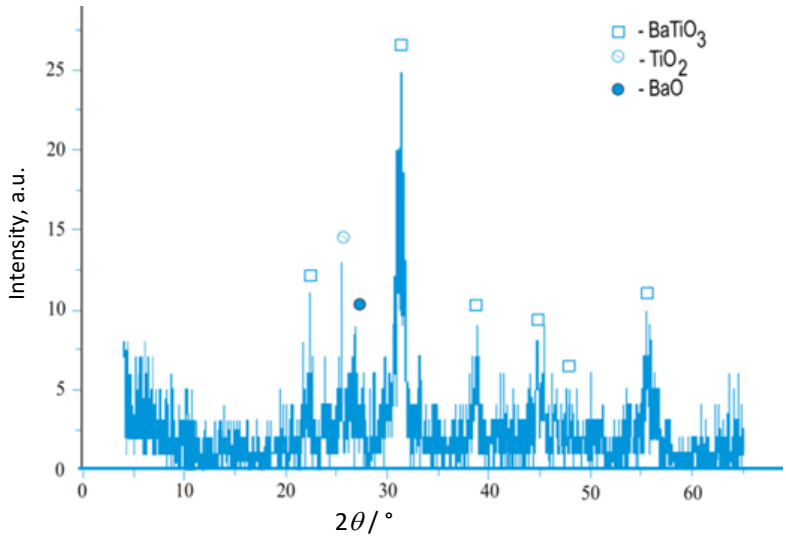

Figure 4. XRD analysis of the reaction system ($BaO+TiO_2$) after 200 min of the mechanochemical treatment

Table 4. XRD peaks of the reaction system ($BaO+TiO_2$) after 200 min of the treatment (8 peaks registered)

Peak (from Fig. 4)	Assigned phase	*d* / nm	2θ / °
1-□	$BaTiO_3$	0.40145	22.12
2-o	TiO_2	0.35031	25.40
3-●	BaO	0.33105	26.91
4-□	$BaTiO_3$	0.28295	31.59
5-□	$BaTiO_3$	0.23196	38.79
6-□	$BaTiO_3$	0.20133	44.99
7-□	$BaTiO_3$	0.19235	47.21
8-□	$BaTiO_3$	0.16588	55.34

Despite this, the detected peaks still indicate the presence of the starting reactants, barium oxide and titanium dioxide. It is noteworthy that the number of peaks associated with noise has significantly decreased, which clearly indicates a dynamic restructuring of the reaction system. The presence of an amorphous state in the system does not necessarily contradict previous observations; it may simply represent an intermediate phase in the reaction process leading to the formation of the final product's structure. Secondary phases such as $BaTi_2O_5$, Ba_2TiO_4 were not found, they are either absent or below the detection limit of the methods used. The subsequent XRD analysis was conducted on a sample taken from the reaction system after 200 min of mechanochemical activation.

The processes observed in the XRD analysis of the sample treated for 110 min continue and become even more pronounced. The main peak of barium titanate (*d*-value 2.8295) shows a noticeable increase in intensity, and all six characteristic peaks for barium titanate are clearly detected. The characteristic peaks of the reactants have largely disappeared, and the number of peaks associated with noise has further decreased. This indicates that after 200 min of mechanochemical treatment, a new phase- barium titanate-has clearly formed and dominates the reaction system. The increasing intensity of the characteristic peaks suggests the development and ordering of the crystal structure of the newly formed compound.

Table 5 and Figure 5 show the XRD analysis of the sample that underwent mechanochemical treatment for 290 min.

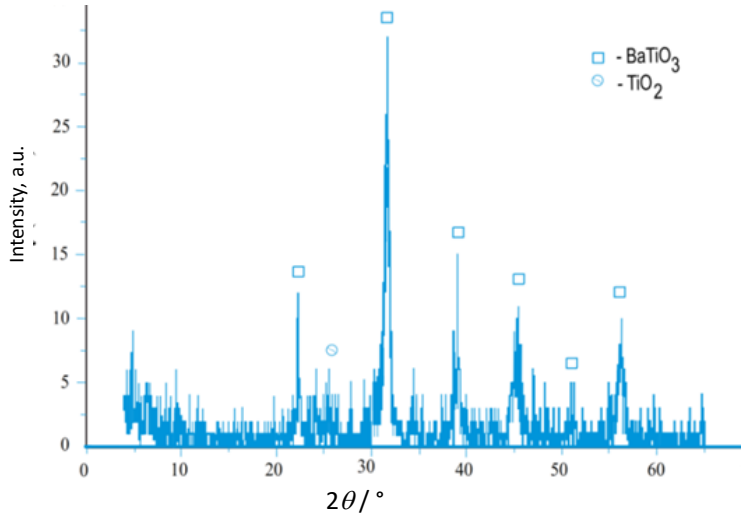

Figure 5. XRD analysis of the reaction system ($BaO+TiO_2$) after 290 min of the mechanochemical treatment

Table 5. XRD peaks of the reaction system ($BaO+TiO_2$) after 290 min of the treatment (7 peaks registered)

Peak (from Fig. 5)	Assigned phase	*d (nm*	2θ / °
1-□	$BaTiO_3$	0.39887	22.27
2-o	TiO_2	0.34910	25.49
3-□	$BaTiO_3$	0.28208	31.69
4-□	$BaTiO_3$	0.23017	39.10
5-□	$BaTiO_3$	0.20038	45.21
6-□	$BaTiO_3$	0.19306	47.03
7-□	$BaTiO_3$	0.16322	56.32

At this time, a well-defined crystal structure of the mechanochemical reaction product, barium titanate, had formed from the starting oxides BaO and TiO_2. Traces of the starting reactants were only observed in a remaining peak corresponding to titanium dioxide, while the increased number of peaks associated with the noise domain suggests that the mechanochemical synthesis of barium titanate was not yet complete. Chemical analyses confirming the absence of one of the reactants (barium oxide), along with the fact that the mechanochemical reaction was conducted with a stoichiometric ratio of reactants (as per Equation (1)), are reliable indicators that the mechanochemical neutralization reaction between the acid anhydride (TiO_2) and the oxide base hydroxide (BaO) was fully realized.

Figure 6 and Table 6 display the XRD analysis of the reaction product (Equation (1)) obtained from the mechanochemical reaction of BaO and TiO_2 after 440 min of treatment. Chemical analysis determined that the sample contained only 1.3 % of the starting barium oxide compared to the initial amount, indicating that 440 min represents the duration required for complete synthesis, considering the detection limit of the methods.

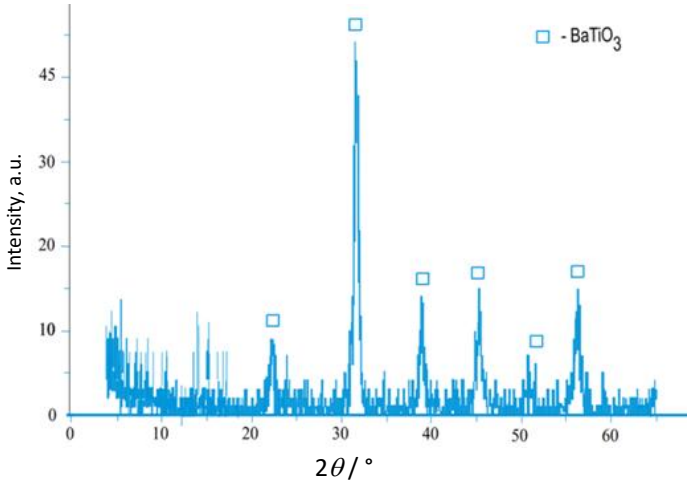

Figure 6. XRD analysis of the reaction system (BaO+TiO_2) after 440 min of the mechanochemical treatment

Table 6. XRD peaks of the reaction system (BaO+TiO_2) after 440 min of the treatment

Peak (from Fig. 6)	Assigned phase	*d* / nm	2θ / °
1-□	$BaTiO_3$	0.39905	22.26
2-□	$BaTiO_3$	0.28217	31.68
3-□	$BaTiO_3$	0.23128	38.91
4-□	$BaTiO_3$	0.19936	45.46
5-□	$BaTiO_3$	0.17929	50.89
6-□	$BaTiO_3$	0.16343	56.24

Analysis of the diffraction maxima (Figure 6) revealed that the peak intensities correspond to the crystalline phases of barium titanate ($BaTiO_3$, *i.e* $BaO{\cdot}TiO_2$). This suggests that after 440 min of mechanochemical treatment, the reaction described in Equation (1), has essentially reached completion, considering the detection limit of methods. The well-defined diffraction peaks of barium titanate, along with the absence of peaks corresponding to the starting reactants—barium oxide and titanium dioxide - could indicate the successful completion of the mechanochemical synthesis of barium titanate. Considering that the vibrating mill we used in researching the possibility of mechanochemical synthesis of barium titanate, at the end of the activation it was determined by X-ray structural analysis that the product is almost completely obtained in a stable crystalline state with the chemical formula $BaTiO_3$.

A detailed analysis of the diagrams presented in Figures 1 to 6 provides valuable insights into the mechanochemical synthesis of barium titanate ($BaTiO_3$). By analysing the progression of the crystal structures and recognizability of the peaks, the entire process can be divided into three experimental stages based on XRD and AAS analyses:

1. First stage (up to 30 min): During this initial phase, the crystal structure of the reaction system collapses significantly. It is challenging to draw conclusions about the crystalline and chemical structures due to the extensive amorphization of the reactants.

2. Second stage (up to 110 min): This phase represents the "transition state" of the reaction system. At this point, it remains difficult to ascertain the crystalline and chemical structures. The mechanical energy introduced during this stage primarily contributes to the destruction of the reactants' crystal structures. The mechanochemical activation accumulates mechanical energy in the material, leading to increased potential energy and chemical reactivity.
   The peak of energy flow in the second stage represents the minimum amount of energy required to transform reactants into products in a chemical reaction. The value of the activation energy is equivalent to the difference in potential energy between particles in an intermediate configuration (known as the transition state or activated complex) and particles of reactants in their initial state. The activation energy thus can be visualized as a barrier that must be overcome by reactants before products can be formed [32].
3. Third stage (after 200 min): In this stage, formation of a distinct crystal structure of barium titanate becomes evident. Diffraction maxima at d-values characteristic for barium titanate increase in intensity. The energy introduced during the third stage, along with the energy accumulated in previous stages, is primarily used for forming stable chemical bonds and constructing the crystal structure of the product. The remaining reactants and the activated complex are sufficiently exciting, ensuring that the newly formed crystal structure of barium titanate remains intact despite the continued mechanical energy input.

Throughout the activation process, mechanical energy is introduced into the reaction system, which drives these transitions. Initially, in the first stage, energy is mainly expended on the breakdown of the crystal structures of the starting reactants, causing significant amorphization [33,34]. Mechanochemical activation also promotes transformation of the released mechanical energy into stored energy within the material, manifesting as accumulated crystal lattice distortions and an increase in the specific surface area. This enhances the potential energy and chemical reactivity of the material.

The second stage of the process represents the peak of this energy flow, where the entire reaction mass enters a transition state. After 110 min of the mechanochemical treatment, the chemical analysis of the reaction mixture sample dissolved in a 10 % acetic acid solution revealed the presence of both barium and titanium in the solution. Notably, barium titanate and titanium dioxide remained insoluble in the dilute acid, leading to two important conclusions:

- Titanium detected in the solution does not originate from free titanium dioxide or barium titanate.
- Barium detected does not come from barium titanate; part of it likely originates from unreacted barium oxide, which had not yet fully participated in the reaction described by Equation (1).

These two findings suggest the total titanium present in the acetic acid solution, along with the corresponding stoichiometric portion of barium, originates from a complex intermediate compound, *$BaO*TiO_2$*, with amorphous characteristics (hence undetectable by XRD) and partial solubility in 10 % acetic acid. Repeating XRD measurements after a three-month relaxation period did not show any changes, indicating relative stability of this intermediate phase. Based on both XRD and chemical analyses, the reaction system after 110 min of the treatment can be described as consisting of the following phases:

- amorphous titanium dioxide (TiO_2), insoluble in acetic acid,
- amorphous barium oxide (BaO), soluble in acetic acid,
- the amorphous activated complex (*$BaO*TiO_2$*), partially soluble in acetic acid,
- crystalline barium titanate ($BaTiO_3$), insoluble in acetic acid.

The third stage of the process is dominated by the formation of a clear and recognizable crystalline structure of barium titanate. From the amorphous structure characteristic for the second stage, the continued mechanochemical treatment results in the gradual emergence and intensification of diffraction maxima at d-values (Table 6) characteristic for barium titanate (JCPDS card No. 5-626). During this stage, the energy introduced into the reaction system via the mechanochemical reactor, along with the energy accumulated in the previous two stages, is largely consumed in forming stable chemical bonds and constructing the crystalline structure of the chemical reaction product. The remaining reactants and the assumed activated complex become so energetically excited that the formation of the product, particularly its well-defined crystalline structure, remains unaffected even by the direct influence of mechanical energy on the newly formed product crystals. The third stage represents formation of the crystalline structure during the mechanochemical synthesis, as the process of growth and development of the compound's crystal structure occurs precisely while the compound itself is being subjected to mechanical energy.

Based on the performed chemical analyses of the samples taken at different time intervals, dependence of the degree of synthesis (*S* / %) on the mechanochemical treatment duration was determined and the resulting kinetic diagram is shown in Figure 7.

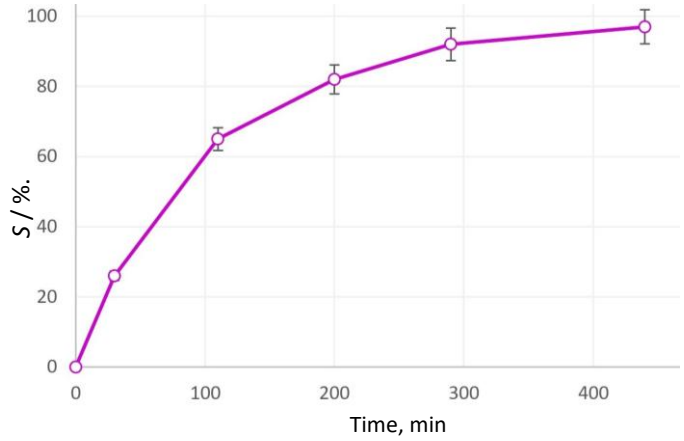

Figure 7. Kinetics of the mechanochemical synthesis of barium titanate

Based on the obtained kinetic diagram, the shape of the curve could be analysed. Given the nature of the chemical reaction, it can first be noted that the investigated mechanochemical process resembles a typical second-order reaction of the form: A + B → products.

However, considering the general form of the chemical reaction (Equation (1)) and the kinetic diagram, and the diffusion driven nature of the process it can be concluded that the mechanochemical process can be approximated as a pseudo-first-order reaction [21,35]. The results, which are used to generate the diagram in Figure 8, align well with the mathematical relations applicable to first-order reactions of the form: A → products, where only one reactant is involved, and the reaction rate is directly proportional to the concentration of that reactant, Equation (3) [36]:

$$-\frac{\mathrm{d}c}{\mathrm{d}t} = kc \tag{3}$$

where *c* represents the concentration of the reactant, *t* is the time, and *k* is the reaction rate constant. Introducing the variable *x*, defined as the amount of reactant consumed in the reaction over time *t*, and after performing the integration, Equation (4) is obtained:

$$\ln\frac{a}{a-x} = kt \tag{4}$$

i.e. Equation (5)*:*

$$\ln\frac{1}{1-S/100} = kt \tag{5}$$

where *S* / %, represents the degree of synthesis achieved at the time *t*. When the Equation (5) is applied to the results presented in Figure 7, the resulting diagram shown in Figure 8 is obtained.

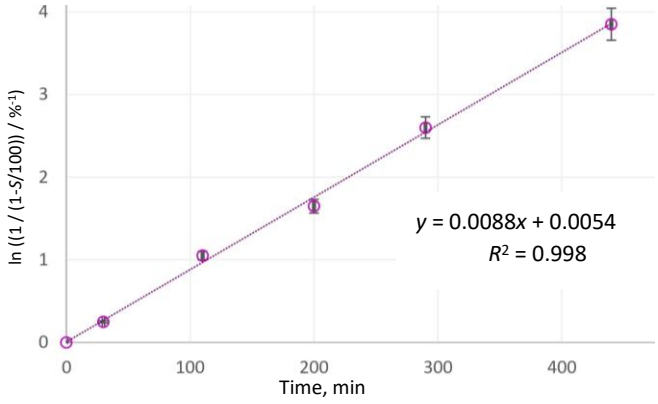

Figure 8. Application of Equation (5) (line) on the experimental results of the mechanochemical synthesis (symbols)

A linear dependence in Figure 8 is evident, as mathematically expressed by Equations (4) and (5), where the rate constant *k* in this graphical representation corresponds to the slope of the line. This confirms that the mechanochemical neutralization reaction (Equation (1)), *i.e.* the mechanochemical synthesis of barium titanate follows the kinetic law of a first-order reaction. The fitted line showed a negligible intercept (0.0054), which can be attributed to experimental uncertainty, while the theoretical model predicts passage through the origin (0,0).

Given that the reaction begins with pure and inactivated reactants, which exist as elementary particles (BaO and TiO_2) during the mechanochemical process, it is concluded that the synthesis of barium titanate proceeds through two kinetic phases. The first phase involves collisions between the molecules of the two reactants, forming an activated complex that stoichiometrically corresponds to barium titanate but represents a unique compound in terms of its structure and chemical bonds, while the second phase involves the introduction of energy into the system, which overcomes the energy barrier along the reaction pathway, driving the chemical reaction irreversibly toward the formation of the desired product, Equation (6):

$$BaO+TiO_2 \xrightarrow{k_0} *BaO*TiO_2* \xrightarrow{k_1} BaTiO_3 \quad (6)$$

where k_0 and k are the rate constants of the first and second phases of the reaction, respectively. According to the conclusion that the reaction follows first-order kinetics, the second stage of reaction (6) represents the slower phase of the overall mechanochemical synthesis of barium titanate, which means that $k_0 >> k_1$.

It can be concluded that the activation energy required to initiate the first phase of the reaction is significantly lower than the activation energy needed to convert the activated complex into the final product of barium titanate, *i.e.* to complete the second phase. The hypothesis regarding the existence of an activated complex (as an intermediate product) during mechanochemical synthesis reactions, coupled with the fact that XRD analysis of the samples after 110 min of the mechanochemical treatment did not show any changes even when repeated three months after the synthesis, supports the conclusion about the stability of the activated complex and the irreversibility of the first-phase reactions (Equation (6)), despite the transition of the reaction system from a lower to a higher energy state. The diagram showing the change in potential energy of the reactants during the mechanochemical reaction is illustrated in Figure 9.

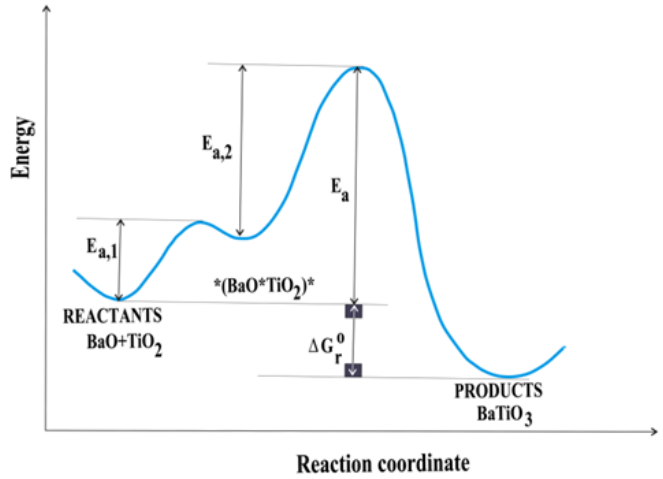

Figure 9.Change in potential energy along the reaction coordinate

In this study, the experiments were not conducted at varying temperatures, so it is not possible to quantitatively determine the activation energies. However, the difference in potential energy between the reactants and the products corresponds to the Gibbs free energy of reaction (Equation (1)), with a value of $\Delta G°_r$= -157.8 kJ mol^{-1}. The diagram representing the potential energies of the reactants and the activated complex illustrates the reaction mechanism of the mechanochemical synthesis of barium titanate, as depicted in reaction (Equation 6).

Therefore, it can be concluded that the activation energy for the first phase of reaction (Equation 6) is lower than that of the second phase. This difference in activation energies causes the rate constant for the second phase to be lower than that of the first phase, leading to the kinetic profile of a first-order reaction.

The solid-state reactions initiated by intensive milling in high-energy mills could be good choice for $BaTiO_3$ powder preparation. Intensive milling (mechanical activation) of the starting materials increases the area of contact between the reactant powder particles due to reduction in particle size and allows surfaces to come into contact [18]. In this study, high-energy mechanical activation accelerated the formation of $BaTiO_3$ without secondary phases, while previous reports also indicate that such activation can reduce the formation temperature [21].

4. CONCLUSION

The results of the experimental research presented in this paper have shown that $BaTiO_3$ can be obtained through a dry mechanochemical process by a neutralization reaction between BaO, as the basic reactant, and TiO_2, as the acidic reactant. Identification of crystalline phases formed during the reaction; monitoring of phase transformations and determination of the synthesis dynamics were successfully performed by using XRD analyses. Composition of the reaction mixture during the synthesis of $BaTiO_3$, was quantitatively analysed by AAS to determine the reaction model and reaction kinetics. To achieve a high conversion rate of 0.99, which can be considered a complete synthesis of $BaTiO_3$, it is necessary for the activation process to last 440 min. By analysing the progression of the formation of crystalline structures and by their identification, the entire process of obtaining $BaTiO_3$ can be divided into three stages: 1. the crystal structure of the BaO-TiO_2 reaction system is disrupted; 2. accumulation of mechanical energy increases the system's potential energy and chemical reactivity forming intermediate compounds; 3. formation of crystalline $BaTiO_3$ becomes evident. This approach highlights mechanochemical synthesis as an energy-efficient route enabling precise monitoring of reaction kinetics, while the obtained results provide a basis for optimizing similar solid-state reactions and potential industrial applications.

Acknowledgement: *The authors would like to thank the Ministry of Science, Technological Development and Innovation of the Republic of Serbia for financially supporting this research (Grant Nos: 451-03-66/2024-03/200023, 451-03-65/2024-03/200131, 451-03-66/2024-03/200026).*

REFERENCES

[1] Vijatović M, Bobić J, Stojanović B. History and Challenges of Barium Titanate: Part I. Sci Sinter. 2008; 10L: 155-165 https://doi.org/10.2298/SOS0802155V

[2] Prado L, Resende N, Silva R, Egues S, Salazar-Banda G. Influence of the synthesis method on the preparation of barium titanate nanoparticles. Chem Eng Process: Process Intensif**.** 2016; 103: 12-20 https://doi.org/10.1016/j.cep.2015.09.011

[3] Kubota K, Seo T, Koide K, Hasegawa Y, Ito H. Olefin-accelerated solid-state C-N cross-coupling reactions using mechanochemistry. Nat Commun. 2019; 10: 111 https://doi.org/10.1038/s41467-018-08017-9

[4] Zhang X, Zhou KS, Liu M, Deng CM, Deng CG,Deng ZQ. Adsorbability and spreadability of calcium-magnesium-alumino-silicate (CMAS) on Al-modified 7YSZ thermal barrier coating. Ceram Int. 2016; 42(16): 19349-19356 https://doi.org/10.1016/j.ceramint.2016.09.106

[5] Oleynikov NN, Tretyakov YD, Shumyantzev AV. Concerning the activation energy of solid state reactions. J Solid State Chem. 1974;11 (4):340-343 https://doi.org/10.1016/S0022-4596(74)80039-3

[6] Gomes W. Definition of Rate Constant and Activation Energy in Solid State Reactions. Nature. 1961;192: 865-866 https://doi.org/10.1038/192865a0

[7] Behrens M. Meso-and nano-structuring of industrial Cu/ZnO/(Al_2O_3) catalysts. J Catal.2009;267 (1):24-29 https://doi.org/10.1016/j.jcat.2009.07.009

[8] Criado JM. On the determination of the activation energy of solid-state reactions from the maximum reaction rate of isothermal runs. J Therm Anal. 1981; 21: 155-157 https://doi.org/10.1007/BF01913708

[9] Lewis GN. The atom and the molecule. J Am Chem Soc. 1916; 38 (4): 762-785 https://doi.org/10.1021/ja02261a002

[10] Avvakumov EG. Mekhanicheskiemetodyaktivaciikhimicheskihprocesov.2rd ed., Novosibirsk, Nauka; 1986 (in Russian)

[11] Boldyrev VV. Mechanochemistry and mechanical activation of solids. Solid State Ion. 1993; 63-65:537-543 https://doi.org/10.1016/0167-2738(93)90157-X

[12] Lazarević ZŽ, Bobić J, Romčević NŽ, Paunović N, Stojanović BD. Study of Barium Bismuth Titanate Prepared by Mechanochemical Synthesis. Sci Sinter.2009; 41: 329-335 https://doi.org/10.2298/SOS0903329L

[13] Obradović N, Filipović S, Pavlović V, Mitrić M, Marković S, Mitić V,Đorđević N, Ristić MM. Isothermal sintering of barium-zinc-titanate ceramics. Ceram Int. 2011; 37(1): 21-27 https://doi.org/10.1016/j.ceramint.2010.07.001

[14] Zdujić M, Poleti D, Jovalekić C, Karanović L. The evolution of structure induced by intensive milling in the system $2Bi_2O_3•3TiO_2$. J Non-Cryst Solids. 2006;352 (28-29): 3058-3068 https://doi.org/10.1016/j.jnoncrysol.2006.03.072
[15] Buscaglia V, Randall CA. Size and scaling effects in barium titanate. J Eur Ceram. 2020; 40: 3744-3758 https://doi.org/10.1016/j.jeurceramsoc.2020.01.021
[16] Reynolds GJ. Electrical Properties of Thin-Film Capacitors Fabricated Using High Temperature Sputtered Modified Barium titanate. Materials. 2012; 5: 644-660 https://doi.org/10.3390/ma5040644
[17] Wei X, Liu Y, Zhao D, Ge SS. 3D printing of piezoelectric barium tinatate with high density form milled powders. J Eur Ceram. 2020; 43 (8):3297-3306 https://doi.org/10.1016/j.jeurceramsoc.2020.06.021
[18] Brzozowski E, Castro MS. Synthesis of barium titanate improved by modications in the kinetics of the solid state reaction. J Eur Ceram. 2000;20: 2347-2351 https://doi.org/10.1016/S0955-2219(00)00148-5
[19] Kozawa T, Onda A, Yanagisawa K. Accelerated formation of barium titanate by solid-state reaction in water vapour atmosphere. J Eur Ceram. 2009; 29: 3259-3264 https://doi.org/10.1016/j.jeurceramsoc.2009.05.031
[20] Apaydin F, Parlak TT, Yıldız K. Low temperature formation of barium titanate in solid state reaction by mechanical activation of $BaCO_3$ and TiO_2. Mater Res Express. 2019; 6: 126330 https://doi.org/10.1088/2053-1591/ab6c0d
[21] Ashiri R. On the solid-state formation of BaTiO3 nanocrystals from mechanically activated $BaCO_3$ and TiO_2 powders: innovative mechanochemical processing, the mechanism involved, and phase and nanostructure evolutions. RSC Adv. 2016; 6: 17138 https://doi.org/10.1039/C5RA22942A
[22] Ziegmann A, Schubert DW. Influence of the particle size and the filing degree of barium titanate filled silicone elastomers used as potential dielectric elastomers on the mechanical properties and the crosslinking density. MaterToday Commun. 2018; 14: 90-98 https://doi.org/10.1016/j.mtcomm.2017.12.013
[23] Uttam R, Yadav N, Kumar S, Dhar R. Strengthening of columnar hexagonal phase of a room temperature discotic liquid crystalline material by using ferroelectric barium titanate nanoparticles. J Mol Liq. 2019; 294: 111609 https://doi.org/10.1016/j.molliq.2019.111609
[24] Gu L, Li T, Xu Y, Sun C, Yang Z, Zhu D, Chen D. Effects of the particle size of $BaTiO_3$ fillers on fabrication and dielectric properties of $BaTiO_3$/Polymer/Al films for capacitor energy-storage application. Materials. 2019;12: 439 https://doi.org/10.3390/ma12030439
[25] Binhayeeniyi N, Sukwisute P, Nawae S, Muensit N. Energy conversion capacity of barium zirconatetitanate. Materials. 2020; 13: 315 https://doi.org/10.3390/ma13020315
[26] Polley C, Distler T, Detsch R, Lund H, Springer A, Boccaccini AR, Seitz H. 3D Printing of Piezoelectric Barium Titanate-Hydroxyapatite Scaffolds with Interconnected Porosity for Bone Tissue Engineering. Materials.2020; 13: 1773 https://doi.org/10.3390/ma13071773
[27] Jelinek M, Vanek P, Tolde Z. Buixaderas E, Kocourek T, Studnicka V, Drahokoupil J, Petzelt J, Remsa J, Tyunina M. PLD preparet bioactive $BaTiO_3$ films on TiNb implants. Mater Sci Eng. C. 2017; 70: 334-339 https://doi.org/10.1016/j.msec.2016.08.072
[28] Stojanović BD, Simoes AZ, Paiva-Santos CO, Jovalekić C, Mitic VV, Varela JA. Mechanochemical synthesis of barium titanate. J Eur Ceram. 2005; 25: 1985-1989 https://doi.org/10.1016/j.jeurceramsoc.2005.03.003
[29] Đorđević NG, Matijašević SD, Mihajlovic SR, Stojanović JN, Radulović AM, Savić LjB. The Effect of Particle Size on the Crystallization $LiGe_2(PO_4)_3$ Phase from Glass. Sci Sinter. 2025; 57: 43-52 https://doi.org/10.2298/SOS231111064D
[30] Vidojkovic VM. Proučavanje mehanizma i kinetike mehanohemijske sinteze neorganskih soli kod reakcija neutralizacije, Doktorska disertacija, Univerzitet u Beogradu, 2001.
[31] Roine A. HSC Chemistry for Windows Chemical Reaction and Equilibrium Software with Extensive Database. Version 2.03, Outokumpu Research Oy, Pori, Finland 1994
[32] Ptaček P, Opravil T, Šoukal F. Introducing the Effective Mass of Activated Complex and the Discussion on the Wave Function of this Instanton. IntechOpen, London UK, 2018. https://doi.org/10.5772/intechopen.70734
[33] Đorđević N, Vlahović M, Mihajlović S. X-ray structural analysis of the BaO and TiO_2 starting compounds and initial mechanochemical activation. Undeground Mining Engineering.2023; 42: 37-46 https://doi.org/10.5937/podrad2342037Q
[34] Botta PM, Aglietti EF, López JMP. Mechanochemical effects on the kinetics of zinc titanate formation. J Mater Sci. 2004; 39:5195-5199 https://doi.org/10.1023/B:JMSC.0000039209.48875.25
[35] Revellame ED, Fortela DL, Sharp W, Hernandez R, Zappi ME. Adsorption kinetic modeling using pseudo-first order and pseudo-second order rate laws: A review. Clean Eng Technol. 2020; 1: 100032 https://doi.org/10.1016/j.clet.2020.100032
[36] Dondur V. Hemijska kinetika, Beograd, Fakultet za fizičku-hemiju; 1992 (in Serbian)

Kinetika faznih transformacija u sintezi barijum-titanata mehanohemijskom obradom

Nataša G. Đorđević[1], Srđan D. Matijašević[1], Nenad M. Vušović[2], Slavica R. Mihajlović[1] i Milica M. Vlahović[4]

[1]Institut za tehnologiju nuklearnih i drugih mineralnih sirovina, Beograd, Srbija
[2]Univerzitet u Beogradu, Tehnički fakultet u Boru, Bor, Srbija
[3]Univerzitet u Beogradu, Institut za hemiju, tehnologiju i metalurgiju-Institut od nacionalnog značaja Republike Srbije, Beograd, Srbija

(Naučni rad)

Izvod

U radu su prikazani rezultati istraživanja sinteze barijum titanata ($BaTiO_3$) na niskim temperaturama suvim mehanohemijskim postupkom. Bazni reaktant u eksperimentima je barijum oksid (BaO), dok je kao kiseli reaktant bio titanijum dioksid (TiO_2). Optimalna količina polaznih uzoraka za aktivaciju je bila od 50 do 150 g. U cilju praćenja reakcije između polaznih uzoraka, reakciona smeša je uzorkovana nakon 30, 110, 200, 290 i 440 min aktivacije. Za reakcije neutralizacije između BaO i TiO_2 korišćen je visokoenergetski vibracioni mlin sa torzionim oprugama i prstenastim radnim elementima. Produkti mehanohemijske reakcije su hemijski analizirani u cilju identifikacije neizreagovanih ostataka oksida zemnoalkalnih metala čija količina može da ukaže na stepen konverzije ili sinteze. Za identifikaciju kristalnih formi nastalih tokom reakcije i praćenje faznih transformacija korišćena je difrakciona rendgenska analiza praha (engl. X-ray powder diffraction, XRD). Dobijeni rezultati ovom analizom su omogućili definisanje dinamike sinteze. Sastav reakcione smeše, u tačno definisanim vremenskim intervalima tokom postupka sinteze, kvantitativno je analiziran atomskom apsorpcionom spektroskopijom. Cilj ovog istraživanja je bio da se tokom sinteze $BaTiO_3$ odredi reakcioni model kao i kinetika reakcije. Rezultati dobijeni u prikazanom eksperimentu su pokazali da je tokom reakcije sinteze $BaTiO_3$ u čvrstom stanju postignut izuzetno visok stepen konverzije (0,99). Uzorkovanjem reakcione smeše u pet različitih vremenskih intervala potvrđeno je prisustvo početnih prahova BaO i TiO_2, zatim intermedijarnih jedinjenja i na kraju konačnog proizvoda, kristalnog $BaTiO_3$. Analizom nastanka kristalnih struktura i njihove identifikacije ceo proces dobijanja $BaTiO_3$ može se podeliti u tri etape: prva etapa u kojoj se urušava kristalna struktura reakcionog sistema BaO-TiO_2 (do 30 min); druga etapa je nastanak prelaznog stanja gde je teško utvrditi kristalnu i hemijsku strukturu, dovedena mehanička energija sistemu se akumulira u materijalu što ima za posledicu povećanje potencijalne energije i hemijske reaktivnosti (do 110 min); treća etapa u kojoj dolazi do značajnog formiranja kristalnog $BaTiO_3$ (posle 200 min). Rezultati su pokazali da je za dati sistem potrebno 440 min mehaničke aktivacije da se izvrši potpuna reakcija neutralizacije.

Ključne reči: reakcija u čvrstom stanju; BaO; TiO_2; mehanizam reakcije; kinetika; mehanohemijska sinteza

Biogasoline synthesis by catalytic cracking of used cooking oil catalysed by chicken eggshell-based CaO impregnated onto γ-Al_2O_3

Aman Santoso, Leni Wulandari, Ahmat Fanani Hidayatulloh, Sumari Sumari, Muntholib Muntholib, Muhammad Roy Asrori and Eli Hendrik Sanjaya

Department of Chemistry, Faculty of Mathematics and Natural Sciences, Universitas Negeri Malang, Jl. Semarang No. 5, Malang, 65145, Indonesia

Abstract

This research aims to synthesize biogasoline from used cooking oil using a catalyst of chicken eggshell based CaO impregnated with γ-Al_2O_3 through catalytic cracking, as well as to characterize the final product. Cracking optimization was carried out by varying the catalyst calcination temperature (650, 750 and 850 °C) and the catalyst concentration (1, 2 and 3 wt.%). The stages of this research were (1) characterization of used cooking oil (density, viscosity, refractive index, and iodine number) (2) synthesis of the CaO/γ-Al_2O_3, (3) catalytic cracking of used cooking oil with the use of the synthesized catalyst, and (4) characterization and identification of biogasoline. The results showed that the optimum condition for catalytic cracking was obtained at the calcination temperature of 650 °C. The synthesized biogasoline has the following characteristics, *i.e.* density of 0.776 g mL^{-1}, viscosity of 1.84 mm^2 s^{-1}, a refractive index of 1.43, and the iodine number of 22.85 g I_2 *per* 100 g. The synthesized biogasoline contained alkane, alkene and carboxylic acid compounds, C_2-C_{19}. This composition was dominated by compounds belonging to biogasoline (C_5-C_{12}) amounting to 94.5 wt.% as confirmed by gas chromatography-mass spectrometry analyses.

Keywords: biofuel; biomass; heterogeneous catalyst; oxide; waste oil; modified material.

Available on-line at the Journal web address: http://www.ache.org.rs/HI/

ORIGINAL SCIENTIFIC PAPER

UDC: 665.73:544.473:544.77

Hem. Ind. **79(4)** 233-241 (2025)

1. INTRODUCTION

The increase in the number of motorized vehicles results in increasing fuel consumption, which is mostly supplied from petroleum. However, this increasing need for fuel does not align with the decreasing availability of petroleum resources. It is estimated that the oil demand in 2050 will increase to 943.3 BL of oil in a rapid energy transition scenario [1]. For this reason, the transition from petroleum to renewable energy sources began to be encouraged.

One of the renewable energies is biogasoline produced by conversion of used cooking oil. Cooking oil consumption in Indonesia reached 16.2 billion litters in 2019. It can be estimated that the average used cooking oil produced is in the range of 40 to 60 % of the oil or in the range of 6.46 to 9.72 billion litters [2]. Used cooking oil is obtained by repeated heating the cooking oil. As a result, used cooking oil contains ~42 % oleic acid ($C_{18}H_{34}O_2$) and ~35 % palmitic acid ($C_{16}H_{32}O_2$) [3]. Currently, used cooking oil has been utilized as a raw material in biogasoline synthesis [4–6]. To become a low fraction such as fuel, it is necessary to break down the long hydrocarbon chains through the cracking process [7]. There are two main types of cracking: thermal cracking and catalytic cracking [8]. Since the thermal cracking requires high temperatures [9], catalytic cracking is considered to be safer due to lower temperatures and higher product conversion, making this process more efficient and economically favourable [10].

In this research, a CaO catalyst derived from chicken eggshells impregnated onto γ-Al_2O_3 was used for catalytic cracking. CaO was selected due to its alkaline nature, high catalytic activity, easy preparation process, abundant availability and environmental friendliness. On the other hand, CaO also has a high decarboxylation capacity with low solubility in fuel [11], and reduces the acidity of cracking products [12]. One of CaO sources in nature is chicken eggshells,

Corresponding author: Aman Santoso, Department of Chemistry, Faculty of Mathematics and Natural Sciences, Universitas Negeri Malang, Jl. Semarang No. 5, Malang, 65145, Indonesia, E-mail: aman.santoso.fmipa@um.ac.id; https://orcid.org/0000-0001-9603-5686
Co-authors: Leni Wulandari https://orcid.org/0009-0009-1372-022X, Ahmat Fanani Hidayatulloh https://orcid.org/0000-0001-9803-1945, Sumari Sumari https://orcid.org/0000-0002-1788-2113, Muntholib Muntholib https://orcid.org/0000-0002-3335-5380, Muhammad Roy Asrori https://orcid.org/0000-0002-6963-4154, Eli Hendrik Sanjaya https://orcid.org/0000-0002-6513-5198

Paper received: 18 February 2025; Paper accepted: 14 December 2025; Paper published: 22 December 2025.
https://doi.org/10.2298/HEMIND250218016S

which contain 97 % CaO, 0.263 % Fe_2O_3 and 0.123 % SO_3 [13]. Eggshell based CaO has been used in the production of biogasoline from used cooking oil with a yield of 4.5 % [6]. Cracking of used cooking oil with the CaO/SBA-15 catalyst resulted in a biogasoline yield of 69.70 % [4]. To increase the catalytic activity of CaO, it was impregnated onto γ-Al_2O_3, which is a metastable form of alumina, most often used as a catalyst [14]. It has a large pore volume and surface area and is stable in various catalytic reaction temperature ranges [15]. In addition, it has Brønsted acid sites and Lewis acid sites that contribute to the catalytic cracking process [16]. γ-Al_2O_3 as a catalyst in palm oil cracking resulted in a biogasoline yield of 45.35 % [17]. Also a Co-Mo/Al_2O_3 catalyst was used in cracking of Nyamplung oil with a biogasoline yield of 25.63 % [18], while the use of Ni-Mo/Al_2O_3 in another study resulted in a biogasoline yield of 59.50 % [5]. The present research aims to synthesize and characterize biogasoline from used cooking oil utilizing a catalyst composed of chicken eggshell based CaO impregnated onto γ-Al_2O_3 through catalytic cracking.

2. MATERIALS AND METHODS

Along with the standard laboratory tools (*e.g.* pycnometer, Otswald viscometer, cracking tool sets), the following instruments were used: X-ray diffractometer (XRD), PANanalytical X'pert Pro, PANalytical B.V., Netherland; X-ray fluorescence (XRF) spectrometer, PANanalytical Minimal 4, PANalytical B.V., Netherland; scanning electron microscope (SEM), Inspect-S50 FEI type, FEI Company, Netherland; gas chromatography-mass spectrometry instrument (GC-MS), Shimadzu QP2010S, Japan and Fourier transform infrared (FT-IR) spectroscope, IRPrestige 21, Shimadzu, Japan. Furthermore, the materials used in this study were used cooking oil, chicken eggshells, $Al(NO_3)_3{\times}9H_2O$ *p.a.* (Merck, Germany), HCl *p.a.* (Sigma Aldrich, USA), NH_4OH *p.a.* (Merck, Germany), ethanol 96 % and distilled water.

2. 1. Synthesis of γ-Al_2O_3

γ-Al_2O_3 was prepared using a precipitation method. First, 1 M $Al(NO_3)_3{\times}9H_2O$ precursor was prepared in 0.5 M HCl solution. 0.5 M NH_4OH was then added dropwise until the pH 9, under stirring using a magnetic stirrer for 3 h at 70 °C. After that, the solution was filtered using a Buchner funnel and the precipitate was washed by distilled water and ethanol. The precipitate was dried in an oven at 75 °C for 24 h [19]. Then the precipitate was calcined at 600 °C for 6 h. The obtained γ-Al_2O_3 was analysed by XRD.

2. 2. Synthesis of chicken eggshell-based CaO

Chicken eggshells were washed in distilled water, crushed and sieved to a 100 mesh size. Then the eggshell particles were dried in an oven at 110 °C for 6 h, followed by calcination at 900 °C for 3 h [20]. The eggshell particles were then analysed by XRF and XRD.

2. 3. Production of chicken eggshell-based CaO/γ-Al_2O_3 catalysts

γ-Al_2O_3 was mixed with the eggshell particles (in water) in a mass ratio of 1:1. The obtained suspension was then stirred using a hand stirrer for 15 min, followed by sonication (42 kHz) at 60 °C for 1 h. Next, the solution was filtered using a Buchner funnel and the precipitate was washed with distilled water and dried in the oven at 110 °C for 4 h. The catalyst precursor was then calcined at various temperatures of 650, 750 and 850 °C for 3 h. The obtained catalysts were analysed by XRD, XRF and SEM.

2. 4. Catalytic cracking of used cooking oil

Used cooking oil was first filtered before cracking with the use of a filter paper. Characterization of the oil included determination of density, viscosity, acid number, refractive index, and composition by using FT-IR analysis.

For the catalytic cracking process, used cooking oil (100 g) and CaO/γ-Al_2O_3 (1 g) were put into the cracking reactor. The batch reactor was constructed by authors using a stainless steel cylinder (5 cm diameter, 10 cm height, 62.5 mL volume), supplied with a temperature sensor for measuring the steam temperature, and connected to a condenser and a bottle by a steel pipe. The reactor was placed on an electric stove, heated to the temperature of 600 °C, followed by the increase in the temperature by 100 °C every 20 min to 1500 °C, and the process was continued for 4 h. The distillate

resulting from cracking was collected into 3 fractions based on the temperature ranges: fraction F1 (100 to 125 °C), fraction F2 (125 to 150 °C) and fraction F3) (150 to 175 °C). In this study, the catalytic cracking process varied regarding the calcination temperature of the catalyst (650, 750 and 850 °C) and catalyst concentration (1, 2 and 3 wt.% of the oil). The resulting product was characterized regarding the refractive index, density, viscosity, iodine number and composition by using GC-MS and FT-IR analyses.

3. RESULTS AND DISCUSSION

3. 1. Characterizations of γ-Al_2O_3 and chicken eggshell based CaO

Formation of γ-Al_2O_3 was confirmed qualitatively by XRD showing peaks at the diffractogram at 2θ = 39.37, 45.75, 66.91 and 85.07° (Figure 1). These results correspond to γ-Al_2O_3 peaks in the XRD pattern database with COD ID. 00-101-0461 at 2θ = 39.48, 45.91, 66.95 and 84.99°. The same result is reported in the previous study [21]. Therefore, it was concluded that γ-Al_2O_3 in this study was successfully synthesized.

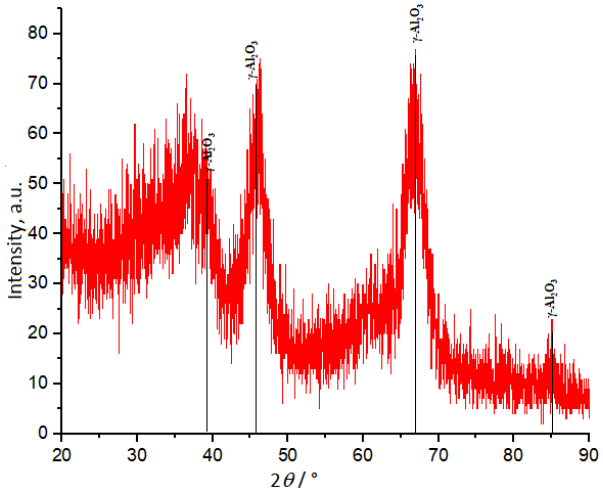

Figure 1. XRD results of the synthesized γ-Al_2O_3

In the final calcination process, the obtained white powder (*i.e.* CaO from chicken eggshells) was analysed by XRD and XRF. Typical CaO peaks were recorded, namely 2θ = 37.47, 53.97, 64.25, 67.47, 79.77 and 86.63° (Figure 2) according to the XRD database with COD ID. 00-101-1095, at 2θ = 37.40, 53.93, 64.24, 67.47, 79.77 and 86.63°. Furthermore, based on XRF analysis the composition of chicken eggshells calcined at 900 °C for 3 h, was determined as: 0.090 wt.% SO_3, 99.590 wt.% CaO, 0.069 wt.% Fe_2O_3, and 0.100 wt.% Co_3O_4. In the other study, the result was obtained at more than 95 wt.% CaO [22]. Therefore, chicken eggshell based CaO in this study showed high purity after the synthesis.

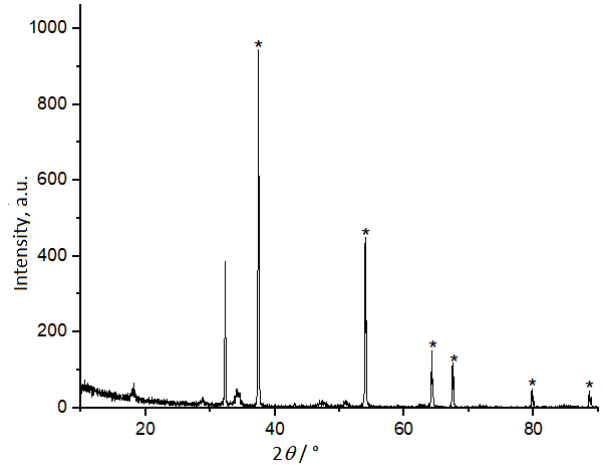

Figure 2. XRD results of chicken eggshell based CaO after calcination at 900 °C

3. 2. Synthesis of chicken eggshell based CaO/γ-Al_2O_3 catalyst

CaO/γ-Al_2O_3 catalyst was synthesized by impregnation of chicken eggshell based CaO onto γ-Al_2O_3 in a mass ratio of 1:1 under ultra-sonication (42 kHz). The catalyst was then calcined at different temperatures of 650, 750 and 850 °C for 3 h. The obtained catalysts were analysed next by XRD, XRF and SEM.

XRD diffractograms of the synthesized CaO/γ-Al_2O_3 catalysts (Fig. 3a) show typical CaO peaks, namely 2θ = 31.66, 36.61 and 52.79° in accordance with the XRD database with COD ID: 00-900-6719, namely 2θ= 31.61, 36.66, and 52.82°. Furthermore, γ-Al_2O_3 peaks were recorded 2θ= 39.49, 46.03 and 66.99° in accordance with the XRD database with COD ID: 00-101-0461, namely 2θ = 39.48, 45.91 and 66.95°. Results of the XRF analysis of all three CaO/γ-Al_2O_3 catalysts obtained at different calcination temperatures are presented in Table 1.

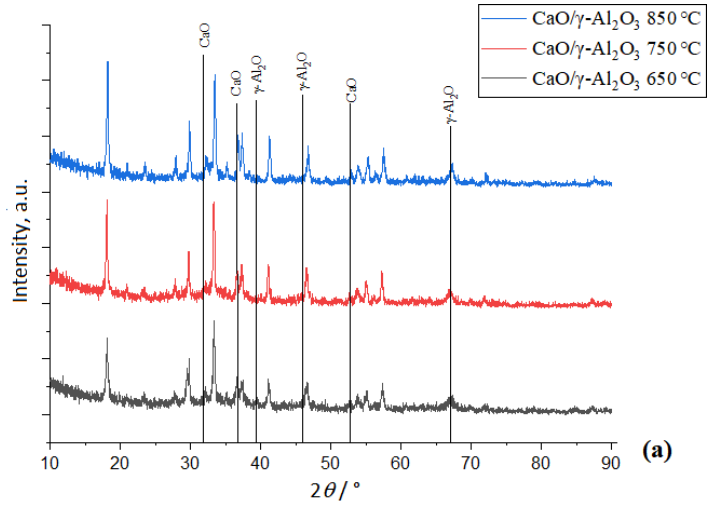

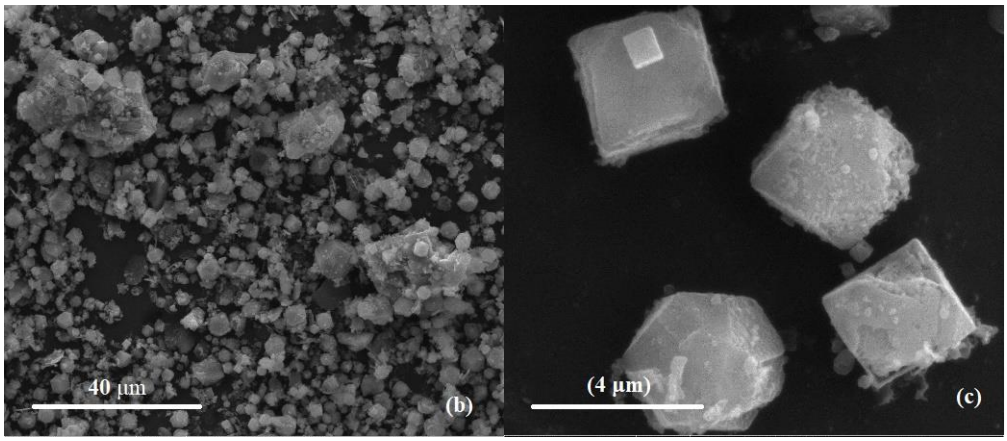

Figure 3. Characterization of chicken eggshell based CaO/γ-Al_2O_3 catalyst (various calcination temperatures of 650, 750, 850 °C): XRD results (a) and scanning electron micrographs of the catalyst calcined at 850 °C (b) and (c)

Table 1. XRF results for chicken eggshell based CaO/γ-Al_2O_3 catalysts calcined at different temperatures

Compound	Calcination temperature, °C		
	650	750	850
	Content, wt.%		
Al_2O_3	24.40	25.70	25.70
CaO	71.72	70.46	70.46
SiO_2	2.80	2.80	2.80
Fe_2O_3	0.10	0.10	0.10
CuO	0.03	0.03	0.03
ZnO	0.02	0.02	0.02
MoO_3	0.57	0.58	0.58
Yb_2O_3	0.25	0.24	0.24

The XRF analysis (Table 1) has indicated the CaO/γ-Al_2O_3 mass ratios in the catalysts of 2.9:1 for the calcination temperature of 650 °C and 2.75:1 for the two other calcination temperatures of 750 °C and 850 °C.

Morphology of the CaO/γ-Al_2O_3 catalyst calcined at 850 °C can be seen in Figure 3b,c. Regularity of the particle size in a cubic shape originating from γ-Al_2O_3 [23] can be seen (Fig. 3b). Meanwhile, the catalyst surface contains lumps (Figure 3c) indicating attachment of CaO to the γ-Al_2O_3 surface. Based on the presented results of XRD, XRF, and SEM analyses, it can be deduced that CaO/γ-Al_2O_3 catalysts were successfully synthesized generally retaining characteristics of the raw materials.

3. 3. Catalytic cracking of used cooking oil

Cracking of used cooking oil produces a polar phase, a nonpolar phase, gas, and the remaining reaction residue. We have focused here on the nonpolar phase, namely the oil products. Three types of catalyst regarding the calcination temperature (*i.e*. 650, 750, and 850 °C) were used at three different concentrations (*i.e*. 1, 2 and 3 wt% of the oil). The reaction mixture was heated to 600 °C and subsequently increased every 20 min by 100 °C up to 1500 °C. The cracking process was carried out for 4 h. The yield of cracking products can be seen in Figure 4.

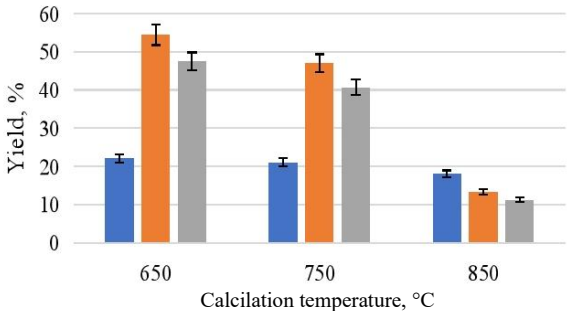

Figure 4. Effects of the calcination temperature (650, 750, and 850 °C) and CaO/γ-Al_2O_3 concentration (1 ■, 2 ■, and 3 ■ wt.% of the oil) on the yield of cracking of used cooking oil

Based on Figure 4, the yields of cracking products decrease with increasing the catalyst calcination temperature. Increasing the calcination temperature of the catalyst will cause the pores in γ-Al_2O_3 to collapse and merge with each other, so the available surface of the catalyst decreases [24]. Therefore, the optimal catalyst calcination temperature was found to be 650 °C.

Increasing the catalyst concentration from 1 to 2 wt.% resulted in increasing the yield of cracking products at catalyst calcination temperatures of 650 and 750 °C. However, when the catalyst concentration was increased to 3 wt.%, the cracking product yield decreased because of excessive catalytic reactions, which resulted in the formation of relatively large amounts of residue [32]. The product yield for the catalyst calcination temperature of 850 °C decreased as the catalyst concentration increased. Therefore, at the catalyst calcination temperature of 850 °C, the catalytic cracking gave the worst results as compared to the other two calcination temperatures.

3. 4. Characterizations of cracking products

The obtained mixtures of cracking products were yellow and had a sharp odour in contrast to the physical appearance of used cooking oil, which is brownish in colour and has a rancid odour. Characteristics of cracking products in 3 fractions (F1: 100 to 125 °C, F2: 125 to 150 °C and F3: 150 to 175 °C) obtained at 650 °C calcination temperature and 2 wt.% catalyst concentration together with those of standard gasoline and the starting used cooking oil are shown in Table 2.

Table 2. Characteristics of the catalytic cracking products of used cooking oil with the use of 2 wt% catalyst calcined at 650 °C. F1, F2 and F3 represent distillate fractions based on the temperature ranges

Parameter	F1	F2	F3	Conventional gasoline	Used cooking oil
Density at 25 °C, g mL^{-1}	0.779	0.776	0.774	0.770	0.910
Viscosity at 25 °C, mm^2 s^{-1}	1.92	1.84	1.78	0.48	58.01
Reflective index at 25 °C	1.44	1.43	1.42	-	1.46
Iodine number, g I_2 *per* 100 g	28.2	22.6	17.76	-	20.51

It can be deduced that the cracking products have characteristics close to those of conventional gasoline. A previous study also obtained the characteristics similar to the present study with the higher value, *i.e*. cracking product of off grade crude palm oil under condition of 0.5 % Co-Mo 1:1/α-Fe_2O_3 catalyst in a batch reactor [8].

3. 5. FT-IR and GC-MS analyses of the cracking products

The product resulting from catalytic cracking of used cooking oil by utilizing the CaO/γ −Al_2O_3 catalyst calcined at 650 °C at the content of 2 wt.% was analysed using FT-IR and GC-MS techniques. Three product fractions F1, F2 and F3 were analysed. The results of FT-IR and GC-MS analyses are shown in Figures 5 and 6, respectively. Based on the results presented in Figure 5, several functional groups induced increases in peak intensity, namely the alkene and carboxylic acid groups [8].

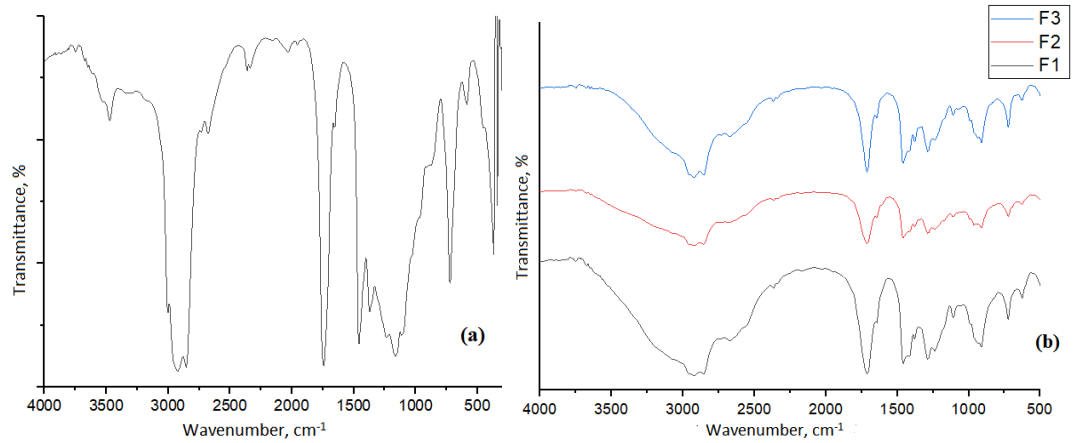

Figure 5. FT-IR spectra of (a) used cooking oil (raw material), and (b) catalytic cracking product fraction

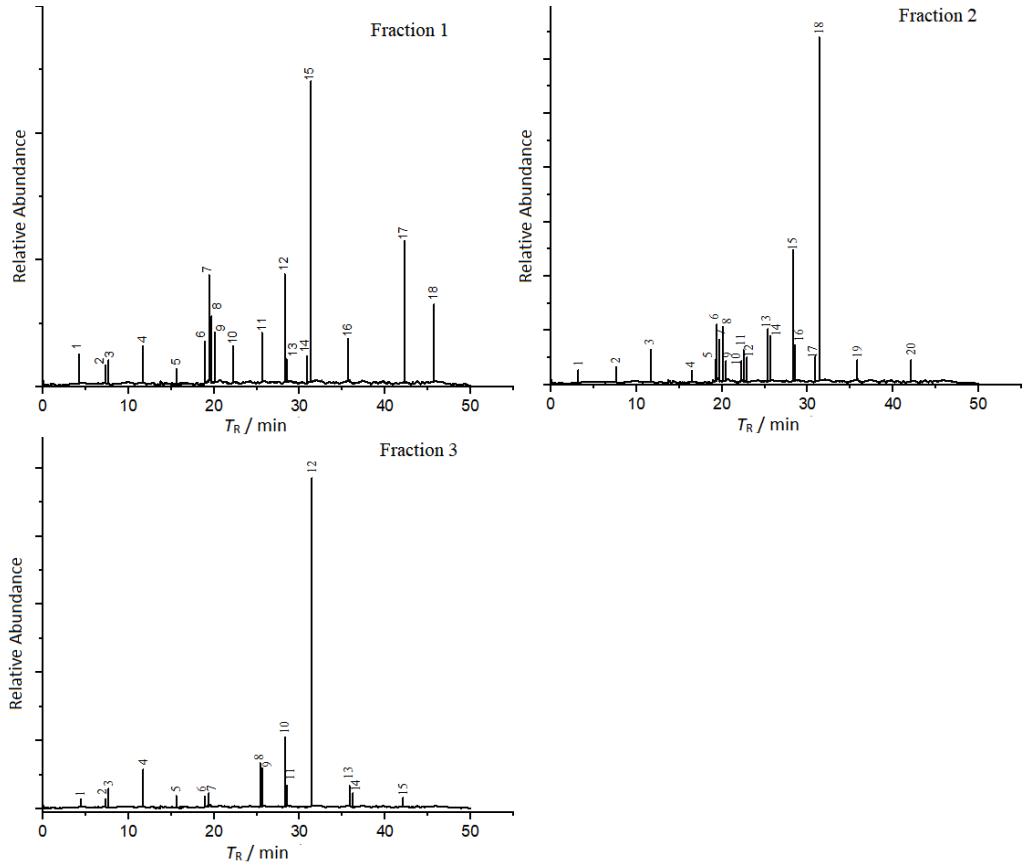

Figure 6. GC-MS chromatograms for the catalytic cracking products in the fractions

Mass spectra at each retention time (T_R) corresponding to the GC-MS chromatograms (Figure 6) are compared for similarities with library data (Table 3).

Table 3. Compound identification and contents (C) of different compounds in 3 fractions of the cracking products

Fraction 1			Fraction 2			Fraction 3		
T_R / min	Compound	*C* / wt.%	T_R / min	Compound	*C* / wt.%	T_R / min	Compound	*C* / wt.%
11.652	n-nonane	3.22	11.651	n-nonane	3.23	4.374	n-heptane	1.41
18.906	1-undecene	3.55	19.387	cis-3-undecene	5.61	7.274	1-hexene	1.40
19.404	cis-3-undecene	8.82	20.076	1,7-octadiene	5.37	7.623	n-octane	2.97
19.675	1-decene	5.55	20.448	heptanoic acid	2.22	11.690	n-nonane	5.82
20.087	1-decune	4.25	22.507	2-methyl decane	3.20	25.369	1-nonene	6.70
25.619	2,7-dimethyl octane	4.25	25.360	1-undecene	5.19	25.641	n-decane	5.93
28.492	Trans-3-undecene	8.88	25.628	2,7-dimethyl octane	4.50	28.286	1-undecene	10.46
31.312	n-decane	24.12	28.297	1-dodecene	12.38	28.525	2-methyl nonane	2.94
35.675	1-dodecene	3.80	28.504	n-undecane	3.65	31.420	n-undecane	48.50
42.273	decanoic acid	11.51	31.358	n-decane	31.98	35.833	1-dodecene	3.35
45.713	9-octadecenoic acid	6.50						

Based on the results of the GC-MS analysis shown in Table 3, F1 consisted of a hydrocarbon with a C_6 - C_{18} bond, *i.e* alkane, alkene and carboxylic acid compounds. In this fraction, biogasoline (C_5 - C_{12}) is dominant, with a content of 93.5 wt.%. Among the compounds found in this fraction, n-decane has the highest concentration of 24.12 wt.%. On the other hand, F2 is hydrocarbons with C_2 - C_{18} bonds consisting of alkane, alkene and carboxylic acid compounds. In this fraction, biogasoline (C_5 - C_{12}) is also dominant, with a similar content of 94.02 wt.%. Here, also, n-decane is found in the highest concentration of 31.98 wt.%. F3 is composed of hydrocarbons with C_6 - C_{19} bonds consisting of alkane, alkene and carboxylic acid compounds with biogasoline (C_5 - C_{12}) being dominant, with the content of 96.08 wt.%. Among the compounds found in this fraction, n-undecane has the highest concentration of 48.50 wt.%. Thus, the average biogasoline content of all three fractions was 94.53 wt.%. Similar hydrocarbon contents in the cracking product were also obtained in a previous study [8]. It should be noted that the catalytic reaction product is a mixture of various compounds [25], so that tracking of cracking products formation is necessary in further research.

4. CONCLUSION

Chicken eggshell-based CaO/γ-Al_2O_3 has been successfully synthesized by an impregnation method that was assisted by sonication. The catalyst composition has been confirmed by XRD, XRF and SEM analyses. Impregnation of CaO obtained from chicken eggshells onto γ-Al_2O_3 resulted in the CaO/γ-Al_2O_3 mass ratios of 2.9:1 for calcination at 650 °C and 2.75:1 for calcination at the other two temperatures of 750 and 850 °C. The best conditions for catalytic cracking of used cooking oil were determined as: the CaO/γ-Al_2O_3 catalyst with the mass ratio of 2.9:1 obtained at the calcination temperature of 650 °C and used at the concentration of 2 wt.% of the oil, by which a biogasoline yield of ~55 % was obtained. Furthermore, by characterization of the produced biogasoline, the following results were obtained: density of 0.76 g mL^{-1}, viscosity of 1.84 mm^2 s^{-1}, refractive index of 1.43, and the iodine number of 22.85 g I_2/100 g. The biogasoline contained C_2 - C_{19}, compounds consisting of alkane, alkene and carboxylic acid compounds. This composition is dominated by compounds characteristic for biogasoline (C_5 - C_{12}) with the content of about 94 % as determined by GC-MS analyses. In further studies, there is a need for optimization of the catalyst component ratio as well as duration and temperature of the cracking reaction to produce an economically higher product yield. In addition, analyses of the cracking products formation will be a valuable topic for further research.

Acknowledgements: Thanks are expressed to the Directorate of Research, Technology and Community Service (DRTPM) which provided funding for this research.

REFERENCES

[1] Davies A, Simmons MD. Demand for 'advantaged' hydrocarbons during the 21st century energy transition. *Energy Reports*. 2021; 7: 4483-4497. https://doi.org/10.1016/j.egyr.2021.07.013

[2] Diputra IGYM, Sunardi, Siyaranamual MD. The correlation between formal education and knowledge of used cooking oil management at Kampung Tersenyum society in South Jakarta. *E3S Web Conf*. 2024; 495: 03006. https://doi.org/10.1051/e3sconf/202449503006
[3] Zein YM, Anal AK, Prasetyoko D, Qoniah I. Biodiesel Production from Waste Palm Oil Catalyzed by Hierarchical ZSM-5 Supported Calcium Oxide. *Indones J Chem*. 2016; 16(1): 98-104. https://doi.org/10.22146/ijc.21184
[4] Ge S, Ganesan R, Sekar M, Xia C, Shanmugam S, Alsehli M, Brindhadevi K. Blending and emission characteristics of biogasoline produced using CaO/SBA-15 catalyst by cracking used cooking oil. *Fuel*. 2022; 307: 121861. https://doi.org/10.1016/j.fuel.2021.121861
[5] Mampuru MB, Nkazi DB, Mukaya HE. Hydrocracking of waste cooking oil into biogasoline in the presence of a bi-functional Ni-Mo/alumina catalyst. *Energy Sources, Part A Recover Util Environ Eff*. 2020; 42(20): 2564-2575. https://doi.org/10.1080/15567036.2019.1610527
[6] Hassan SN, Nurdin S, Yaakob Z, Mahmud MS. Biogasoline synthesis via fluid catalytic cracking of waste cooking oil using treated eggshell. *IOP Conf Ser Mater Sci Eng*. 2020; 736(2): 22069. https://doi.org/10.1088/1757-899X/736/2/022069
[7] Santoso A, Sumari, Joharmawan R, Hutami LB. Catalytic cracking of waste frying oil using Ni-Fe/activated zeolite catalyst as a source of renewable energy. *IOP Conf Ser Mater Sci Eng*. 2019; 509: 12009. https://doi.org/10.1088/1757-899x/509/1/012009
[8] Santoso A, Mulyaningsih A, Sumari S, Retnosari R, Aliyatulmuna A, Pramesti IN, Asrori MR. Catalytic cracking of off grade crude palm oil to biogasoline using Co-Mo/α-Fe_2O_3 catalyst. *Energy Sources, Part A Recover Util Environ Eff*. 2023; 45(1): 1886-1899. https://doi.org/10.1080/15567036.2023.2183998
[9] A'issyah EWN, Santoso A, Aliyatulmuna A. Synthesis Bio-gasoline from Crude Palm Oil Offgrade via Catalytic Cracking Using CaO/α-Fe_2O_3 Heterogeneous Catalyst. *E3S Web Conf*. 2024; 481. https://doi.org/10.1051/e3sconf/202448101003
[10] Hassan SN, Sani YM, Abdul Aziz AR, Sulaiman NMN, Daud WMAW. Biogasoline: An out-of-the-box solution to the food-for-fuel and land-use competitions. *Energy Convers Manag*. 2015; 89: 349-367. https://doi.org/10.1016/j.enconman.2014.09.050
[11] Xu J, Jiang J, Chen J, Sun Y. Biofuel production from catalytic cracking of woody oils. *Bioresour Technol*. 2010; 101(14): 5586-5591. https://doi.org/10.1016/j.biortech.2010.01.148
[12] Zhang G, Yu F, Wang W, Wang J, Ji J. Influence of Molten Salts on Soybean Oil Catalytic Pyrolysis with/without a Basic Catalyst. *Energy & Fuels*. 2014; 28(1): 535-541. https://doi.org/10.1021/ef4015845
[13] Ayodeji AA, Modupe OE, Rasheed B, Ayodele JM. Data on CaO and eggshell catalysts used for biodiesel production. *Data Br*. 2018; 19: 1466-1473. https://doi.org/10.1016/j.dib.2018.06.028
[14] Santoso A, Kusumah TN, Sumari S, Wijaya AR, Retnosari R, Rachman IB, Marfuah S, Roy Asrori M. Synthesis of biodiesel from waste cooking oil using heterogeneous catalyst of Na2O/γ-Al_2O_3 assisted by ultrasonic wave. *AIMS Energy*. 2022; 10(5): 1059-1073. https://doi.org/10.3934/energy.2022049
[15] Stuart NM, Sohlberg K. The Microstructure of γ-Alumina. *Energies*. 2021; 14(20): 6472. https://doi.org/10.3390/en14206472
[16] Feng R, Liu S, Bai P, Qiao K, Wang Y, Al-Megren HA, Rood MJ, Yan Z. Preparation and Characterization of γ-Al_2O_3 with Rich Brønsted Acid Sites and Its Application in the Fluid Catalytic Cracking Process. *J Phys Chem C*. 2014; 118(12): 6226-6234. https://doi.org/10.1021/jp411405r
[17] Wijanarko A, Mawardi DA, Nasikin M. Biogasoline Production from Palm Oil Via Catalytic Hydrocracking over Gamma-Alumina Catalyst. *Makara J Technol*. 2006; 10(2): 51-60. https://doi.org/10.7454/mst.v10i2.423
[18] Rasyid R, Prihartantyo A, Mahfud M, Roesyadi A. Hydrocracking of Calophyllum inophyllum Oil With Non-sulfide CoMo Catalysts. *Bull Chem React Eng Catal*. 2015; 10(1): 61-69. https://doi.org/10.9767/bcrec.10.1.6597.61-69
[19] Marbun MJ, Kurniawansyah F, Prajitno DH, Roesyadi A. Production of Diethyl Ether Over Cr-Co/γ-Al2O3 Catalyst. *IOP Conf Ser Mater Sci Eng*. 2019; 543(1): 12058. https://doi.org/10.1088/1757-899X/543/1/012058
[20] Oko S, Feri M. Pengembangan Katalis CaO dari Cangkang Telur Ayam dengan Impregnasi KOH dan Aplikasinya terhadap Pembuatan Biodiesel dari Minyak Jarak. *J Teknol*. 2019; 11(2): 103-109. https://doi.org/10.24853/jurtek.11.2.103-110
[21] Chauruka SR, Hassanpour A, Brydson R, Roberts KJ, Ghadiri M, Stitt H. Effect of mill type on the size reduction and phase transformation of gamma alumina. *Chem Eng Sci*. 2015; 134: 774-783. https://doi.org/10.1016/j.ces.2015.06.004
[22] Kalaycı T, Altuğ DT, Kınaytürk NK, Tunalı B. Characterization and potential usage of selected eggshell species. *Sci Rep.* 2025; 15, 6241. https://doi.org/10.1038/s41598-025-87786-y
[23] Ayoola HO, House SD, Bonifacio CS, Kisslinger K, Saidi WA, Yang JC. Evaluating the accuracy of common γ-Al2O3 structure models by selected area electron diffraction from high-quality crystalline γ-Al_2O_3. *Acta Mater*. 2020; 182: 257-566. https://doi.org/10.1016/j.actamat.2019.10.027
[24] Tang W, Yuan Y, Hu G, Zhu J, Dai Y, Zhang J, Fu C. Ammonium salt-assisted preparation of porous high-purity γ-Al2O3 with a high specific surface area. *Ceram Int*. 2024; 50(5): 7255-7265. https://doi.org/10.1016/j.ceramint.2023.11.294
[25] Asrori MR, Santoso A, Sumari S. Initial defect product on immiscible mixture of palm oil: Ethanol by amphiphilic chitosan/Zeolite LTA as optimization of microemulsion fuel. *Ind Crops Prod*. 2022; 180: 114727. https://doi.org/10.1016/j.indcrop.2022.114727

Sinteza biobenzina katalitičkim krekovanjem korišćenog ulja za kuvanje katalizovanim CaO na bazi ljuske kokošjeg jajeta impregniranog na γ-Al_2O_3

Aman Santoso, Leni Wulandari, Ahmat Fanani Hidayatulloh, Sumari Sumari, Muntholib Muntholib, Muhammad Roy Asrori and Eli Hendrik Sanjaya

Department of Chemistry, Faculty of Mathematics and Natural Sciences, Universitas Negeri Malang, Malang, Indonesia

(Naučni rad)

Izvod

Cilj ovog istraživanja je sinteza biobenzina iz korišćenog ulja za kuvanje korišćenjem katalizatora na bazi ljuske kokošjeg jajeta impregniranog sa γ-Al_2O_3 putem katalitičkog krekovanja, kao i karakterizacija finalnih proizvoda. Optimizacija krekovanja je sprovedena variranjem temperature kalcinacije katalizatora (650, 750 i 850 °C) i koncentracije katalizatora (1, 2 i 3 mas.%). Faze ovog istraživanja bile su (1) karakterizacija korišćenog ulja za kuvanje (gustina, viskoznost, indeks prelamanja i jodni broj), (2) sinteza CaO/γ-Al_2O_3, (3) katalitičko krekovanje korišćenog ulja za kuvanje korišćenjem sintetisanog katalizatora i (4) karakterizacija i identifikacija biobenzina. Rezultati su pokazali da su optimalni uslovi za katalitičko krekovanje dobijeni na temperaturi kalcinacije od 650 °C. Sintetizovani biobenzin ima sledeće karakteristike, *tj.* gustinu od 0,776 g ml^{-1}, viskoznost od 1,84 mm^2 s^{-1}, indeks prelamanja od 1,43 i jodni broj od 22,85 g I_2 na 100 g. Sintetizovani biobenzin sadrži jedinjenja alkana, alkena i karboksilnih kiselina, C_2-C_{19}. U ovom sastavu dominirala su jedinjenja koja pripadaju biobenzinu (C_5-C_{12}) u iznosu od 94,5 mas.%, što je potvrđeno analizama gasnom hromatografijom sa masnom spektrometrijom.

Ključne reči: biogorivo; biomasa, heterogeni katalizator; oksid; otpadno ulje; modifikovani materijal

Tehnološko-metalurški fakultet Univerziteta u Beogradu - sto godina znanja, istraživanja i akademske tradicije

Mirjana Kijevčanin i Mirjana Kostić

Tehnološko-metalurški fakultet, Univerzitet u Beogradu, Beograd, Srbija

Ovaj tekst napisan je u želji da se, povodom jubileja, podsetimo ključnih događaja i ljudi koji su oblikovali Fakultet, kao i da izrazimo zahvalnost generacijama profesora, saradnika i studenata čije znanje, rad i vizija već sto godina stvaraju Tehnološko-metalurški fakultet Univerziteta u Beogradu.

Ključne reči: sto godina postojanja Tehnološko-metalurškog fakulteta; razvoj nastave hemijske tehnologije; doprinos nauci.

Available on-line at the Journal web address: http://www.ache.org.rs/HI/

PRIKAZ KNJIGA I DOGAĐAJA

Hem. Ind. **79(4)** 243-248 (2025)

Povod za ovaj kratak osvrt na početke i razvoj nastave tehnologije i metalurgije, kao i na dostignuća nastavnika i saradnika Tehnološko-metalurškog fakulteta, jeste izuzetno važan jubilej – 100 godina od osnivanja samostalnog Tehnološkog odseka Tehničkog fakulteta Univerziteta u Beogradu. Zvanični dokument o njegovom osnivanju potpisan je 16. novembra 1925. godine, te se taj datum smatra danom utemeljenja današnjeg Tehnološko-metalurškog fakulteta.

Pripreme za razvoj nastave iz ovih oblasti počele su mnogo ranije, zahvaljujući malobrojnim pojedincima i vizionarima koji su prepoznali značaj hemije, hemijske tehnologije i metalurgije. Jedan od njih bio je Mihailo Rašković (Slika 1a), prvi profesor hemije i tehnologije na Liceju, jedinoj visokoškolskoj ustanovi u tadašnjoj Srbiji. On je još 1853. godine držao predavanja iz ovih oblasti, uprkos tome što u nerazvijenoj zemlji gotovo da nije postojala hemijska industrija, već svega nekoliko pivara, fabrika sapuna, tekstila, šećerana, špiritana i mlinova (Slika 2).

Slika 1. *a) Mihailo Rašković – prvi profesor hemijske tehnologije i autoritet svog vremena; b) prof. Sima Lozanić – autor prvih udžbenika iz tehnologije; c) Todor – Toša Selesković – profesor na Katedri za mehaničku tehnologiju i poznati konstruktor*

Figure 1. *a) Prof. Mihailo Rašković – the first professor of chemical technology and an authority of his time; b) prof. Sima Lozanić - author of the first textbooks on chemical technology; c) Todor - Toša Selesković - professor at the Department of Mechanical Technology and a well-known engineer and designer*

Corresponding authors: Mirjana Kijevčanin, E-mail: mirjana@tmf.bg.ac.rs, https://orcid.org/0000-0001-7126-3965 and
Mirjana Kostić, E-mail: kostic@tmf.bg.ac.rs, https://orcid.org/0000-0001-9925-4884, Tehnološko-metalurški fakultet, Univerzitet u Beogradu, Srbija

Slika 2. *Nastava tehnologije od Liceja do Tehnološkog odseka Tehničkog fakulteta*
Figure 2. *Teaching of technology from the Lyceum to the Technological Department of the Technical Faculty*

Zakonom iz 1863. godine Licej je postao Velika škola sa tri fakulteta, Filozofskim, Tehničkim i Pravničkim, pri čemu su predmeti hemija i hemijska tehnologija pripala Tehničkom fakultetu. Te iste godine formirana je i Katedra za hemiju i hemijsku tehnologiju. Od 1872. godine nastavu preuzima profesor Sima Lozanić (Slika 1b), autor prvog udžbenika iz hemijske tehnologije, koji je bio podeljen na četiri knjige: O vodi i gorivu (1887. g.), Osnovi metalurgije (1887. g.), Staklo, keramika, kreč, cement, gips (1892. g.) i Hemijski proizvodi (1894. g.).

Nove promene usledile su 1894. godine, kada je na zahtev Tehničkog fakulteta osnovana zasebna Katedra za hemijsku tehnologiju i Katedra za mehaničku tehnologiju, na čelu sa Todorom Seleskovićem (Slika 1c), poznatim konstruktorom i projektantom. Podignuti su objekti po njegovim projektima, kao što su barutana u Obilićevu kod Kruševca, parni mlin u Kragujevcu, Keramička fabrika, a posebno je značajan njegov doprinos razvoju Topolivnice u Kragujevcu.

Zakonom iz 1905. godine Velika škola postaje Univerzitet, a na Tehničkom fakultetu predaju se brojni hemijski i tehnološki predmeti. Nastava je u potpunosti obustavljena tokom Prvog svetskog rata, a obnovljena 1919. godine. Zbog velikog značaja hemije i tehnoloških disciplina, 1920. g. formira se Tehnološka grupa pri Mašinskom odseku, a 1923. g. uvodi se i tehnološki smer, čime je načinjen ključni korak ka kasnijem osnivanju samostalnog odseka 1925. g. i fakulteta 1948. godine (Slika 3).

Drugi svetski rat ponovo prekida rad Univerziteta, da bi se nastava obnovila u novembru 1945. Reorganizacijom Univerziteta 1948. godine, Tehnički fakultet prerasta u Tehničku veliku školu, a njegovi odseci postaju samostalni fakulteti. Za prvog dekana Tehnološkog fakulteta imenovan je profesor Panta S. Tutundžić (Slika 4), jedan od najzaslužnijih za izgradnju današnje zgrade Fakulteta. Njegova izuzetna dostignuća u oblasti fizičke i elektrohemije priznala je Srpska akademija nauka i umetnosti izborom za dopisnog člana 1958. godine, a za redovnog člana 1961. godine. U čast svog prvog dekana, Fakultet danas najboljim studentima dodeljuje nagradu koja nosi njegovo ime.

Iako je nastava tehnologije od početka obuhvatala i metalurgiju, Metalurški odsek zvanično je osnovan 1949. godine, a Fakultet je 1966. godine dobio naziv Tehnološko-metalurški fakultet.

Tokom jednog veka postojanja, profesori Fakulteta ostavili su trajan trag u razvoju Univerziteta: profesori Rajko Vračar i Ivanka Popović obavljali su funkcije rektora i prorektora, dok su prorektori bili i profesori Panta Tutundžić, Dragomir Malić, Slobodan Radosavljević i Dušan Vučurović.

Slika 3. *Od Tehnološkog odseka Tehničkog fakulteta do Tehnološko-metalurškog fakulteta*

Figure 3. *From the Technological Department of the Technical Faculty to the Faculty of Technology and Metallurgy*

Slika 4. *Profesor Panta S Tutzndžić - prvi dekan Tehnološko-metalurškog fakulteta*

Figure 4. *Professor Panta S Tutundžić - the first dean of the Faculty of Technology and Metallurgy*

Fakultet su činile generacije studenata, od prvih 15 upisanih 1925. godine do rekordnih 791 studenta 1980. godine (Slika 5). Danas Fakultet ima oko 1600 studenata na osnovnim studijama. Od osnivanja do danas diplomiralo je preko 12.000, master ili magistarske studije završilo je više od 2.500, a doktoriralo preko 1.000 studenata. Broj nastavnika i saradnika rastao je od 3 (1925. g.), preko 20 (1948. g.), 190 (1980. g.), dok ih danas Fakultet ima 105. Nastava se odvija kroz 17 studijskih programa na svim nivoima studija.

Slika 5. *Broj studenata i zaposlenih kroz vreme*

Figure 5. *Number of students and employees over time*

Pored obrazovanja inženjera, profesori i saradnici Fakulteta decenijama su doprinosili privredi i nauci. Još 1946. profesor Panta S. Tutundžić pisao je o značaju naučnog rada za obnovu hemijske industrije, naglašavajući da se održivi razvoj industrije ne može ostvariti bez stalnog naučnog napretka.

U periodu od 1961. do 1971. g. Fakultet je, iako tada formalno neregistrovan kao istraživačka ustanova, ostvario preko 300 studija, elaborata i patenata za privredu. Godine 1973. Fakultet je zvanično registrovan kao naučno-istraživačka organizacija. Danas je saradnja sa privredom usmerena na optimizaciju procesa, razvoj novih tehnologija i stručnu podršku industriji, dok se naučni rad potvrđuje objavljivanjem radova u vodećim nacionalnim i međunarodnim časopisima. Nastavnici Fakulteta doprinose pozicioniranju Univerziteta u Beogradu na ARWU listi, a neki se nalaze i na Stanfordovoj listi najuticajnijih naučnika sveta.

Srećni smo i ponosni što ove godine obeležavamo 100 godina rada Tehnološko-metalurškog fakulteta Univerziteta u Beogradu i nadamo se da ćemo i dalje, u duhu vek duge tradicije i kao neizostavan činilac razvoja celokupnog društva, nastaviti da dajemo doprinos u obrazovanju mladih inženjera i naučnika u oblastima hemijskih i srodnih tehnologija i metalurgije.

Faculty of Technology and Metallurgy, University of Belgrade
A century of knowledge, research and academic tradition

Mirjana Kijevčanin and Mirjana Kostić

Faculty of Technology and Metallurgy, University of Belgrade, Belgrade, Serbia

(Book and Event Review)

This brief reflection on the beginnings and growth of education in technology and metallurgy, as well as on the achievements of the professors and researchers of the Faculty of Technology and Metallurgy, marks an important milestone: the 100th anniversary of the establishment of the independent Department of Technology within the Technical Faculty of the University of Belgrade. The official founding document was signed on November 16, 1925, a date celebrated as the birth of today's Faculty of Technology and Metallurgy University of Belgrade.

Keywords: 100th anniversary of the Faculty of Technology and Metallurgy; history of chemical technology teaching; contribution to science

Preparations for education in these fields began much earlier, when a handful of visionary scholars recognized the importance of chemistry, chemical technology, and metallurgy. One of them was Mihailo Rašković (Figure 1a), the first professor of chemistry and technology at the Liceum, the only institution of higher education in Serbia at the time, who began lecturing as early as 1853, despite the fact that the country had virtually no chemical industry, save for a few breweries, soap factories, textile plants, sugar refineries, distilleries, and mills (Figure 2).

The 1863 Law transformed the Liceum into the Great School with three faculties: Philosophical, Technical, and Law, assigning chemistry and chemical technology to the Technical Faculty, where the Department of Chemistry and Chemical Technology was established the same year. In 1872, Professor Sima Lozanić (Figure 1b) assumed responsibility for teaching chemistry and chemical technology. He later authored the first textbook on chemical technology, published in four parts between 1887 and 1894.

Significant changes occurred in 1894 with the establishment of a separate Department of Chemical Technology and a new Department of Mechanical Technology led by Todor Selesković (Figure 1c), a well-known engineer and designer. Several industrial facilities were built according to his designs, including the gunpowder factory in Obilićevo near Kruševac and the steam mill in Kragujevac.

The Great School became the University of Belgrade in 1905, where chemistry and technology courses continued to expand. Teaching was completely suspended during World War I and resumed only in 1919. Given the growing importance of these disciplines, the Technological Group was formed in 1920 within the Mechanical Department, and by 1923 the technological track became an official study path, paving the way for the creation of the independent department in 1925 and, later, the Faculty in 1948 (Figure 3).

World War II again interrupted university activities until November 1945. The 1948 reorganization of the University formed the Technical High School, and former departments became independent faculties. The first Dean of the newly established Faculty of Technology was Professor Panta S. Tutundžić (Figure 4), who played a crucial role in the obtaining of the Faculty's current building. His achievements in physical and electrochemistry earned him membership in the Serbian Academy of Sciences and Arts (SASA) in 1958 and full membership in 1961. Today, the Faculty honours his legacy by awarding a student prize that bears his name.

Although teaching in technology had always included metallurgy, the Department of Metallurgy was officially established in 1949, and in 1966 the Faculty adopted the name it carries today, the Faculty of Technology and Metallurgy.

Throughout its century-long history, the Faculty's professors have made a profound impact on the University of Belgrade. Professors Rajko Vračar and Ivanka Popović served as Rectors and Vice-Rectors, while Professors Panta Tutundžić, Dragomir Malić, Slobodan Radosavljević, and Dušan Vučurović also held Vice-Rector positions.

The Faculty has always been defined by its students. Their numbers grew from the initial 15 enrolled in 1925 to a peak of 791 first-year students in 1980 (Figure 5). Today, the Faculty has around 1,600 undergraduate students. Since its founding, more than 12,000 students have graduated, over 2,500 have earned master's degrees, and more than

1,000 have completed doctoral studies. The number of professors and researchers also evolved, from 3 in 1925, to 20 in 1948, to 190 in 1980, while today the Faculty employs 105 academic staff members. Teaching is organized across 17 academic programs at all study levels.

Beyond educating generations of engineers, the Faculty's professors and researchers have played a vital role in industrial development and scientific advancement. In 1946, Professor Panta S. Tutundžić wrote about the importance of scientific work for rebuilding the chemical industry, arguing that sustainable industrial progress is impossible without continuous investment in research and expertise.

Between 1961 and 1971, although not yet formally registered as a research institution, the Faculty completed over 300 studies, reports, and patents for industry. It became an officially recognized research institution in 1973. Today, the Faculty's collaboration with industry focuses on process optimization, technology development, and technical consulting, while its scientific output appears in leading national and international journals. The Faculty significantly contributes to the University of Belgrade's ranking in ARWU fields and proudly has professors among Stanford's list of the world's most influential scientists.

This text is written in honour of the Faculty's centennial, to remember the key events and individuals that shaped its history, and to express gratitude to the generations of professors, researchers, and students whose dedication, expertise, and vision built the Faculty of Technology and Metallurgy over the past hundred years.

Nova razvojna faza Elixir grupe: tehnološka modernizacija, održivost i jačanje domaće hemijske industrije

Aleksandar Stanković

Hemijska divizija, Elixir grupa, Novi Sad, Srbija

Elixir grupa ulazi u 2026. godinu sa snažnim razvojnim zamahom, potvrđujući svoju poziciju jednog od najznačajnijih industrijskih sistema u regionu i pouzdanog nosioca modernizacije domaće hemijske industrije. Tokom prvih pet meseci 2026. godine, Elixir grupa će sukcesivno pustiti u rad tri nova industrijska postrojenja: pogon za proizvodnju kristalnih mineralnih đubriva u januaru, novi pogon fosforne kiseline u aprilu i energanu za termički tretman i energetsko iskorišćenje industrijskog otpada u maju. Ovi projekti predstavljaju zaokruženu investicionu celinu koja istovremeno unapređuje proizvodne kapacitete, tehnološki nivo, ekološke standarde i dugoročnu konkurentnost Elixir grupe.

Available on-line at the Journal web address: http://www.ache.org.rs/HI/

VESTI

Hem. Ind. **79(4)** 249-252 (2025)

Kristalna đubriva – odgovor na zahteve savremene poljoprivrede

Puštanjem u rad pogona za proizvodnju kristalnih đubriva početkom 2026. godine, Elixir grupa pravi iskorak ka segmentu visokovrednih, specijalizovanih mineralnih đubriva namenjenih intenzivnoj i preciznoj poljoprivredi. Kristalna, odnosno potpuno vodotopiva đubriva, predstavljaju neizostavan element savremenih agro-tehnoloških sistema, posebno u fertirigaciji, plasteničkoj i stakleničkoj proizvodnji, kao i u visokointenzivnim zasadima.

Novi pogon projektovan je u skladu sa najvišim tehnološkim standardima, sa naglaskom na stabilnost kvaliteta, preciznu kontrolu hemijskog sastava i fleksibilnost u formulacijama. Vertikalnom i horizontalnom integracijom novog pogona sa već postojećim, postignuta je visoka energetska efikasnost, i maksimalno iskorišćenje sirovina; praktično bez otpada i nusproizvoda. Time se dodatno smanjuje ekološki otisak proizvodnje.

Ulazak u segment kristalnih đubriva predstavlja i strateški odgovor Elixir grupe na promene u poljoprivredi, gde se sve veći akcenat stavlja na preciznu ishranu biljaka, optimizaciju prinosa i smanjenje gubitaka hraniva u životnoj sredini. Time se jača veza između hemijske industrije i održive poljoprivredne proizvodnje, što je jedan od ključnih izazova savremenog agroindustrijskog kompleksa.

Dodatna tržišna prilika za glavni proizvod ovog pogona (monoamonijum fosfat) ogleda se u njegovoj primeni u naprednim energetskim i elektrohemijskim procesima, koji beleže snažan razvoj na globalnom nivou.

Novi pogon fosforne kiseline – jačanje sirovinske osnove i tehnološke nezavisnosti

U aprilu 2026. godine planirano je puštanje u rad novog pogona za proizvodnju fosforne kiseline, koji predstavlja jedan od najznačajnijih investicionih projekata Elixir grupe u poslednjih nekoliko godina. Fosforna kiselina je ključna sirovina u proizvodnji kompleksnih mineralnih đubriva, a njen stabilan i pouzdan izvor od suštinskog je značaja za kontinuitet i razvoj celokupnog poslovnog sistema.

Novi pogon projektovan je sa ciljem povećanja kapaciteta, unapređenja energetske efikasnosti i smanjenja specifičnih emisija po toni proizvoda. Primena savremenih tehnoloških rešenja omogućava bolju iskorišćenost fosfatne rude, efikasnije upravljanje nusproizvodima i viši stepen kontrole procesa. Ovim projektom se povećava obim proizvodnje fosforne kiseline, što obezbedjuje sirovinu za nove, buduće pogone.

Elixir grupa u svom proizvodnom portfoliju ima fosfornu kiselinu prehrambenog kvaliteta, a naredni investicioni ciklus biće usmeren ka proizvodnji food grade fosfatnih soli.

Sa aspekta šire industrijske slike, novi pogon fosforne kiseline doprinosi jačanju domaće hemijske industrije i njenoj integraciji u regionalne i evropske lance vrednosti. Povećani kapaciteti i viši tehnološki standardi stvaraju osnovu za dalji razvoj novih proizvoda, kao i za unapređenje izvoznog potencijala Elixir grupe.

Energana za termički tretman i energetsko iskorišćenje otpada – zatvaranje industrijskog kruga i odgovorno upravljanje resursima

Treći ključni projekat, čije se puštanje u rad očekuje u maju 2026. godine, jeste energana na otpad. Ovo postrojenje ima poseban značaj ne samo za Elixir grupu, već i za širu industrijsku i ekološku zajednicu u Srbiji. Reč je o savremenom postrojenju za termički tretman industrijskog otpada, projektovanom u skladu sa najstrožim domaćim i evropskim ekološkim propisima.

Izgradnjom energane, Elixir grupa uspostavlja zatvoreniji i održiviji industrijski ciklus, u kojem se otpadni tokovi iz industrijskih sistema, tretiraju na bezbedan i kontrolisan način. Time se značajno smanjuje potreba za odlaganjem

otpada, umanjuju rizici po životnu sredinu i doprinosi principima cirkularne ekonomije. Energija dobijena na taj način se konvertuje u vodenu paru koja se dalje koristi u proizvodnim pogonima Elixir grupe

Posebna vrednost ovog projekta ogleda se u njegovoj ulozi u unapređenju industrijske infrastrukture Srbije, s obzirom na hronični nedostatak kapaciteta za bezbedan tretman opasnog i industrijskog otpada. Energana Elixir grupe predstavlja primer kako industrija može preuzeti aktivnu ulogu u rešavanju sistemskih ekoloških izazova, uz istovremeno poštovanje najviših standarda bezbednosti i zaštite životne sredine.

Integrisana vizija razvoja

Tri nova postrojenja koja Elixir grupa uvodi u rad tokom 2026. godine ne treba posmatrati kao pojedinačne investicije, već kao deo integrisane razvojne vizije. Reč je o strateškom pristupu koji povezuje tehnološki napredak, ekonomsku i resursnu efikasnost i odgovornost prema životnoj sredini. Ovakav pristup omogućava Elixir grupi da odgovori na rastuće zahteve tržišta, regulatorne izazove i očekivanja društva u celini.

Ulaskom u novu fazu razvoja, Elixir grupa potvrđuje svoju dugoročnu opredeljenost ka modernoj, konkurentnoj i održivoj hemijskoj industriji. Investicije u kristalna đubriva, fosfornu kiselinu i tretman industrijskog otpada predstavljaju snažan signal da domaća industrija ima znanje, kapacitete i viziju da bude ravnopravan učesnik u savremenim globalnim tokovima. Za stručnu javnost, ali i za celokupnu privredu, ovi projekti predstavljaju primer kako se strateškim planiranjem i tehnološkim ulaganjem gradi stabilna i održiva industrijska budućnost.

Kristalna đubriva – odgovor na zahteve savremene poljoprivrede

Puštanjem u rad pogona za proizvodnju kristalnih đubriva početkom 2026. godine, Elixir grupa pravi iskorak ka segmentu visokovrednih, specijalizovanih mineralnih đubriva namenjenih intenzivnoj i preciznoj poljoprivredi. Kristalna, odnosno potpuno vodotopiva đubriva, predstavljaju neizostavan element savremenih agro-tehnoloških sistema, posebno u fertirigaciji, plasteničkoj i stakleničkoj proizvodnji, kao i u visokointenzivnim zasadima.

Novi pogon projektovan je u skladu sa najvišim tehnološkim standardima, sa naglaskom na stabilnost kvaliteta, preciznu kontrolu hemijskog sastava i fleksibilnost u formulacijama. Vertikalnom i horizontalnom intergacijom novog pogona sa već postojećim, postignuta je visoka energetska efikasnost, i maksimalno iskorišćenje sirovina; praktično bez otpada i nusproizvoda. Time se dodatno smanjuje ekološki otisak proizvodnje.Ulazak u segment kristalnih đubriva

predstavlja i strateški odgovor Elixir grupe na promene u poljoprivredi, gde se sve veći akcenat stavlja na preciznu ishranu biljaka, optimizaciju prinosa i smanjenje gubitaka hraniva u životnoj sredini. Time se jača veza između hemijske industrije i održive poljoprivredne proizvodnje, što je jedan od ključnih izazova savremenog agroindustrijskog kompleksa.

Dodatna tržišna prilika za glavni proizvod ovog pogona (monoamonijum fosfat) ogleda se u njegovoj primeni u naprednim energetskim i elektrohemijskim procesima, koji beleže snažan razvoj na globalnom nivou.

Novi pogon fosforne kiseline – jačanje sirovinske osnove i tehnološke nezavisnosti

U aprilu 2026. godine planirano je puštanje u rad novog pogona za proizvodnju fosforne kiseline, koji predstavlja jedan od najznačajnijih investicionih projekata Elixir grupe u poslednjih nekoliko godina. Fosforna kiselina je ključna sirovina u proizvodnji kompleksnih mineralnih đubriva, a njen stabilan i pouzdan izvor od suštinskog je značaja za kontinuitet i razvoj celokupnog poslovnog sistema.

Novi pogon projektovan je sa ciljem povećanja kapaciteta, unapređenja energetske efikasnosti i smanjenja specifičnih emisija po toni proizvoda. Primena savremenih tehnoloških rešenja omogućava bolju iskorišćenost fosfatne rude, efikasnije upravljanje nusproizvodima i viši stepen kontrole procesa. Ovim projektom se povećava obim proizvodnje fosforne kiseline, što obezbedjuje sirovinu za nove, buduće pogone.

Elixir grupa u svom proizvodnom portfoliju ima fosfornu kiselinu prehrambenog kvaliteta, a naredni investicioni ciklus biće usmeren ka proizvodnji food grade fosfatnih soli.

Sa aspekta šire industrijske slike, novi pogon fosforne kiseline doprinosi jačanju domaće hemijske industrije i njenoj integraciji u regionalne i evropske lance vrednosti. Povećani kapaciteti i viši tehnološki standardi stvaraju osnovu za dalji razvoj novih proizvoda, kao i za unapređenje izvoznog potencijala Elixir grupe.

Energana za termički tretman i energetsko iskorišćenje otpada – zatvaranje industrijskog kruga i odgovorno upravljanje resursima

Treći ključni projekat, čije se puštanje u rad očekuje u maju 2026. godine, jeste energana na otpad. Ovo postrojenje ima poseban značaj ne samo za Elixir grupu, već i za širu industrijsku i ekološku zajednicu u Srbiji. Reč je o savremenom postrojenju za termički tretman industrijskog otpada, projektovanom u skladu sa najstrožim domaćim i evropskim ekološkim propisima.

Izgradnjom energane, Elixir grupa uspostavlja zatvoreniji i održiviji industrijski ciklus, u kojem se otpadni tokovi iz industrijskih sistema, tretiraju na bezbedan i kontrolisan način. Time se značajno smanjuje potreba za odlaganjem otpada, umanjuju rizici po životnu sredinu i doprinosi principima cirkularne ekonomije. Energija dobijena na taj način se konvertuje u vodenu paru koja se dalje koristi u proizvodnim pogonima Elixir grupe

Posebna vrednost ovog projekta ogleda se u njegovoj ulozi u unapređenju industrijske infrastrukture Srbije, s obzirom na hronični nedostatak kapaciteta za bezbedan tretman opasnog i industrijskog otpada. Energana Elixir grupe predstavlja primer kako industrija može preuzeti aktivnu ulogu u rešavanju sistemskih ekoloških izazova, uz istovremeno poštovanje najviših standarda bezbednosti i zaštite životne sredine.

INTEGRISANA VIZIJA RAZVOJA

Tri nova postrojenja koja Elixir grupa uvodi u rad tokom 2026. godine ne treba posmatrati kao pojedinačne investicije, već kao deo integrisane razvojne vizije. Reč je o strateškom pristupu koji povezuje tehnološki napredak, ekonomsku i resursnu efikasnost i odgovornost prema životnoj sredini. Ovakav pristup omogućava Elixir grupi da odgovori na rastuće zahteve tržišta, regulatorne izazove i očekivanja društva u celini.

Ulaskom u novu fazu razvoja, Elixir grupa potvrđuje svoju dugoročnu opredeljenost ka modernoj, konkurentnoj i održivoj hemijskoj industriji. Investicije u kristalna đubriva, fosfornu kiselinu i tretman industrijskog otpada predstavljaju snažan signal da domaća industrija ima znanje, kapacitete i viziju da bude ravnopravan učesnik u savremenim globalnim tokovima. Za stručnu javnost, ali i za celokupnu privredu, ovi projekti predstavljaju primer kako se strateškim planiranjem i tehnološkim ulaganjem gradi stabilna i održiva industrijska budućnost.